Swiss Journal of Palaeontology

RESEARCH Open Access

Dental remains of '*Parachleuastochoerus*' *valentini* (Suidae: Tetraconodontinae) from the early Late Miocene of Sant Quirze (Vallès-Penedès Basin, NE Iberian Peninsula): taxonomic and phylogenetic implications

David M. Alba[1*], Souzanna Siarabi[1], Sara G. Arranz[1], Sharrah McKenzie[1] and Isaac Casanovas-Vilar[1]

Abstract

The distinctiveness and genus allocation of '*Parachleuastochoerus*' *valentini* (Suidae: Tetraconodontinae), from the Miocene of Europe, has been controversial, being alternatively considered a junior synonym of *Conohyus simorrensis*. Recently described material from the Vallès-Penedès Basin (NE Iberian Peninsula) supported its distinct species status but did not discount an alternative ascription to *Conohyus*, largely because the lower male canine remained unknown. Here we describe all the tetraconodontine dentognathic material from the earliest Late Miocene sites of Trinxera del Ferrocarril–Sant Quirze (~11.6–11.2 Ma, MN7+8), as well as Can Feliu 2 and Poble Nou de Sant Quirze (≤11.2 Ma, MN9), comprising 134 specimens. The former locality played an important role in the resurrection of '*Pa.*' *valentini* but ~70% of the available material remained unpublished. Based on metrical and qualitative comparisons with published material of this species and similarly sized tetraconodontines from Europe, we attribute the whole studied sample to '*Pa.*' *valentini*. Previous reports of *Parachleuastochoerus huenermanni* from the site are erroneous (owing to specimen mislabeling). Our results reinforce the distinctiveness of *'Pa.' valentini*, while its lower male canine morphology (first described herein) does not support its transfer to *Conohyus*. However, a cladistic analysis favors closer phylogenetic relationships with *Retroporcus matritensis* (a potential junior synonym of *C. simorrensis*) and even *Versoporcus steinheimensis* than with *Parachleuastochoerus crusafonti* (the type species of the genus). Our results thus indicate that *Parachleuastochoerus*, as currently conceived, is polyphyletic, although pending an in-depth revision of other European tetraconodontines we refrain from providing a new combination for '*Pa.*' *valentini*.

Keywords Suids, Dental morphology, Taxonomy, Systematics, Phylogeny, Evolution, Miocene, Spain, Europe

Introduction

Tetraconodontines are a suid clade characterized—among other craniodental features (for further details, see Harris & Liu, 2007)—by hypertrophied distal premolars and comparatively reduced mesial premolars, even though dental proportions vary widely within the group (Van der Made, 1999). The Tetraconodontinae Lydekker, 1876 were originally erected at the family rank based on genus *Tetraconodon* Falconer, 1868, which was not yet recognized as a suid. Simpson (1945) first classified

Handling editor: Gabriel Aguirre Fernández

*Correspondence:
David M. Alba
david.alba@icp.cat
[1] Institut Català de Paleontologia Miquel Crusafont (ICP-CERCA), Universitat Autònoma de Barcelona, Edifici ICTA-ICP, c/ Columnes s/n, Campus de la UAB, 08193 Cerdanyola del Vallès, Barcelona, Spain

tetraconodontines as an extinct subfamily of suids, further encompassing the genera *Conohyus* Pilgrim, 1925 and *Sivachoerus* Pilgrim, 1926. It was not until the end of the twentieth century that Van der Made (1999) arranged the tetraconodontine genera known by then into tribes: Tetraconodontini Lydekker, 1876, including *Tetraconodon* and *Sivachoerus*; Nyanzachoerini Van der Made, 1999, including among others *Conohyus* and *Nyanzachoerus* Leakey, 1958; and the monotypic Parachleuastochoerini, based on *Parachleuastochoerus* Golpe-Posse, 1972. This distinction was based on biometric evolutionary trends, especially regarding the premolars, with tetraconodontins having large or even extremely enlarged premolars, nyanzachoerins having moderately sized or even reduced premolars, and parachleuastochoerins having relatively elongate but narrow premolars (Van der Made, 1999). This arrangement was subsequently criticized because it relies entirely on dental proportions while disregarding other sources of craniodental morphology (e.g., Bernor et al., 2004). Indeed, these tribes are frequently ignored in systematic papers dealing with suids (e.g., Bishop, 2010; Harris & Liu, 2007; Hünermann, 1999; Pickford, 2016; Pickford & Laurent, 2014), and subsequent cladistic analyses of suids (admittedly, not focused on tetraconodontines) have thus far been unable to substantiate this systematic arrangement (Hou & Deng, 2014; Orliac et al., 2010).

Pickford (1993) hypothesized that tetraconodontines evolved from a hyotheriine stock later than listriodontines (implying that hyotheriines are paraphyletic), while Van der Made (1999) considered that tetraconodontines share a last common ancestor with suines, exclusive of other suid subfamilies. The latter view was supported by subsequent cladistic analyses, which further placed hyotheriines as the sister taxon of tetraconodontines + suines (Hou & Deng, 2014; Orliac et al., 2010). Given their earliest record in Asia, tetraconodontines are considered to have originated there and later dispersed into the rest of the Old World during the Middle Miocene (Harris & Liu, 2007; Van der Made, 1999). Van der Made (1999) concluded that tetraconodontines dispersed into Europe in two different events, given the older first appearance datum of *Conohyus* (MN5) as compared with that of *Parachleuastochoerus* s.l. (MN6)—i.e., including other species other than the type, which is dated to the Vallesian. These considerations were based on a simplified taxonomic scheme that only recognized these two tetraconodontine genera in Europe (e.g., Hünermann, 1999; Van der Made, 1999). Over the years, the boundaries of these two genera (and the species included therein) have proven very controversial. Part of the problem is whether *Chaeropotamus steinheimensis* Fraas, 1870 belongs to *Conohyus* (Bernor et al., 2004; Chen, 1984), *Parachleuastochoerus* (Fortelius et al., 1996; Hünermann, 1999; Van der Made, 1997, 1999, 2020; Van der Made et al., 2014), or an entirely different genus (Pickford, 2014, 2016)—the latter being the opinion followed here (see below). Implicit in these taxonomic disagreements is whether the aforementioned species shares a closest last common ancestor with *Conohyus simorrensis* (Lartet, 1851) (the type species of *Conohyus*), *Parachleuastochoerus crusafonti* Golpe-Posse, 1972 (the type species of *Parachleuastochoerus*), or both.

Van der Made (1999) raised the possibility that *Parachleuastochoerus* s.l. might have evolved from a *Conohyus*-like ancestor (implying a single dispersal event into Europe), while noting that it was unclear whether the narrower premolars of the former were indeed derived or plesiomorphic as compared with *Conohyus*. The latter view is tentatively favored by a cladistic analysis of dental features on a few tetraconodontine species (Bernor et al., 2004) as well as by large-scale cladistic analyses of suids (Hou & Deng, 2014; Orliac et al., 2010), which recovered the type species of *Parachleuastochoerus* as more basal than the other tetraconodontines. Nevertheless, these analyses were based on a very limited number of tetraconodontine taxa and, more importantly, could not consider recent developments in the systematics of European tetraconodontines (e.g., Pickford, 2014, 2016), which unfolded following Pickford and Laurent's (2014) lectotype designation for *C. simorrensis*. Among other taxonomic actions, Pickford and Laurent (2014) and Pickford (2014, 2016): (1) erected the genera *Versoporcus* Pickford, 2014 and *Retroporcus* Pickford, 2016—with *Versoporcus steinheimensis* (Fraas, 1870) and *Retroporcus complutensis* Pickford & Laurent, 2014 (the latter based on material previously included in *C. simorrensis*; Van der Made & Salesa, 2004) as their respective type species; (2) resurrected the nominal taxa *Sus doati* Lartet, 1851, *Sus valentini* Filhol, 1882, *Sus grivensis* Gaillard, 1899, and *Hyotherium soemmeringi matritensis* Golpe-Posse, 1972—respectively, within the genera *Conohyus*, *Parachleuastochoerus*, *Versoporcus*, and *Retroporcus*; and (3) considered that *Conohyus simorrensis goeriachensis* Van der Made, 1989 and *Conohyus olujici* Bernor et al., 2004 are respective junior synonyms of *Retroporcus matritensis* (Golpe-Posse, 1972) and *Parachleuastochoerus huenermanni* (Heissig, 1989)—instead of belonging to *C. simorrensis* s.s. and constituting a distinct subspecies of *Pa. steinheimensis*, respectively (Van der Made, 2020; Van der Made et al., 2014).

The above-mentioned taxonomic opinions and nomenclatural acts by Pickford and colleagues have been criticized (Van der Made, 2020), questioned (Iannucci & Begun, 2022), or modulated to some extent (Alba et al., 2024; McKenzie et al., 2023a, 2023b, 2024) by subsequent

authors. Central among the disagreements emerged from the aforementioned revisions of European tetraconodontines is the controversial distinctiveness and genus ascription of '*Parachleuastochoerus*' *valentini* (Filhol, 1882), which rely on both dental and cranial remains. Unlike in previous papers, and for the reasons that will be explained in greater detail in the Discussion, here we will use the genus name within quotes to denote its uncertain applicability to this species. After being initially resurrected by Pickford (2013a) and Pickford and Laurent (2014), the distinctiveness of '*Pa.*' *valentini* was better justified by Pickford (2014), who relied only on dental morphology but also referred to cranial differences relative to *V. steinheimensis*. These differences were in fact the main basis to justify the erection of *Versoporcus*. Later on, Pickford (2016) added additional remains from various European sites to the hypodigm of '*Pa.*' *valentini*, whereas Van der Made (2020) criticized the inclusion of this species in *Parachleuastochoerus* and considered it to be a junior subjective synonym of *C. simorrensis*. McKenzie et al. (2023a) supported Pickford's (2014, 2016) taxonomy and included further remains in the hypodigm of the species. However, McKenzie et al. (2023a) excluded from the latter the type material of *Conohyus melendezi* Golpe-Posse, 1972, which they considered, like Van der Made (2020), a junior synonym of *C. simorrensis* (instead of '*Pa.*' *valentini* as argued by Pickford, 2014, 2016). McKenzie 2024) further argued that *C. doati* is a *nomen dubium* and that most of the material attributed by Pickford (2013a, 2014, 2016) and Pickford and Laurent (2014) to this species should be assigned instead to '*Pa.*' *valentini*—including *Conohyus ebroensis* Azanza, 1986, which would be a junior subjective synonym of '*Pa.*' *valentini* (instead of *C. simorrensis*, as argued by Van der Made, 2020).

Based on the above, the classification of '*Pa.*' *valentini* in *Parachleuastochoerus* is tentatively supported by distal premolar vs. molar size proportions (McKenzie et al., 2024; Pickford, 2014). However, Van der Made's (2020) opinion that this material belongs to *Conohyus* is not unreasonable, given the poorly defined and controversial boundaries among European tetraconodontine genera. This is further supported by disagreements among Pickford (2014, 2016), Van der Made (2020), and McKenzie et al. (2023a, 2024) about the composition of the hypodigms and/or the distinctiveness of *C. simorrensis*, *C. doati*, and '*Pa.*' *valentini* (e.g., the material originally used to erect *C. melendezi* and *C. ebroensis*; see above). McKenzie et al. (2024) concluded that, albeit '*Pa.*' *valentini* is a distinct species, its alternative allocation into *Conohyus* cannot be confidently ruled out because (1) no cranial remains are known for the type species of *Parachleuastochoerus* and, hence, the cranial differences between '*Pa.*' *valentini* and *V. steinheimensis* noted by Pickford (2014) would also be compatible with an ascription of the former to *Conohyus* and the latter to *Parachleuastochoerus* (Iannucci & Begun, 2022); and (2) the male lower canine (c1m) morphology of '*Pa.*' *valentini* is unknown, precluding to ascertain whether it displays the diagnostic c1m morphology of *Conohyus* (Pickford & Laurent, 2014; Pickford, 2013b, 2014, 2016).

All these taxonomic debates have far-reaching implications for the reliability of previous cladistic analyses (Hou & Deng, 2014; Orliac et al., 2010) regarding European tetraconodontines. First, because '*Pa.*' *valentini* had yet to be resurrected and was not considered in the coding of *Parachleuastochoerus*, which was based on the type species. Second, because the coding of *Conohyus* was based on the remains of species currently included in different genera. According to Orliac et al. (2010), *Conohyus* was based on both *Conohyus grivensis* (Gaillard, 1899) from La Grive-Saint-Alban and *C. simorrensis* from Simorre and Le Fousseret. However, following the aforementioned revisions, the former would belong to *Versoporcus* (McKenzie et al., 2023b, 2024; Pickford, 2014, 2016) or else *Parachleuastochoerus* (Van der Made, 2020), whereas the latter material could represent both *Conohyus* and *Retroporcus* (Pickford & Laurent, 2014). Given the restricted cladistic results for tetraconodontines and the diverging taxonomic opinions of several authors, many uncertainties persist about the evolutionary history of this group in Europe. For example, it is uncertain whether European tetraconodontines originated from a single or multiple dispersal events from Asia, and even which is their plesiomorphic condition regarding the hypertrophy of the distal premolars (see discussion in Pickford, 2014; Van der Made, 2020). This kind of questions cannot be reliably tackled without an accurate phylogeny of the Tetraconodontinae, which in turn would require to clarify most if not all of the aforementioned taxonomic controversies about the European taxa.

As a first step toward the resolution of the aforementioned issues, here we provide a detailed description of the dental morphology of '*Pa.*' *valentini* based on the abundant material from the early Late Miocene Sant Quirze localities. Together with the material from France, the Sant Quirze material played a prominent role in Pickford's (2014) taxonomic validation of this nominal species within *Parachleuastochoerus*. However, only a portion of the available sample was considered (see Materials and methods), so that the rest is herein figured and described in detail for the first time. To reassess the genus ascription and phylogenetic relationships of '*Pa.*' *valentini*, we further provide detailed comparisons not only with previously described material of '*Pa.*' *valentini*, but also with other medium to large-sized tetraconodontines from

Europe (namely, *R. matritensis*, *C. simorrensis*, and *V. steinheimensis*). Some of these species overlap with '*Pa.*' *valentini* in chronostratigraphic range (McKenzie et al., 2023a, 2023b, 2024; Pickford, 2014, 2016) and, therefore, the possibility that more than a single species was present at the site could not be discounted a priori. Based on the comparisons reported in this paper—and contrary to previous reports of *Pa. huenermanni* at the site (Pickford, 2014, 2016; Van der Made, 1990, 1997)—we conclude that the whole tetraconodontine sample can be assigned to '*Pa.*' *valentini*, thereby supporting its distinctiveness. This represents an unprecedented opportunity to ascertain the intraspecific variation of '*Pa.*' *valentini* within a single site and further enables the description of some tooth loci that were previously unknown for the species, including the c1m. We further report the first cladistic analysis including this species, together with *V. steinheimensis* and *R. matritensis*. Given current uncertainties about the genus allocation of '*Pa.*' *valentini* and its possession of reduced distal premolars (similarly to *Pa. crusafonti* and *V. steinheimensis*), deciphering its closest systematic affinities is key to better understanding the evolutionary history of European tetraconodontines.

Historical background

Most of the fossil remains from the municipality of Sant Quirze del Vallès (Barcelona, Catalonia, Spain) come from the site currently known as Trinxera del Ferrocarril–Sant Quirze (SQ-TF). Originally, this site was referred with former toponyms (no longer official) of this municipality, including Sant Quirze de Terrassa (Bataller, 1924, 1926; Villalta-Comella & Crusafont-Pairó, 1941a) and Sant Quirze de Galliners (Villalta-Comella & Crusafont-Pairó, 1933, 1941b, 1944b, 1944c, 1945; Schaub, 1944, 1947; Villalta & Crusafont, 1934, 1946; Crusafont & Truyols, 1954; Bergounioux & Crouzel, 1962; Crusafont-Pairó, 1969), which were frequently provided with the Spanish spellings of "San Quirce" or especially "San Quirico" in the oldest literature (e.g., Bataller, 1926; Bergounioux, 1938; Crusafont-Pairó, 1935, 1944; Villalta-Comella & Crusafont-Pairó, 1941a, 1941b, 1943a, 1943b, 1944a, 1944b, 1944c, 1945; Schaub, 1944, 1947). Over time, the site was just referred to as "Sant Quirze" (e.g., Aldana Carrasco, 1992a, 1992b; Bergounioux, 1958; Casanovas-Vilar et al., 2016a; Crusafont-Pairó et al., 1948; Freudenthal, 1966; Harrison et al., 2002), with Trinxera del Ferrocarril being considered a synonym (e.g., Casanovas-Vilar et al., 2016b; Luján et al., 2016). Nevertheless, the presence of other localities within the municipality (see below) makes it recommendable to favor Trinxera del Ferrocarril ("Trinchera del Ferrocarril" in Spanish), which has also been widely used in the literature (Agustí Ballester, 1977a; Agustí et al., 1985; Crusafont-Pairó & Golpe, 1972; Crusafont-Pairó & Golpe-Posse, 1972; Crusafont-Pairó, 1965, 1975a; Golpe-Posse, 1971, 1972, 1974), as the name of the site.

The oldest fossil vertebrate finds from this area correspond to hipparionin remains originally described by Almera and Bofill y Poch (1887). These authors did not mention the name of the site, just a vineyard in the surrounding of Sabadell. However, the name of the locality, Mas Duran (MDU), was mentioned by later authors (Bataller, 1918; Hernández-Pacheco, 1914). The fossils were found by Francesc de P. Benessat (Bataller, 1918; Crusafont-Pairó, 1969, 1975c) alongside the Sec River (riu Sec) near the farmhouse of Mas Duran in Sant Quirze (Fig. 1A–B). The second find corresponds to a gomphotheriid mandibular fragment from Can Canals (CCA), also close to the Sec River, found in 1908 and initially housed in the private collection of Josep M. Vives i Lucena (Bataller, 1918; Bergounioux & Crouzel, 1958; Crusafont-Pairó et al., 1948; Villalta-Comella & Crusafont-Pairó, 1943a). Bataller (1918) incorrectly attributed the site to Sant Pere de Terrassa, but later authors attributed it to Sant Quirze (Bataller, 1924; Bergounioux & Crouzel, 1958; Crusafont & Truyols, 1954; Crusafont-Pairó, 1969; Villalta-Comella & Crusafont-Pairó, 1943a, 1943b). This specimen was subsequently housed in the rectory at the entrance of Sant Quirze and lost during the Spanish Civil War (Crusafont-Pairó, 1969). The toponym corresponded to a former farmhouse located more than 1.3 km S-SE from MDU and currently included within the homonymous industrial park (Polígon Industrial de Can Canals), formerly also known as Polígon Industrial del Sud-Est (Fig. 1A–B).

The SQ-TF site was not discovered until the early 1920s, owing to the excavation of a railway trench of the company Ferrocarrils de Catalunya between Sant Cugat del Vallès and Sabadell in the early 1920s (Fig. 1C–D). There are some disagreements in the literature about the exact date of discovery, from ca. 1923 (Crusafont-Pairó & Villalta, 1948) to 1925 (Golpe-Posse, 1974) or even 1926 (Crusafont-Pairó, 1975a). Nevertheless, it must have been discovered not later than 1922, when the Sant Quirze train station was inaugurated (Salmerón i Bosch, 1988), and certainly before 1924, when fossil remains from the site (including suids) were first published (Bataller, 1924). The site was reported to be located at about 500 m (Bataller, 1924; Villalta-Comella & Crusafont-Pairó, 1943a) or 600 m (Bataller Calatayud, 1938) southward from the Sant Quirze train station, at about the level of Can Canals farmhouse (Villalta-Comella & Crusafont-Pairó, 1943a) but slightly westward. The geological section of the site provided by Bataller (1924) corresponded to kilometer 6.9 of the railway, which according to old maps would roughly coincide with Can Canals, in further

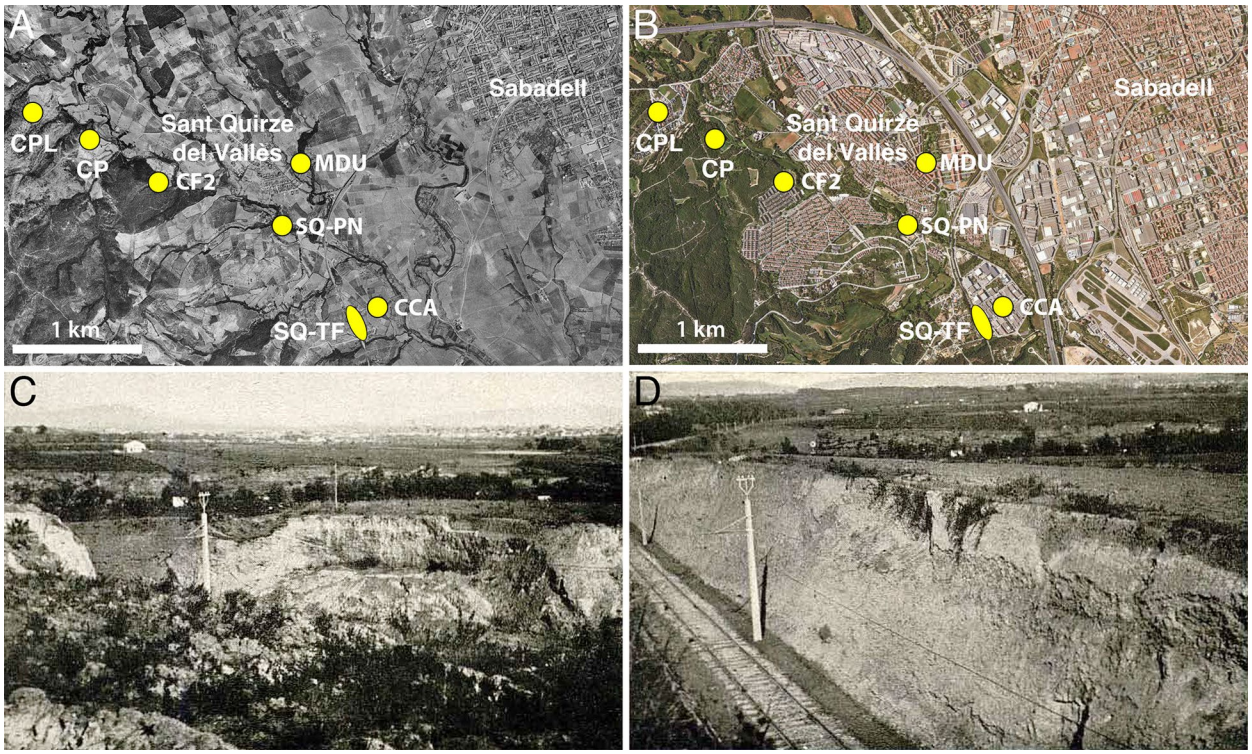

Fig. 1 **A–B** Orthophotomap of the Sant Quirze area from 1945 (**A**) and 2022 (**B**), indicating the approximate position of the various sites discussed in this paper. **C–D** Two views of the SQ-TF site in the 1920s. Abbreviations: CCA, Can Canals; CF2, Can Feliu2; CP, Can Poncic; CPL, Can Pallars i Llobateres; MDU, Mas Duran; SQ-PN, Poble Nou de Sant Quirze; SQ-TF, Trinxera del Ferrocarril-Sant Quirze. The UTM coordinates (31N / ETRS89) employed for each site are the following: CCA (424360, 4597110) and MDU (423670, 4598280) correspond to the homonymous farmhouses; CP (421900, 4598475) and CPL (421450, 4598750) approximate location after Alba et al. (2018); CF2 (422480, 4598150) is located based on the current toponym of Can Feliu; SQ-PN has been placed between the Can Barra farmhouse (423430, 4597810) and Los Rosales (423800, 4597620) neighbourhood; finally, SQ-TF has been situated according to Galindo i Torres et al.'s (2001) map (424100, 4597060), approximately coinciding with Sant Quirze C based on Quintana Cardona (1995), although according to the old literature (see main text) it would have extended >200 m along the railway (i.e., approximately 424190, 4596840). Base orthophotomaps for panels **A–B** © Institut Cartogràfic i Geològic de Catalunya, downloaded from VISSIR v. 3.35 and reproduced with permission by means of a Creative Commons license CC BY 4.0 (Institut Cartogràfic i Geològic de Catalunya 2024). Panels **C–D** reproduced from Bataller (1924)

agreement with the current geologic map of the area (Galindo i Torres et al., 2001). In any case, the 8 m-deep trench where the site was located extends along 200–250 m (Crusafont-Pairó & Villalta, 1948; Villalta-Comella & Crusafont-Pairó, 1941a, 1943a), indicating that the site was loosely delimited (Fig. 1A–B), although the stratigraphic thickness of the exposed stratigraphic section is uncertain.

Since the early 1920s, most finds were initially made by amateur collector Mario Guérin (also known as Màrius Guerín), who kept them in his private collection (as it was customary at the time) but allowed them to be published by Josep R. Bataller (Bataller, 1924, 1926; Bataller Calatayud, 1938), from the Museu Geològic del Seminari de Barcelona (MGSB). However, some of the first published material belonged to the private collection of Josep Colominas (Bataller, 1924), while other specimens were apparently collected by Bataller himself. All this material is currently housed in the MGSB, following the donation of Guérin's collection sometime after his death in 1968 (Crusafont-Pairó, 1975a). During the 1930s, landslides in the trench walls caused by rainfall led to further excavation works aimed to reduce the steepness of the slopes, enabling the recovery of additional fossils (Crusafont-Pairó, 1935; Villalta-Comella & Crusafont-Pairó, 1933). By then, Miquel Crusafont-Pairó had already intermittently surveyed the site (Crusafont-Pairó, 1969). However, from 1933 onward, Crusafont started to survey it more regularly, together with Josep F. de Villalta-Comella and various collaborators of the Sabadell Museum (Crusafont-Pairó, 1944, 1969, 1975a; Villalta-Comella & Crusafont-Pairó, 1941b), coinciding with some of their first publications (Villalta & Crusafont, 1934; Villalta-Comella & Crusafont-Pairó, 1933). The Spanish Civil War (1936–1939) temporarily halted such activities, which were nevertheless resumed with renewed vigor since

the early 1940s (Villalta-Comella & Crusafont-Pairó, 1941a, 1941b, 1943a), beginning with the discovery of barbourofelid remains by Joan Andrés in 1940 (Crusafont-Pairó, 1969). These fossils were described soon thereafter (Villalta-Comella & Crusafont-Pairó, 1943a, 1943b) and systematic excavations of the site followed in 1942 (Villalta-Comella & Crusafont-Pairó, 1943b). Prospections of the site continued for many years, until vegetation growth made it impossible to continue surveying it (Golpe-Posse, 1974). By the early 1970s, the site was considered almost exhausted (Crusafont-Pairó & Golpe-Posse, 1972). However, new conditioning works of the trench in 1995, performed under paleontological surveillance by personnel linked to the Institut de Paleontologia M. Crusafont in Sabadell, led to the recovery of additional macrovertebrate remains (including two tetraconodontine molars) from the so-called Sant Quirze C (SQ-TFC) locality (Quintana Cardona, 1995). New microvertebrate samples were also collected by that time from trench layers labeled Sant Quirze A (SQ-TFA), Sant Quirze B (SQ-TFB), and Sant Quirze G (SQ-TFG) by Llenas i Avellaneda (1996).

Besides the aforementioned sites of MDU, CCA, and SQ-TF, there are many other fossil localities in the municipality of Sant Quirze del Vallès, such as Can Poncic and Can Pallars i Llobateres (e.g., Alba et al., 2018; Casanovas-Vilar et al., 2016a; Crusafont & Truyols, 1954; Fig. 1A–B). Nevertheless, here we will only focus on two sites that are not very far from SQ-TF and have yielded tetraconodontine remains: Can Barra or Poble Nou de Sant Quirze (SQ-P) and Can Feliu (CF). The former was first reported as Can Barra by Crusafont-Pairó and Villalta (1948) and Crusafont and Truyols (1954) and as SQ-PN by Crusafont and Truyols (1956). Although this duplicity of names might suggest otherwise, the subsequent literature indicates the two sites are the same. First, the carnivoran remains originally described by Crusafont-Pairó (1962) from SQ-PN were later attributed to Can Barra (Crusafont-Pairó & Golpe-Posse, 1973). Second, although the two sites were mentioned as separate in multiple works (Crusafont-Pairó & Casanovas Cladellas, 1973; Golpe-Posse, 1971, 1972, 1974), when reporting the material Golpe-Posse (1971, 1972) made it clear that they were synonyms. According to Golpe-Posse (1971, 1974), the locality of SQ-PN was located on the right side of the road from Sabadell to Rubí, in a former exploitation of yellowish to greenish clays. In the Sant Quirze area, the toponym "Can Barra" is located next to the Can Barra Creek near the neighborhood of Los Rosales—indeed, the fossil remains from Los Rosales (Sant Quirze) housed in the Institut Català de Paleontologia Miquel Crusafont (ICP) are considered to come from this site—being located ca. 1 km NW from SQ-TF (Fig. 1A–B).

Some confusion further surrounds the site of CF because a careful reading of the literature indicates that the suid remains did not come from the site originally named as such (Crusafont & Truyols, 1954; Crusafont-Pairó & Villalta, 1948), which yielded tortoise remains. The site of CF was mentioned again in multiple papers during the 1970s, often together with SQ-PN and/or Can Barra (Crusafont-Pairó & Casanovas Cladellas, 1973; Crusafont-Pairó & Golpe, 1972; Crusafont-Pairó & Golpe-Posse, 1972; Crusafont-Pairó, 1975a; Golpe-Posse, 1971, 1972, 1974), and sometimes in isolation (Agustí Ballester, 1977b; Crusafont-Pairó, 1975c), especially following the discovery of a primate tooth (Crusafont-Pairó, 1975b). The latter find was also referred to the site of Can Sant Feliu (Crusafont-Pairó & Golpe-Posse, 1981, 1982; Golpe-Posse, 1982). We have been unable to find a toponym of Can Sant Feliu in the area and, with a single exception (Ginsburg, 1986), later authors referred the primate find to just Can Feliu (Aldana Carrasco, 1992a, 1992b; Andrews et al., 1996; Begun, 2002; Harrison et al., 2002; Moyà-Solà et al., 1990), with Can Sant Feliu being considered a synonym (Alba & Moyà-Solà, 2012; Casanovas-Vilar et al., 2016a; Marigó et al., 2014). In turn, Golpe-Posse (1971, 1972) frequently referred the suids to Can Feliu, but sometimes specified that Can Feliu 1 (CF1) had no mammals and that the latter came from Can Feliu 2 (CF2), with Can Pagès being its synonym (Agustí, 1981; Golpe-Posse, 1974). This agrees with the fact that Crusafont-Pairó and Golpe (1972) reported Can Feliu as a new outcrop of mudstones that did not allow for a systematic excavation. Therefore, we conclude that the mammal remains came from a locality discovered during the early 1970s that should be termed CF2, whereas CF1 was discovered in the 1940s and only yielded tortoise remains. The toponym of Can Feliu is located about 2 km NW from SQ-TF and 1 km W-NW from Can Barra/SQ-PN (Fig. 1A–B), being indeed closer to the fossiliferous area Can Poncic (Alba et al., 2018). Its exact location cannot be determined with certainty but in the 1990s it was already considered that the outcrop had been destroyed (Llenas i Avellaneda, 1996).

The suid assemblage from Sant Quirze

The suid remains described in this paper, housed in the ICP and the MGSB, mostly come from SQ-TF, as evidenced by the historical background provided above. Only a few specimens housed in the ICP come from the SQ-TFC locality (excavated in 1995) or other nearby sites (SQ-PN and CF2). In the case of SQ-TF, Bataller (1924) originally reported the suids *Sus palaeochoerus* Kaup, 1833—currently, *Propotamochoerus palaeochoerus* (Kaup, 1833)—and *Listriodon splendens* Von Meyer, 1846. However, the inspection of his figures shows that

some of the suid remains were attributed to a machairodontine carnivoran and an indeterminate mammal. In a subsequent faunal list of this site, Bataller Calatayud (1938) added two additional species, *Hyotherium grivense* (Gaillard, 1899) and *Sus major* Gervais, 1850—currently, *V. grivensis* (considered a synonym of *V. steinheimensis* by McKenzie et al., 2024) and *Hippopotamodon major* (Gervais, 1850), respectively. In turn, Villalta-Comella and Crusafont-Pairó (1941b) reported from Sant Quirze *Hyotherium simorrense* var. *Doati* Lartet, 1851 (currently, *C. doati*, considered a *nomen dubium* by McKenzie et al., 2024), *Hyotherium* cf. *Soemmeringii* Von Meyer, 1834, *S. palaeochoerus*, *L. splendens* var. *major* Roman, 1907, and *Choeromorus pygmaeus* Depéret, 1892—although the citation of *H.* cf. *soemmeringi* corresponded to Can Barra/SQ-PN instead of SQ-TF (Crusafont-Pairó & Villalta, 1948; Golpe-Posse, 1971, 1972). Villalta-Comella and Crusafont-Pairó (1941b) also noted that Bataller Calatayud (1938) had further reported *H. grivense* and *S. major*. These species, like *S. palaeochoerus*, were subsequently omitted by Villalta and Crusafont (1946). Then, Crusafont-Pairó and Villalta (1948) reported *H. soemmeringi* from SQ-PN and *H. simorrense* var. *doati*, *L. splendens*, and *Taucanamo pygmaeus* (Depéret, 1892), the latter currently included in *Albanohyus* Ginsburg, 1974 (see Van der Made, 1996b). Finally, Crusafont and Truyols (1954, 1956) reported *H. simorrense* and *L. splendens* from both SQ-PN (as Can Barra) and SQ-TF, as well as *T. pygmaeus* and an indeterminate suid from SQ-TF.

None of the works mentioned in the preceding paragraph except Bataller (1924) described or figured any suid remains to justify their identification. This gap was filled by Golpe-Posse's (1971) unpublished PhD dissertation and derivative publications (Golpe-Posse, 1972, 1974), where she reported *L. splendens* and *H. soemmeringi* from SQ-TF, SQ-PN, and CF2, but not *T. pygmaeus*, despite being cited from SQ-TF in previous works (see also Crusafont-Pairó & Casanovas Cladellas, 1973). Golpe-Posse (1971, 1972) mostly reported material then housed in Sabadell but not that housed in Guérin's collection, which probably had not been donated to the MGSB yet (Crusafont-Pairó, 1975a). Pickford (1981) first reported material of *Pa. crusafonti* from Sant Quirze, while Van der Made (1990) cited from Sant Quirze *L. splendens*, *C. steinheimensis*, *Pa. huenermanni*, and *Korynochoerus palaeochoerus* (Kaup, 1833), and *L. splendens* and *C. steinheimensis* from CF2. Van der Made's (1990) citation of *K. palaeochoerus* is noteworthy, as its presence at Sant Quirze (originally noted by Bataller, 1924) had been discounted by subsequent authors (Golpe-Posse, 1971, 1972; Villalta & Crusafont, 1946). Van der Made (1996a) described in greater detail the material of *L. splendens* from SQ-TF and CF2 housed in the IPS and the MGSB, while Van der Made (1997) repeated his former identifications with only two exceptions: (1) *C. steinheimensis* was transferred to *Parachleuastochoerus*; and (2) *K. palaeochoerus* was no longer reported. More recently, Pickford (2014) described tetraconodontine material housed at the ICP, supposedly coming from SQ-TF, and attributed it to *Pa. valentini* and *Pa. huenermanni*, while Pickford (2016) further reported from Sant Quirze the presence of *L. splendens* but not *Pr. palaeochoerus*.

Our inspection of the old collection numbers of the material of *Pa. huenermanni* reported by Pickford (2014) as from Sant Quirze and their comparison with those reported by Golpe-Posse (1971) unambiguously indicate that these remains come instead from the MN9 site of Can Poncic 1. They were originally attributed by Golpe-Posse (1971, 1972) to *Pa. crusafonti* and are currently attributable to *Pa. huenermanni*, following Van der Made (1990) and Pickford (2014). The mislabeling of these specimens in the ICP collections must have occurred sometime during the early 1970s, given that Pickford (1981) studied the material in 1976. Our inspection of all the available dentognathic suid remains from Sant Quirze from both the ICP and the MGSB, comprising ~300 specimens, indicates that a small suid attributable to *Albanohyus pygmaeus* (Depéret, 1892)—reported from TF-SQ by some authors (Crusafont & Truyols, 1954; Crusafont-Pairó & Villalta, 1948; Villalta-Comella & Crusafont-Pairó, 1941b)—might indeed be present in the samples from SQ-TF and SQ-PN, albeit being represented by very few and poorly diagnostic specimens, just comprising 1% of the sample. The rest of the assemblage is dominated by *L. splendens* (53%) and large tetraconodontine remains (44%), the remaining fossils being only attributable to Suidae indet. As remarked by Pickford (2014), some of the tetraconodontine remains were erroneously attributed to *Pr. palaeochoerus* by some authors (Bataller, 1924; Bataller Calatayud, 1938; Van der Made, 1990; Villalta-Comella & Crusafont-Pairó, 1941b). Its absence from SQ-TF agrees well with the late Aragonian (MN7+8) age of SQ-TF (see below), given that *Pr. palaeochoerus* is currently considered to be restricted to the Vallesian (Alba et al., 2022, 2024; McKenzie et al., 2023a, 2024; Pickford, 2014, 2016).

Age and geological background

Geology and stratigraphy

The Sant Quirze sites are located in the Vallès Sector of the Vallès-Penedès Basin—an elongate half-graben situated in NE Iberian Peninsula, between the Catalan Coastal (Littoral and Prelittoral) Ranges, near Barcelona (Fig. 2). This basin has yielded a rich vertebrate fossil record spanning from the Early to the Late Miocene (Casanovas-Vilar et al., 2016a, 2022). The Sant Quirze

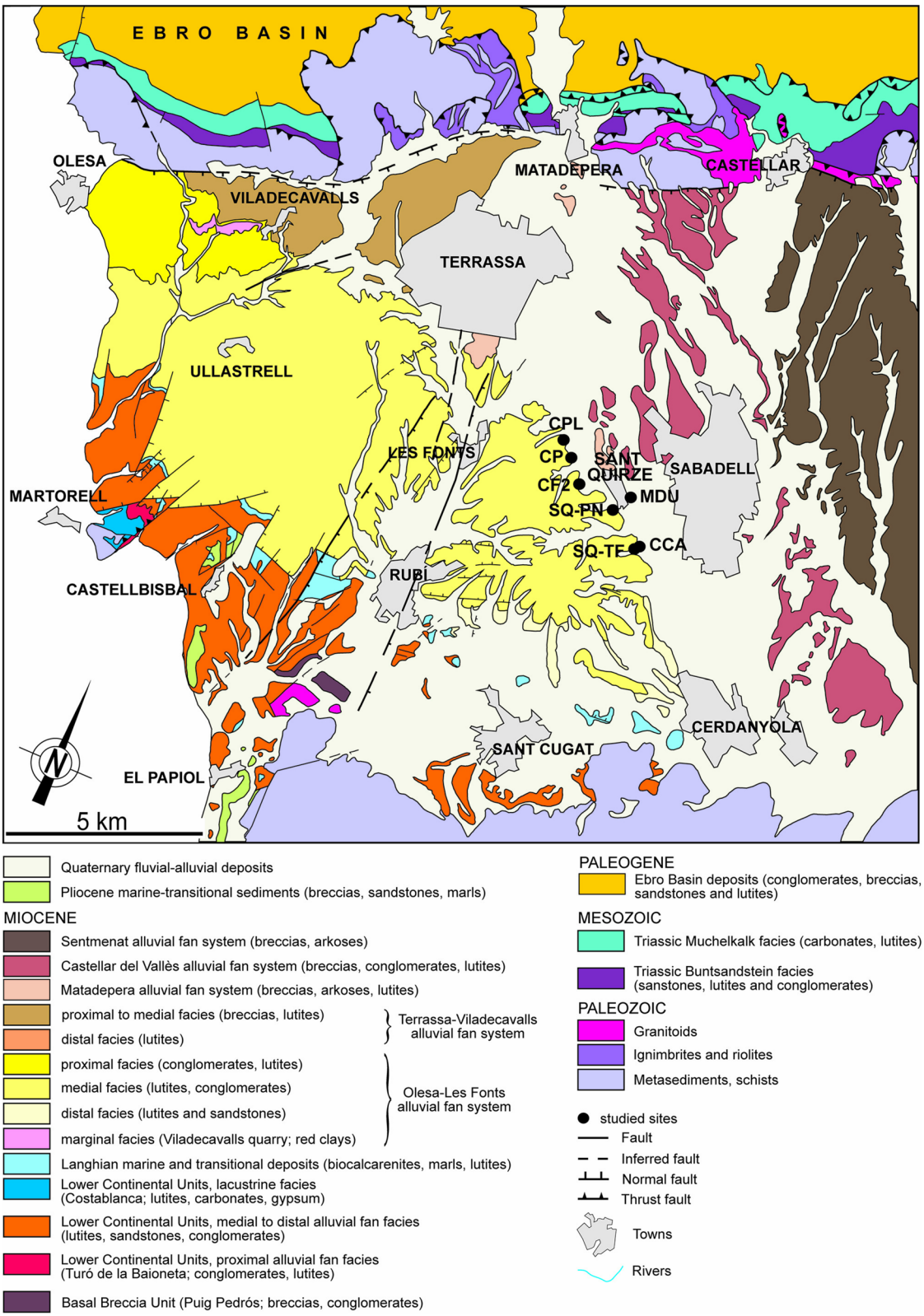

Fig. 2 Schematic geological map of the Vallès-Penedès Basin indicating the location of the Sant Quirze localities from which the described suid material comes from. Abbreviations: CCA, Can Canals; CF2, Can Feliu2; CP, Can Poncic; CPL, Can Pallars i Llobateres; MDU, Mas Duran; SQ-PN, Poble Nou de Sant Quirze; SQ-TF, Trinxera del Ferrocarril-Sant Quirze. Modified from Casanovas-Vilar et al. (2016a: fig. 2)

localities belong to the Upper Continental Units, a continental lithostratigraphic formation that ranges in age from the Middle to the Late Miocene (Agustí et al., 1985; Casanovas-Vilar et al., 2016a, 2022). The deposits of the SQ-TF area, composed of sandstones with interbedded layers of reddish or greyish mudstones and polymictic conglomerates, are interpreted as distal to medial facies of the Olesa-Les Fonts alluvial fan system, ranging in age from the Aragonian to the Vallesian, i.e., Middle to early Late Miocene (Galindo i Torres et al., 2001). This alluvial fan system displays a radius >15 km and is the most extensive of the Vallès-Penedès Basin (Garcés Crespo, 1995). Its source area was located at the Prelittoral Range and its conglomeratic facies are distinguished from those of adjacent alluvial fan systems by being clearly polymictic, including fragments of Paleozoic metamorphic and igneous rocks, as well as Mesozoic and Paleogene carbonates, the latter not only sourced from the Prelittoral Range but also from the Ebro Basin (Garcés Crespo, 1995). In the area surrounding SQ-TF, these conglomerate deposits have great lateral continuity and constitute the base of decametric sequences that progressively fine upward into sandstones with cross-lamination and massive mudstones, which often display carbonaceous nodules and crusts denoting paleosol formation (Galindo i Torres et al., 2001). These decametric sequences denote sedimentary cycles characterized by paleochannel erosion, followed by infill with coarse sediments and, finally, paleochannel abandonment accompanied by the deposition of finer sediments corresponding to a marginal to distal alluvial plain (Garcés Crespo, 1995). The Miocene sediments that formerly cropped out at SQ-PN and CF2 probably corresponded to the same alluvial fan system as SQ-TF, whereas those of MDU would more likely correspond to younger (early Vallesian to early Turolian, i.e., Late Miocene), distal facies of the Matadepera alluvial fan system, which crop out more northeastward (Galindo i Torres et al., 2001; Fig. 2).

Even though Santafé Llopis (1978) described the 150 m-thick stratigraphic sequence outcropping along the railway trench between the train stations of Bellaterra and Sant Quirze (ca. 3.3 km), he did not indicate the exact position of the SQ-TF fossiliferous deposits. In contrast, Bataller (1924) published a geological section of 30 m in length along the railway, indicating the dominance of pinkish and reddish claystones, with some layers of bluish claystones and sandstones, as well as "mollusc beds". In turn, Villalta-Comella and Crusafont-Pairó (1941a, 1943a) reported a more detailed stratigraphic column of the 8 m-thick slope that outcropped at the SQ-TF site. According to Villalta-Comella and Crusafont-Pairó (1943a), the deposits were dominated by very fine and plastic, greenish and greyish "marls" (probably meaning claystones) that yielded the large mammal remains, with some more or less sandy layers interbedded, and some harder and calcareous reddish layers that yielded tortoise remains. In an unpublished report, Llenas i Avellaneda (1996) depicted a similar stratigraphic column naming the various micromammal localities sampled in the mid-1990s but apparently with the wrong scale (a thickness of 16 m instead of the 8 m as originally reported; Villalta-Comella & Crusafont-Pairó, 1941a, 1943a).

Even when corrections are considered, there are some discrepancies in the thickness of the various layers estimated from the published columns; from bottom to top (original thickness reported before that of Llenas i Avellaneda 1996): (1) motley claystones with large mammal remains (60 cm vs. 1.5 m; Sant Quirze A); (2) blackish mudstones with snail shell remains (30 vs. 40 cm; Sant Quirze B); (3) calcareous marls without fossils (70 vs. 30 cm); (4) greenish marls with small mammal remains (70 vs. 50 cm; not sampled in the 1990s); (5) yellow-reddish claystones and sandstones with tortoise remains (3.8 vs. 3.0 m); (6) calcareous marls without fossils (70 vs. 50 cm); (7) greenish marls with small mammal remains (70 cm vs. 1.0 m; Sant Quirze G); and (8) Quaternary (50 vs. 80 cm) on top. Most of the large mammal remains originally collected at SQ-TF can be inferred to come from Sant Quirze A (Villalta-Comella & Crusafont-Pairó, 1941a, 1943a; Llenas i Avellaneda, 1996; contra Casanovas-Vilar et al., 2016b), which is also rich in microvertebrates (Casanovas-Vilar et al., 2016b) and was more intensively sampled than Sant Quirze B and G. This section is short enough so as to assume that age differences are slight: based on the average sedimentation rates for the basin (~20 cm/kyr; Garcés et al., 1996; Alba et al., 2017, 2022), a thickness of 8 m would imply a time lapse of 40 kyr, thus likely representing no more than 0.1 Myr even considering local variations in sedimentation rates.

Age

Bataller (1924) originally correlated SQ-TF to the "Pontian", but soon thereafter rectified and considered it to be "late Vindobonian" in age (Bataller, 1926; Bataller Calatayud, 1938). The same opinion was held by Crusafont and coauthors (Crusafont-Pairó, 1935, 1944, 1951, 1953; Crusafont & Truyols, 1954; Villalta-Comella & Crusafont-Pairó, 1933, 1941a, 1941b, 1943a, 1944a, 1944b, 1944c, 1945), even after he defined the Vallesian land mammal age based on the Vallès-Penedès record, focusing on the dispersal of hipparionins and, to a lesser extent, giraffids (Crusafont-Pairó, 1950, 1951, 1953; Crusafont-Pairó & Truyols-Santonja, 1960). In 1971, Crusafont-Pairó and Golpe-Posse (1974) presented an attempt to refine the biozonation of the late Aragonian and correlated Sant Quirze with zone 19a (La Grive), which preceded a latest

Aragonian zone 19b (Barberà). This biozonation was used by Golpe-Posse (1971, 1972, 1974) but never became mainstream, probably owing to the almost simultaneous establishment of the MN (Mammal Neogene) zonation (Mein, 1975). In parallel, the Aragonian land mammal age was defined (Daams et al., 1977, 1999). Therefore, from the mid-1970s onward, SQ-TF or Sant Quirze more generally were correlated to the late Aragonian MN8 zone (Agustí & Moyà-Solà, 1990; Agustí et al., 1985; Mein, 1975, 1986, 1990), the MN7 zone (Agustí, 1999), or the fused MN7+8 zone (Agustí et al., 1997, 2001; Casanovas-Vilar et al., 2011, 2016a, 2016b; de Bruijn et al., 1992).

In terms of local biozonation of the Vallès-Penedès Basin, Agustí (1981, 1982, 1990) considered SQ-TF the type locality of the *Fahlbuschia crusafonti* Zone, subsequently renamed *Megacricetodon ibericus* Zone (Agustí & Moyà-Solà, 1991; Agustí et al., 1997), *Democricetodon crusafonti*+*Megacricetodon ibericus* Concurrent Range Zone (Casanovas-Vilar et al., 2011), and most recently *Democricetodon crusafonti—Hippotherium* Interval Subzone (Casanovas-Vilar et al., 2016b). The latter has estimated age boundaries between 11.88 and 11.18 Ma (Casanovas-Vilar et al., 2016a, 2016b) and is roughly equivalent to MN8 as originally conceived. The rationale for relying on the first appearance datum of hipparionins at 11.18 Ma (Agustí et al., 1997; Alba et al., 2019, 2022; Casanovas-Vilar et al., 2016b; Garcés Crespo, 1995; Garcés et al., 1996) to define the upper limit of this subzone is that the latest Aragonian and the earliest Vallesian rodent faunas of the Vallès-Penedès Basin have traditionally been considered to be indistinguishable (Agustí, 1990; Agustí et al., 1985, 1997, 2001). Nevertheless, the succession of *Hispanomys* species offers some prospects to distinguish both subzones based on rodents alone, as well as to further refine the biozonation of the latest Aragonian in the Vallès-Penedès Basin (Alba et al., 2022; Casanovas-Vilar et al., 2016a). The presence at SQ-TFA of *Hispanomys lavocati* (Agustí, 1981; Agustí Ballester, 1977a; Casanovas-Vilar et al., 2016a; Freudenthal, 1966) indicates an age not older than 11.6 Ma, when this species is first recorded in the basin (Alba et al., 2022). In turn, the lack of *Hispanomys dispectus* and *Hispanomys daamsi* supports a pre-Vallesian age younger than 11.2 Ma (Alba et al., 2022), in further agreement with the lack of hipparionins and giraffids at the site (e.g., Golpe-Posse, 1974). Therefore, we conclude that the age of SQ-TF ranges between 11.6 and 11.2 Ma, corresponding to the Late Miocene portion of the late Aragonian (MN7+8).

While there is universal agreement about the MN7+8 age of SQ-TF, there have been multiple disagreements about SQ-PN and CF2, owing to their meagerer fauna and the lack of magnetostratigraphic data. The former was originally considered (as Can Barra) to be Vindobonian (Crusafont-Pairó & Villalta, 1948) or Vallesian (Crusafont & Truyols, 1954), and Vindobonian with doubts (Crusafont & Truyols, 1956), Vallesian (Crusafont-Pairó, 1962), or latest Vindobobonian (Crusafont-Pairó & Golpe-Posse, 1973) as SQ-PN, whereas CCA was considered Vindobonian like SQ-TF (Crusafont & Truyols, 1954; Crusafont-Pairó & Villalta, 1948). Following Crusafont-Pairó and Golpe-Posse's (1974) biozonation, both SQ-PN and CF2 were correlated to the latest Vindobonian zone 19b (Barberà) and, hence, considered intermediate in age between SQ-TF and Vallesian sites (Crusafont-Pairó & Golpe, 1972; Crusafont-Pairó & Golpe-Posse, 1973, 1974; Golpe-Posse, 1971, 1972, 1974). Only Ginsburg (1986) considered CF2—and Castell de Barberà (CB)—to be either late Astaracian (i.e., late Aragonian) or else basal Vallesian. Most other authors considered instead that this site is late Aragonian (MN8 or MN7+8; Moyà-Solà et al., 1990; Aldana Carrasco, 1992a; Andrews et al., 1996; Harrison et al., 2002; Alba et al., 2010) until Casanovas-Vilar et al. (2016a) considered it to be Vallesian (MN9).

The latest Aragonian biozone defined by Crusafont-Pairó and Golpe-Posse (1974) was supposedly characterized by the presence of giraffids and the absence of *Hippotherium*. This is the reason why Agustí (1999) and Agustí et al. (2001) correlated SQ-TF to MN7 instead of MN8. However, the other localities correlated with the aforementioned zone 19b (Can Poncic 2, Can Mata 2, and CB) are currently considered to be Vallesian (Alba et al., 2019, 2022; Casanovas-Vilar et al., 2016a, 2016b). Contrary to long held assumptions (Agustí, 1999; Agustí et al., 1985, 1997, 2001; Crusafont-Pairó & Golpe-Posse, 1974), there is no accurately dated evidence of giraffids before hipparionins in the Vallès-Penedès Basin (Alba et al., 2022), and the same applies to the suine *Propotamochoerus*, traditionally considered to have dispersed into Europe during MN7+8 (e.g., Agustí, 1999; Agustí et al., 2001; Alba et al., 2006; Fortelius et al., 1996; Hünerman, 1999; Iannucci et al., 2021; Van der Made, 1990; Van der Made & Moyà-Solà, 1989; Van der Made et al., 1999) but actually not recorded there until earliest MN9 (Alba et al., 2022; McKenzie et al., 2023a, 2024; Pickford, 2014, 2016). As a result, several sites traditionally considered late MN7+8 in age (e.g., Agustí, 1999; Agustí et al., 1985, 2005) are currently correlated to the earliest MN9, based on the presence of hipparionins (Can Missert; Alba et al., 2024; Robles et al., 2011, 2013), magnetostratigraphic data (Can Mata 1; Alba et al., 2022), or both (CB; Alba et al., 2019, 2022). When all this evidence is considered, SQ-PN, based on the presence of giraffids (Golpe-Posse, 1971, 1974), and CF, based on the presence of *H. dispectus* (Agustí, 1981; Agustí Ballester, 1980; Alba et al., 2022), may be correlated to the earliest Vallesian, with an age not older than 11.2 Ma.

Materials and methods

Studied and comparative samples

As noted above, Pickford (2014) only described a portion of the tetraconodontine remains from Sant Quirze. This is partly attributable to the fact that, about a decade ago, part of the collection housed in the ICP was not adequately inventoried yet (and hence likely inaccessible to him). However, the main reason is that he did not study the more abundant collection housed in the MGSB. The described material consists of 134 records, which include 5 tooth series or dentognathic fragments with more than a single tooth plus 129 isolated (complete or partial) teeth or dentognathic fragments with a single tooth from various Sant Quirze localities, amounting to a total of 144 teeth. Most of the material comes from SQ-TF, except for two fossils from SQ-PN and four from CF2. A total of 83 specimens are housed in the MGSB in Barcelona (Catalonia, Spain), while the remaining ones are deposited at the ICP Museum in Sabadell (Catalonia, Spain).

The comparative sample is restricted to '*Pa.*' *valentini* sensu McKenzie et al. (2024) from other sites as well as to other medium to large-sized tetraconodontine species from Europe, namely *C. simorrensis*, *R. matritensis*, and *V. steinheimensis*. Following McKenzie et al. (2024), we included in the hypodigm of '*Pa.*' *valentini* most of the material previously attributed by Pickford (2013a, 2014, 2016) and Pickford and Laurent (2014) to *C. doati*—considered a *nomen dubium* by McKenzie et al. (2024)—except those from the type locality. This material includes the specimens formerly included in *C. ebroensis*, which was synonymized with *C. doati* by Pickford and Laurent (2014; see also Pickford, 2013a, 2014, 2016) or *C. simorrensis* by Van der Made (2020), but is here considered a junior synonym of '*Pa.*' *valentini* following McKenzie et al. (2024). In contrast, the material from Mira originally included in *C. melendezi* and subsequently reassigned to '*Pa.*' *valentini* by Pickford (2014) is here included in *C. simorrensis* following Van der Made (2020) and McKenzie et al. (2023a, 2024). The tetraconodontine sample from Przeworno 1 and 2 is also included in *C. simorrensis* following Kubiak (1981) and Pickford (2016), although other authors (Fortelius et al., 1996; Van der Made, 2020; Van der Made et al., 2014) have attributed it to *V. steinheimensis* (in *Parachleuastochoerus*). Besides the aforementioned controversies regarding the attribution of specific samples, it should be taken into account that the distinction between *C. simorrensis* and *R. matritensis* is controversial, with the latter species being considered a junior synonym of the former by Van der Made (2020). However, pending an in-depth revision of this question we prefer to provisionally keep them separate to better assess their potential morphological differences. Accordingly, attributions of published material to either *C. simorrensis* or *R. matritensis* follow Pickford and Laurent (2014) and Pickford (2016), including some sites (such as Simorre and Villefranche d'Astarac) where the two species have been reported. In the case of Elgg, Pickford and Laurent (2014) attributed the material to *C. simorrensis* (as previously done by other authors; Fortelius et al., 1996; Van der Made et al., 2014), but here we include the whole sample in *R. matritensis* following the more detailed assessment provided by Pickford (2016). The most extensive sample for any of these two species is that from Göriach, formerly attributed to *C. simorrensis* (e.g., Fortelius et al., 1996; Thenius, 1956; Van der Made, 1989) but here included in *R. matritensis* following Pickford and Laurent (2014) and Pickford (2016); this sample serves as a good measure of intraspecific variability to evaluate the differences previously noted between *C. simorrensis* s.s. and *R. matritensis*. It is also noteworthy that *V. steinheimensis* is understood in a broad sense following McKenzie et al. (2024), i.e., including *V. grivensis* as its junior synonym (contra Pickford, 2014, 2016). The tetraconodontine material from Sansan (Pickford, 2012, 2017) is included in the comparative sample but unassigned to species, being provisionally included in '*Sus*' *choerotherium* de Blainville, 1847 *nomen dubium*.

Measurements and iconography of the species included in the comparative sample have been taken from the literature. The measurements employed, for a total of 830 teeth, are reproduced in Additional file 1: Table S1—including species attribution, catalog No., tooth locus, site, and published source—whereas the descriptive statistics derived from them are reported in Additional file 1: Table S2. In turn, published figures of the comparative material that have been consulted are reported in Additional file 1: Table S3—including tooth locus, species attribution, and citations of plates and figures. The literature sources for the comparative sample (measurements and/or iconography) are the following (see Additional file 1: Tables S1 and S3 for sites and details about the figures): '*Pa.*' *valentini* (Alba et al., 2024; Azanza, 1986; McKenzie et al., 2023a, 2024; Pickford, 2013a, 2014, 2016; Roman, 1907; Van der Made, 1989); *V. steinheimensis* (Chen, 1984; Fraas, 1870; Gaillard, 1899; Golpe-Posse, 1972; McKenzie et al., 2023b, 2024; Pickford, 2014, 2016; Stehlin, 1900; Van der Made et al., 2014); *C. simorrensis* (Ginsburg, 1977; Glazek et al., 1971; Golpe-Posse, 1972; Kaup, 1859; Kubiak, 1981; Pickford & Laurent, 2014; Pickford, 2013b, 2014, 2016; Thenius, 1956; Van der Made, 1989, 1998, 2020; Van der Made & Morales, 2003); *R. matritensis* (Hofmann, 1893; Stehlin, 1900; Thenius, 1956; Golpe-Posse, 1971, 1972; Morales & Soria, 1985; Azanza, 1986; Van der Made, 1989, 1998; Pickford,

2014, 2016; Pickford & Laurent, 2014); *C. doati* (*nomen dubium*) (Pickford, 2014; Pickford & Laurent, 2014; Stehlin, 1900; Van der Made, 2020); and '*S.*' *choerotherium* (*nomen dubium*) (Ginsburg, 1977; Pickford, 2012, 2017).

Dental terminology and measurements

Upper and lower teeth are denoted by uppercase and lowercase letters, respectively (see abbreviations below), followed by a number indicating tooth locus and a letter denoting sex for the canines. Standard dental axes are used, except that 'labial' is used for the incisors and canines instead of 'buccal' (restricted to the cheek teeth). Dental terminology follows Van der Made (1996a) with minor modifications (McKenzie et al., 2023a, 2023b, 2024).

Measurements of crown maximum mesiodistal length (MD) and labiolingual/buccolingual breadth (BL) were taken with a digital caliper to the nearest 0.1 mm. BL was measured separately at the mesial and distal (or central, in the third molars) lobes. Crown proportions were measured using a breadth/length index (BLI = maximum BL / MD × 100). Descriptive statistics for the taxa included in the comparative sample include the arithmetic mean, standard deviation (SD), and minimum–maximum (Min–Max) range for each tooth locus; confidence intervals for the mean were not computed because sample sizes are often too small. Dental size and proportions of the permanent cheek teeth and deciduous fourth premolars are further depicted by means of bivariate plots of BL vs. MD. The variation for *V. steinheimensis* and previously reported specimens of '*Pa.*' *valentini* is highlighted using separate convex hulls. The samples of *C. simorrensis*, *R. matritensis* from Göriach, and *R. matritensis* from other localities are depicted using different symbols for illustrative purposes, but united in a single convex hull to facilitate comparisons with the other species. Some *nomina dubia* mentioned in the comparisons are also included.

Cladistic analysis

As our aim was to assess the internal phylogenetic relationships of tetraconodontines, rather than discussing the phylogeny of suoids as a whole, we refrained from replicating previous cladistic analyses based on a wide representation of taxa (Hou & Deng, 2014; Orliac et al., 2010). These include many taxa with a large number of missing data, which introduce too much noise regarding tetraconodontines. However, we relied on the previous character-taxon matrix used by Hou and Deng (2014)—which is an expanded version of Orliac et al.'s (2010) matrix—to perform a more focused analysis including tetraconodontines and a few additional taxa: the suines *Sus* Linnaeus, 1758 and *Hippopotamodon* Lydekker, 1877, the latter previously coded as *Microstonyx* Pilgrim, 1926, which is currently considered a junior subjective synonym of *Hippopotamodon* (Pickford, 2015); a hyotheriine (*Hyotherium* spp., based on the three species previously coded by Hou & Deng, 2014, using variable character states when necessary); and an extant tayassuid (*Tayassu* Fischer, 1814) as outgroup. As a result, only 33 of the 133 characters originally coded were parsimony-informative, the remaining ones being either constant (50) or parsimony-uninformative (differing only in the ingroup). Although these characters were omitted when performing the analyses, so as to compute the various indices, all of the characters (see character numbering and definition in Hou & Deng, 2014: appendix 1) were coded for the tetraconodontines (Additional file 1: Table S4), so that they are available to other authors to perform more comprehensive analyses. Note that, unlike Orliac et al. (2010), Hou and Deng (2014) distinguished only two states for character #53 (#45 of Orliac et al., 2010) but used three character states in the matrix; therefore, we simplified the coding of this character following Hou and Deng's (2014) definition.

To analyze a better representation of European tetraconodontines than previous studies, consider recent developments in their alpha-taxonomy (McKenzie et al., 2024; Pickford, 2014, 2016; Pickford & Laurent, 2014), and take into account the material described in the present work, we coded anew three different species that replaced the '*Conohyus*' of Orliac et al. (2010) and Hou and Deng (2014)—which, as explained above, is a chimera of several genera. Although only dental morphology is discussed in this paper, cranial features for *V. steinheimensis* and '*Pa.*' *valentini* were coded based on data provided in the literature (Chen, 1984; Pickford, 2014). For '*Pa.*' *valentini*, we coded it first from various sites based on recent publications (Pickford, 2014, 2016)—including the portion of the SQ-TF sample described by Pickford (2014), as well as the original material from CCN20 (McKenzie et al., 2023a), CB (McKenzie et al., 2024), and Can Missert (Alba et al., 2024) housed in the ICP. We then compared this coding with the one that can be derived from the specimens described herein, which showed no discrepancies. We were able to code 91 characters based on the literature/material from other sites and 92 from the described sample. Nine characters coded from the literature could not be verified in the described sample (#8, #12–#15, #17–#18, #22, #69) due to missing data, whereas the remains described in this paper enabled the coding of 10 additional characters (#41, #42, #50, #99–#103, #111, #113). This resulted in a total of 101 characters (76% of those included in the matrix) coded for '*Pa.*' *valentini*.

We also coded *V. steinheimensis* based on published literature (Chen, 1984; Gaillard, 1899; Pickford, 2014, 2016; Stehlin, 1900), as well as an examination of the original material from Gratkorn housed in the Universalmuseum Joanneum in Graz, Austria (Van der Made et al., 2014) and from Ca l'Almirall (McKenzie et al., 2023b) and CB (McKenzie et al., 2024) housed in the ICP, resulting in a total of 100 characters coded (75%). In turn, as a preliminary approach to older, similarly-sized tetraconodontines from Europe—and pending a more nuanced approach to the likely synonymy between *R. matritensis* and *C. simorrensis*—we coded the tetraconodontine from Göriach based on the original material housed in the Universalmuseum Joanneum in Graz (see also Thenius, 1956; Van der Made, 1989, 1998), resulting in 88 (66%) coded characters. Finally, pending a revision of *Pa. crusafonti* based on the currently available sample from the type locality (Can Llobateres 1; currently underway by the authors of this paper), the coding for *Pa. crusafonti* was taken directly from Orliac et al.'s (2010) *Parachleuastochoerus*—except for characters #101–#103, which were newly coded based on unpublished observations reported in this paper—resulting in 90 coded characters (68%).

The matrix employed in our cladistic analysis (Additional file 1: Table S5) has 10 taxa and 33 parsimony-informative characters. It was analyzed with PAUP* 4.0a for macOS (Swofford, 2003) by treating characters as unordered and using the branch-and-bound algorithm. Clade support for the newly derived cladogram was assessed using Bremer's indices and bootstrap percentages. Tree length and standard cladistic metrics (CI, RI, RCI) were computed excluding uninformative characters.

Abbreviations

Anatomical abbreviations D/d, Deciduous; C/c, canine; f, female; I/i, incisor; L, left; M/m, molar; P/p, premolar; m, male; R, right

Measurement abbreviations BL, maximum labiolingual or buccolingual breadth; BLd, BL of molars at the distal lobe (or central in the case of third molars); BLI, breadth/length index; BLm, BL of molars at the mesial lobe; Di, maximum distal breadth of the c1m; La, maximum labial breadth of the c1m; Li, maximum lingual breadth of the c1m; Max, maximum; Min, minimum; SD, standard deviation.

Cladistic abbreviations CI, consistency index; RCI, rescaled consistency index; RI, retention index.

Locality abbreviations CB, Castell de Barberà; CF2, Can Feliu 2 (=Can Pagès, Can Sant Feliu); CCN20, Creu de Conill 20; SQ-PN, Poble Nou de Sant Quirze (=Can Barra); SQ-TF, Sant Quirze–Trinxera del Ferrocarril.

Institutional abbreviations ICP, Institut Català de Paleontologia Miquel Crusafont, Sabadell, Barcelona, Spain; IPS, acronym of the ICP collections (following the former informal name of this institution, 'Institut de Paleontologia de Sabadell'); MGSB, Museu Geològic del Seminari de Barcelona, Barcelona, Spain.

Systematic paleontology

Order **Artiodactyla** Owen, 1848
Superfamily **Suoidea** Gray, 1821
Family **Suidae** Gray, 1821
Subfamily **Tetraconodontinae** Lydekker, 1876
Genus ***Parachleuastochoerus*** Golpe-Posse, 1972
'Parachleuastochoerus' valentini (Filhol, 1882)
(Figs. 3, 4, 5, 6, 7, 8, 9, 10, 11)

Referred material See Table 1.

Description

Upper incisors The I1 is represented by two specimens with a moderately worn crown and a partial root (Fig. 3A–B; one already figured by Pickford, 2014: fig. 13A) plus a complete (Fig. 3E) and two incomplete (Fig. 3C–D) germs. The crown is labiolingually compressed, slightly tilted mesially, and somewhat higher than long and pointed when unworn. The lingual side is marked concave, with a thick and obliquely oriented endocrista that runs from the junction of the precrista and lingual cingulum up to the crown apex. The lingual cingulum is moderately developed and obliquely oriented, ending in a cuspule-like swelling where it meets the thick postcrista, which displays minor crenulations when unworn. The precrista is thinner than the postcrista and progressively curves until merging with the lingual cingulum. The cervix displays a moderately developed mesiolingual preanticline and a distolabial endosyncline. The root is only slightly waisted at the cervix and curves distally toward its apex.

Three additional upper incisors are here interpreted as I2s. The best preserved one (Fig. 3F), which includes the almost unworn crown and the entire root, was figured as an i3 of *L. splendens* by Bataller (1924: pl. 5, fig. 9). The other specimens (Fig. 3G–H) only preserve the crown but are similarly worn, showing an entirely comparable morphology. The crown is smaller and proportionally lower-crowned and more labiolingually compressed than that of the I1. It displays a triangular profile in labial/lingual views, with the pointed apex being located toward the mesial half of the crown. The labial crown wall is convex, whereas the lingual is concave except at its swollen central portion. The lingual cingulum is subtle and discontinuous at the level of the lingual swelling, which is V-shaped (apically tapering) but does not constitute a

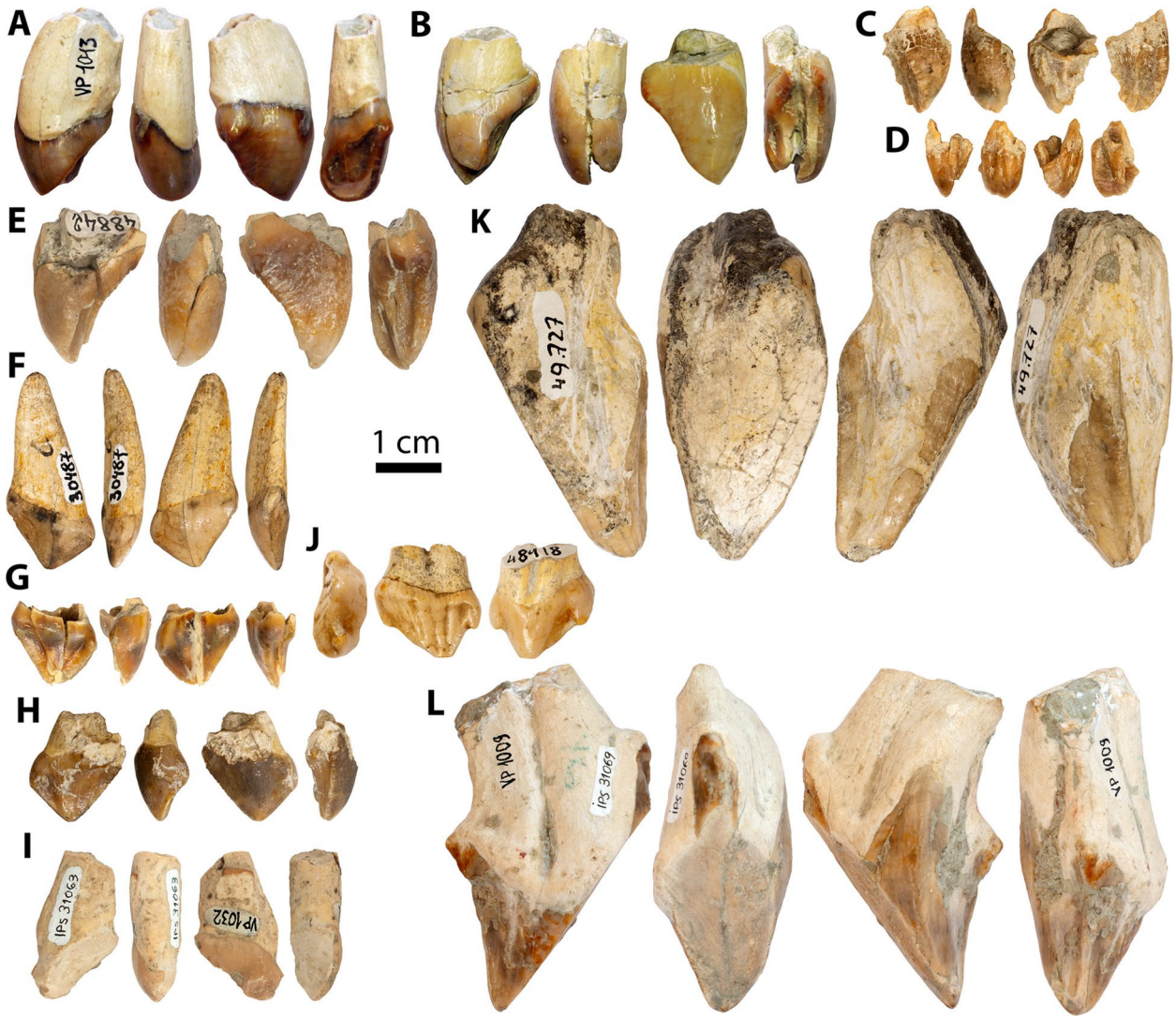

Fig. 3 Permanent upper incisors and canines of '*Parachleuastochoerus' valentini* described in this paper: **A** IPS96058 [VP1013], R I1; **B** IPS30986, R I1; **C** MGSB48853.1, L I1 partial germ; **D** MGSB48853.2, R I1 partial germ; **E** MGSB48842, R I1 germ; **F** MGSB30487, L I2; **G** MGSB48862, damaged L I2; **H** MGSB48559, R I2 crown; **I** IPS96051 [VP1032], R I3; **J** MGSB48918, L C1f; **K** MGSB49727, R C1m; **L** IPS31069 [VP1009], L C1m. All the specimens come from SQ-TF and are depicted, from left to right, in lingual, mesial, labial, and distal views, except for the C1f, which is depicted, from left to right, in occlusal, lingual, and labial views

well-defined endocrista. The crown markedly protrudes from the cervix distally and, especially, mesially. The precrista and postcrista are straight to mildly convex; the former is slightly shorter and steeper than the latter, which appears slightly crenulated (albeit less so than in the I1). The cervix shows no marked anticlines and the root is more labiolingually compressed, lingually curved, and distally tilted than in the I1.

A very worn incisor with partial root (Fig. 3I), only preserving the cervix on the labial side, is tentatively identified as an I3 because the root is more mesially waisted at the cervix and more distally tilted than in the I2. No occlusal details can be ascertained due to the advanced degree of wear.

Upper canines The C1m is represented by two relatively worn specimens (Fig. 3K–L), one of them figured by Pickford (2014: fig. 15A). They are similar to one another when differences in wear are considered, although one of them (Fig. 3K), which shows a more obliquely oriented wear facet (Fig. 3L), appears somewhat stouter. The root is very short compared with the crown, which is largely covered by cementum. The cervix displays marked endoanticline and ectoanticline. The crown is somewhat labiolingually compressed and

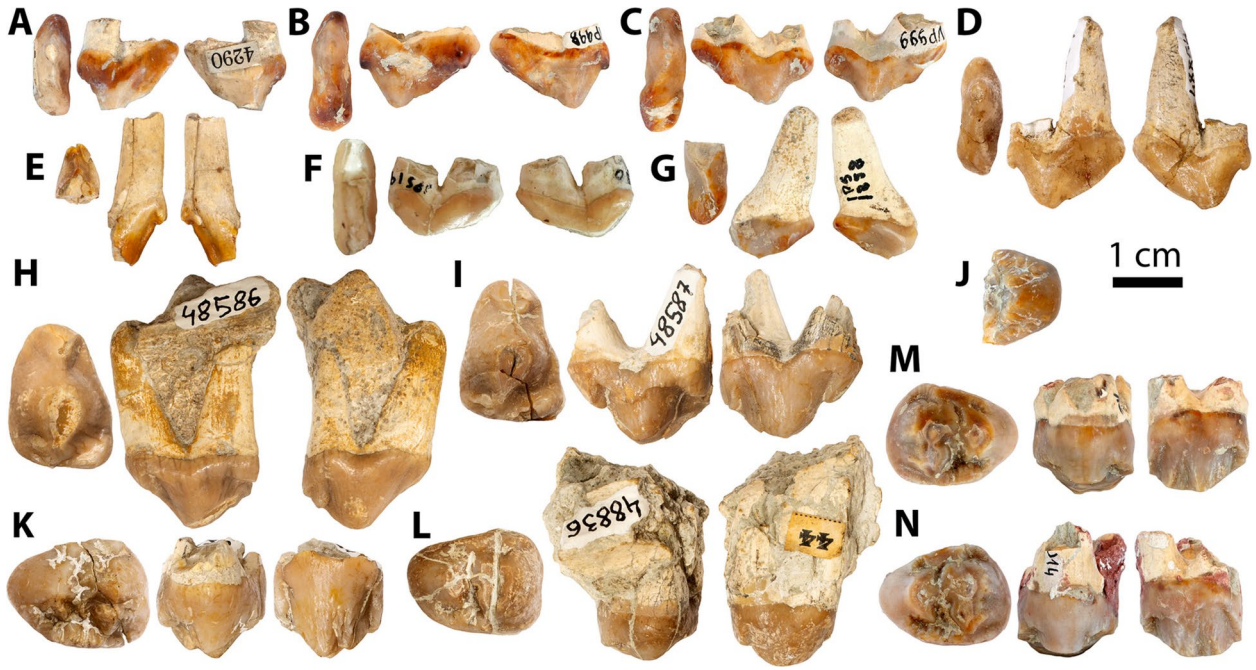

Fig. 4 Permanent upper premolars of '*Parachleuastochoerus*' *valentini* described in this paper: **A** IPS95962 [4290], R P1; **B** IPS96073 [VP998], R P2; **C** IPS96074 [VP999], L P2; **D** MGSB48854, R P2; **E** MGSB48860, L P2 mesial fragment; **F** IPS31028 [IPS1980], R P2 from CF2; **G** IPS96072 [IPS1858], R P2 distal fragment; **H** MGSB48586, R P3; **I** MGSB48587, R P3; **J** IPS138283, R P4 lingual fragment; **K** MGSB48937, L P4; **L** MGSB48836, L P4; **M** IPS96056 [IPS1825], R P4; **N** IPS31065a [VP1014], L P4. All specimens come from SQ-TF unless explicitly indicated; they are depicted, from left to right, in occlusal, lingual, and labial views, except for a partial P4, which is only depicted in occlusal view

slightly curved distolabially. It displays marked basal protrusions both mesially and distally. The mesial protrusion, located at the level of the presyncline, appears to be apically continued by a distinct precrista that is largely eroded by wear. The distal protrusion is more marked and continued by a distinct keel up to the preserved crown apex. In one of the specimens (Fig. 3L), marked labial and lingual apicobasal grooves are present on the cementum surface. The mesial wear facet displays an elliptical to oval shape that more strongly tapers toward the distal side.

A very slightly worn tooth preserving the basal-most portion of the root is here identified as a C1f (Fig. 3J). The crown is labiolingually compressed and reminiscent of that of the mesial upper premolars (see below), except for being labially more bulging and higher crowned. It displays a single main cusp located toward the mesial half of the crown, as well as very distinct mesial and distal styles that considerably protrude from the cervix. The labial crown wall is very convex except for moderately developed clefts that flank the mesial and distal styles. The lingual wall is flat and displays multiple vertical grooves directed toward the crown apex. The lingual cingulum is centrally discontinued and otherwise very subtle except at the level of the prestyle. There are two (mesial and distal) roots fused at least at their base.

Upper premolars A single P1 is available from the sample (Fig. 4A) because, of the four upper premolars from SQ-TF previously identified by Pickford (2014) as such, three are here considered P2s (Pickford, 2014: fig. 14B, G, I; see our Fig. 4B–C, G) and the remaining one (Pickford, 2014: fig. 14A) is considered a DP2 (see later). One of these P2s (Fig. 4G), which is only partially preserved, was formerly identified by Golpe-Posse (1972) as an I2.

The crown of the single available P1 is slightly worn but is missing its apex and it only preserves the basal portion of the mesial root. The crown has an elongate (buccolingually compressed) occlusal contour that becomes markedly convex at the mesial and distal ends, with the latter being lingually twisted. The crown is moderately high-crowned and displays a rather trenchant appearance, with its single main cusp (paracone) being clearly located on the mesial half of the crown. A slightly sinuous and steep paraprecrista descends from the paracone apex toward the very faint prestyle located on the mesial end of the crown. This crest displays minor serrations and shapes a marked concave profile in buccal/lingual views, so that the paracone appears mesially tilted. The parapostcrista emerges in distal direction from the distal aspect of the paracone and is less steep, but thicker, than the paraprecrista. It displays a distinctly protruding portion visible in buccal/lingual views that does not

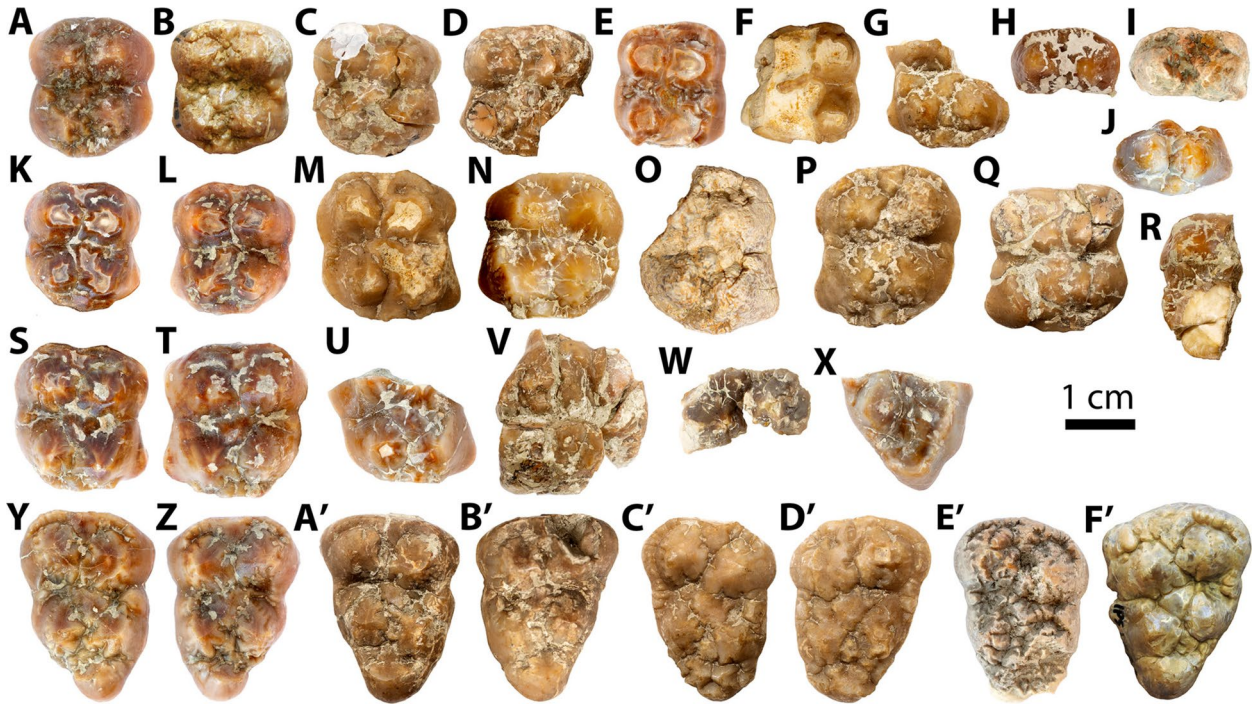

Fig. 5 Permanent upper molars of '*Parachleuastochoerus' valentini* described in this paper: **A** IPS96055 [VP1015], L M1 crown; **B** IPS31026 [IPS1881], L M1 from CF2; **C** MGSB48939, R M1; **D** MGSB48831, partial R M1; **E** IPS96081 [IPS1794], R M1; **F** MGSB48915, damaged L M1; **G** MGSB48824, partial L M1; **H** MGSB49725, R M1 mesial fragment; **I** IPS63283, R M1 mesial fragment; **J** IPS30988, R M1 distal fragment; **K** IPS31061 [VP1007], R M1; **L** IPS31065b [VP1014], L M1; **M** MGSB48914, R M2; **N** MGSB48832, L M2; **O** MGSB48814, R M2 partial germ; **P** MGSB48816, L M2; **Q** MGSB48835, damaged L M2; **R** MGSB49726.2, R M2 buccal fragment; **S** IPS31061 [VP1007], R M2; **T** IPS31065c [VP1014], L M2; **U** IPS31078 [55], R M2 distal fragment; **V** MGSB48833, fragmentary L M2?; **W** MGSB48841, L M2? mesial fragment; **X** IPS38614, R M3 distal fragment from SQ-PN; **Y** IPS31061 [VP1007], R M3; **Z** IPS31065d [VP1014], L M3; **A′** MGSB48829, R M3; **B′** MGSB48830, L M3; **C′** MGSB48815, R M3; **D′** MGSB48813, L M3; **E′** IPS95947 [514], R M3 germ; **F′** IPS31027 [IPS1882], L M3 from CF2. All specimens come from SQ-TF unless explicitly indicated and are depicted in occlusal view

form a distinct (cuspule-like) metacone. Instead, it is continued by a thinner and distolingually oriented portion of the crest that ends close to the distolingual corner of the crown. The crown walls are only moderately convex around the paracone, otherwise being slightly concave. There are no distinct cingula and the crown only slightly protrudes mesially from the cervix, which displays a marked endoanticline (the ectoanticline cannot be adequately assessed). The cervix extends much farther rootward distally than mesially, at least on the lingual side. Two roots, fused at least along their basal-most portion, were apparently present originally, with the basal portion of the mesial root being vertically oriented.

Besides the P2s previously described by Pickford (2014) as P1s (Fig. 4B–C, G), two new P2s (Fig. 4D–E) from SQ-TF and another one from CF2 (Fig. 4F) are described here. Four specimens preserve the complete crown, which is only slightly worn (Fig. 4B–D) except in one of the specimens (Fig. 4F). The distal root is preserved in two P2s (Fig. 4D, G), while the mesial is preserved in a partial specimen (Fig. 4E). The P2s from SQ-TF are larger than but display a similar morphology to the P1 described above, coupled with some differences. Thus, the P2s displays a comparatively lower occlusal relief, a more lingually tilted mesial portion with a more distinct prestyle, and an expanded and/or lingually tilted distalmost portion. There is also some variation in the course of the parapostcrista, although it invariably terminates close to the distobuccal end of the crown. Only in a single specimen (Fig. 4G), the parapostcrista appears to bifurcate at its distal end. The two roots are distinct except at their basal-most portion, the mesial one being verticalized and the distal being apparently slightly stouter and either vertical or slightly tilted distally.

The distal premolars include two P3s (Fig. 4H–I) and five P4s (Fig. 4J–N) from SQ-TF. The former display a moderate degree of wear and, in one of the specimens (Fig. 4H), the roots are completely preserved. The P4s include a lingual crown fragment (Fig. 4J) and four specimens that completely preserve the crown, which is almost unworn in one specimen (Fig. 4K) and moderately worn in the remaining ones. Among the latter, one of the specimens (Fig. 4L) preserves the roots socketed in the maxillary bone; the other two (Fig. 4M–N),

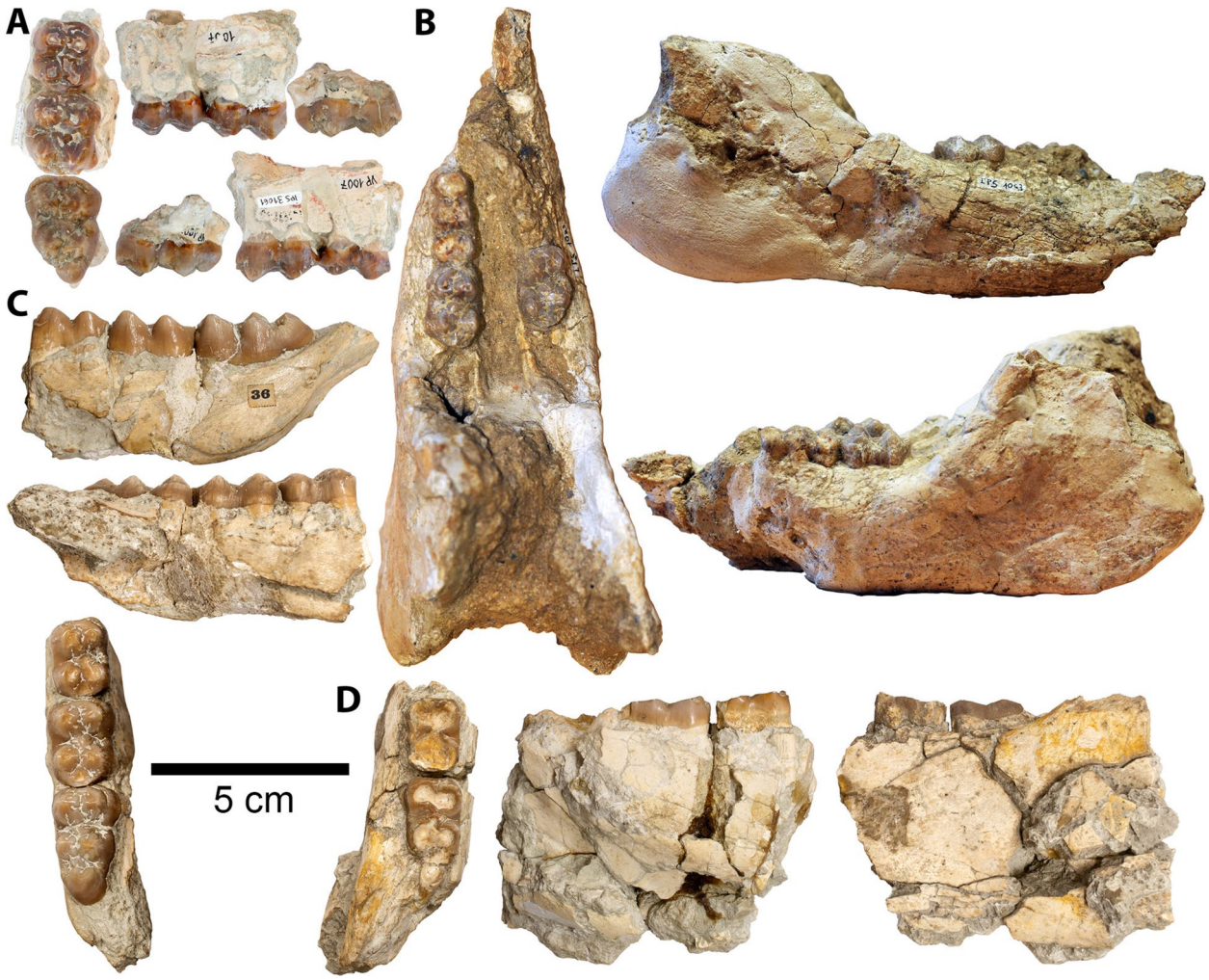

Fig. 6 Dentognathic remains of '*Parachleuastochoerus*' *valentini* described in this paper: **A** IPS31061 [VP1007], R maxillary fragment with M1–M2 with associated M3, in occlusal (left), lingual (top right), and buccal (bottom right) views; **B** IPS27505 [IPS1063], partial juvenile mandible with L dp4–m1 and R m1 from SQ-PN, in occlusal (left), right buccal (top right), and left buccal (bottom right) views; **C** MGSB30480, R mandibular fragment with m1–m3, in lingual (top), buccal (middle), and occlusal (bottom) views; **D** MGSB30490, L mandibular fragment with m2–m3, in occlusal (left), lingual (middle), and buccal (right) views. All specimens come from SQ-TF unless explicitly indicated

which only preserve the basal-most portion of the roots, were reported by Pickford (2014: fig. 12C) and are probably antimeres of the same individual; the left one is also unambiguously associated with an M1–M3 series (see later). The two P3s from SQ-TF display a suboval (Fig. 4H) to subtriangular (Fig. 4I) occlusal contour that is longer than broad and broadest at its distal-most portion, with a markedly convex mesial contour and an almost straight distal one. The paracone is inflated and centrally located. The paraprecrista is steep and progressively becomes concave in buccal/lingual views until merging with a well-developed and slightly mesiolingually tilted prestyle at the mesial end of the crown. The postcrista is short and slightly distobuccally directed, ending in a well-developed poststyle that is higher than the prestyle and located close to the distal end of the crown. Nevertheless, due to wear it is unclear whether a distinct paracone was originally present distally from the paracone. The prestyle is flanked by moderately developed buccal and lingual clefts, whereas a similarly developed cleft separates the buccal base of the paracone from the poststyle. There is no buccal cingulum, whereas a continuous lingual cingulum (albeit narrower at the paracone level) extends from the prestyle until the distolingual corner of the crown, where it becomes ledge-like and bears a poorly developed protocone (basically, a thickening of the lingual cingulum). This premolar is three-rotted, with

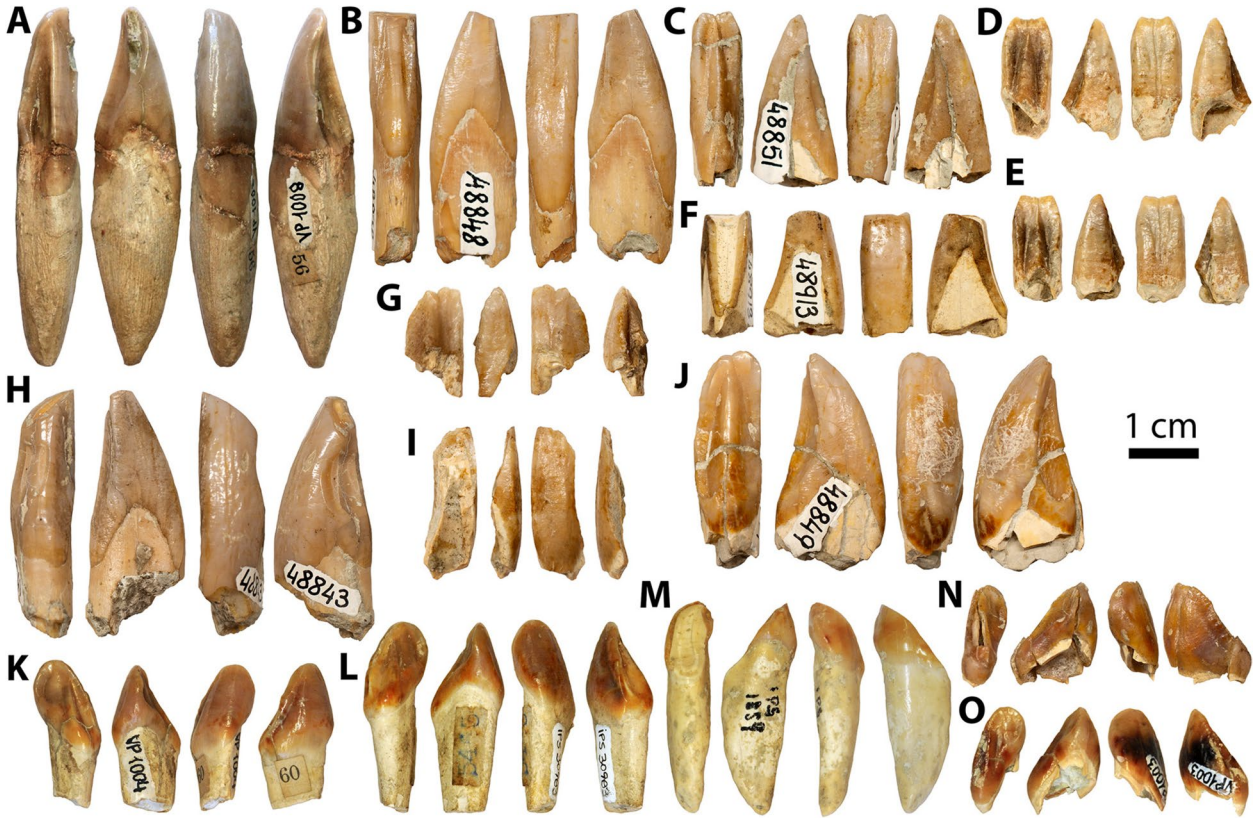

Fig. 7 Permanent lower incisors of '*Parachleuastochoerus*' *valentini* described in this paper: **A** IPS96057 [VP1008, 56], L i1; **B** MGSB48848, R i1; **C** MGSB48851, R i1 crown; **D** MGSB48853.3, L i1 germ; **E** MGSB48853.4, R i1 germ; **F** MGSB48913, L i1; **G** MGSB48850, L i2 germ; **H** MGSB48843, L i2; **I** MGSB48936.1, L i2? partial crown; **J** MGSB48849, L i2; **K** IPS96087 [VP1004, 60], R i3; **L** IPS95966 [5456], L i3; **M** IPS96086 [IPS1859], L i3; **N** MGSB48863, damaged L i3 germ; **O** IPS31060 [VP1003], L i3. All specimens come from SQ-TF and are depicted, from left to right, in lingual, mesial, labial, and distal views

a mesially tilted mesial root and more vertically oriented distal roots that are fused at their base.

The P4s from SQ-TF can be best ascertained based on an almost unworn crown with no dentine exposure (Fig. 4K). Three additional specimens, which preserve the complete and only moderately worn crown (Fig. 4L–N), display a similar occlusal morphology. The crown displays a suboval to subtriangular and lingually tapering occlusal contour that is much broader than long and longer buccally than lingually. The lingual half of the crown appears slightly tilted mesially, owing to a more or less marked angulation of the distolingual crown corner. This angulation appears related to the position of the protocone, which is not located between the paracone and metacone, but more transversely aligned with the former. The protocone, which is the most voluminous cusp, is less peripheral than the buccal cusps. The metacone is subequal in size (lower and smaller) compared with the paracone. Both buccal cusps are closely packed, so that their dentine exposures become confluent at early wear stages. Nevertheless, they are well distinct, with their bases being separated by a transverse groove that runs from the protofossa onto the apical portion of the buccal crown wall. This groove is well distinct but narrow in the least worn specimen (Fig. 4K), more indistinct in another one (Fig. 4L), and broader and cleft-like in the two likely antimeres (Fig. 4M–N). The protofossa is deep and broader distally than mesially, being centrally partly interrupted by the crests radiating from the paracone and protocone apices. The mesial and distal cingula are well developed, display secondary crenulations of the enamel when unworn, and terminate in well-developed styles at the mesiobuccal and distobuccal corners of the crown. None of the specimens displays a lingual cingulum, but the two likely antimeres display a moderately developed but discontinuous buccal cingulum. This premolar is three-rotted, displaying a robust lingual root and two distinct and somewhat diverging lingual roots, which are slenderer and only fused at their basal-most portion.

Upper molars Among the many upper molars included in the sample, only a few are associated: they include an M1–M3 tooth series (Fig. 5L, T, Z)

Fig. 8 Permanent lower canines of '*Parachleuastochoerus*' *valentini* described in this paper: **A** MGSB30471 [24], R c1m; **B** MGSB30471 [23], L c1m; **C** MGSB30471 [22], L c1m; **D** MGSB48852, L c1f. All specimens come from SQ-TF and are depicted, from left to right, in lingual, mesial, labial, and distal views

associated with the P4 (Fig. 4N) of the same individual (of which only the M2 and M3 were figured by Pickford, 2014: fig. 14F, H) and a maxillary fragment with M1–M2 and associated M3 (Figs. 5K, S, Y, 6A) that was also figured by Pickford (2014: fig. 15B–C). Despite having different catalog numbers, these specimens likely belong to a single individual based on similarities in size, shape, and wear stage. The remaining are isolated, either complete or partial, consisting of multiple M1s (Fig. 5A–J), M2s (Fig. 5M–R, U–W), and M3s (Fig. 5X, A'–F'), of which only two M1s were previously figured by Pickford (2014: figs. 14E, 16B). This sample of upper molars mostly comes from SQ-TF, except for an M1 (Fig. 5B) and an M3 (Fig. 5F') from CF2, as well as another M3 (Fig. 5X) from SQ-PN. All the molar positions include some lightly worn crowns or unworn

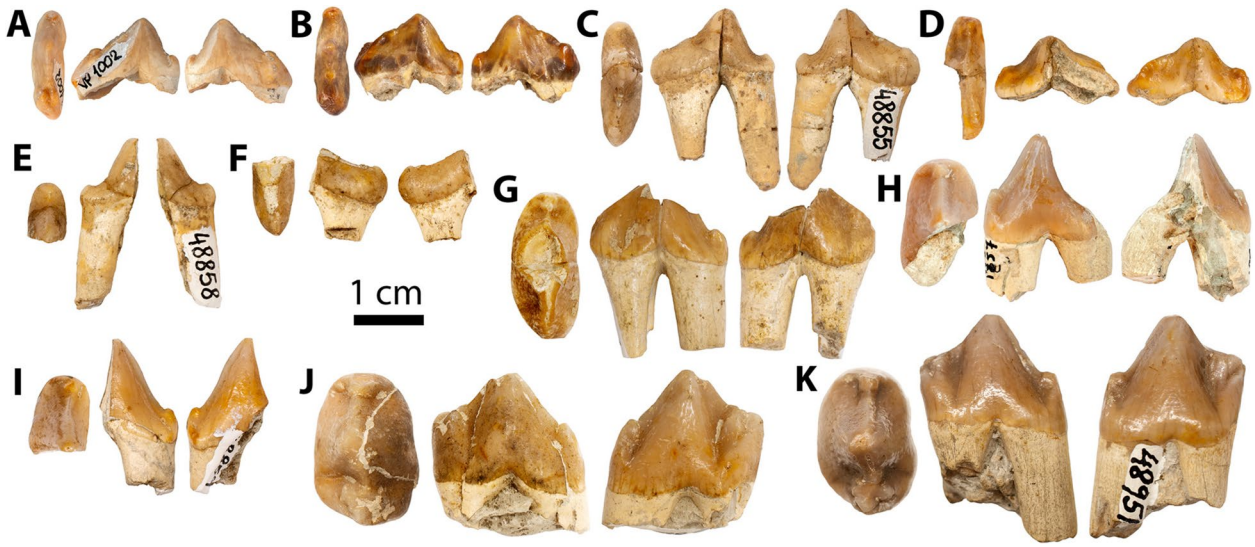

Fig. 9 Permanent lower premolars of '*Parachleuastochoerus' valentini* described in this paper: **A** IPS96063 [VP1002], L p1; **B** MGSB48856, L p1; **C** MGSB48855, L p2; **D** MGSB48857, partial R p2 crown; **E** MGSB48858, R p2 mesial fragment; **F** MGSB48861, R p2 distal fragment; **G** MGSB48817, damaged L p3; **H** IPS96062 [IPS1857], partial R p3; **I** MGSB48859, L p3 mesial fragment; **J** MGSB48588, L p4; **K** MGSB48951, L p4. All specimens come from SQ-TF and are depicted, from left to right, in occlusal, lingual, and labial views

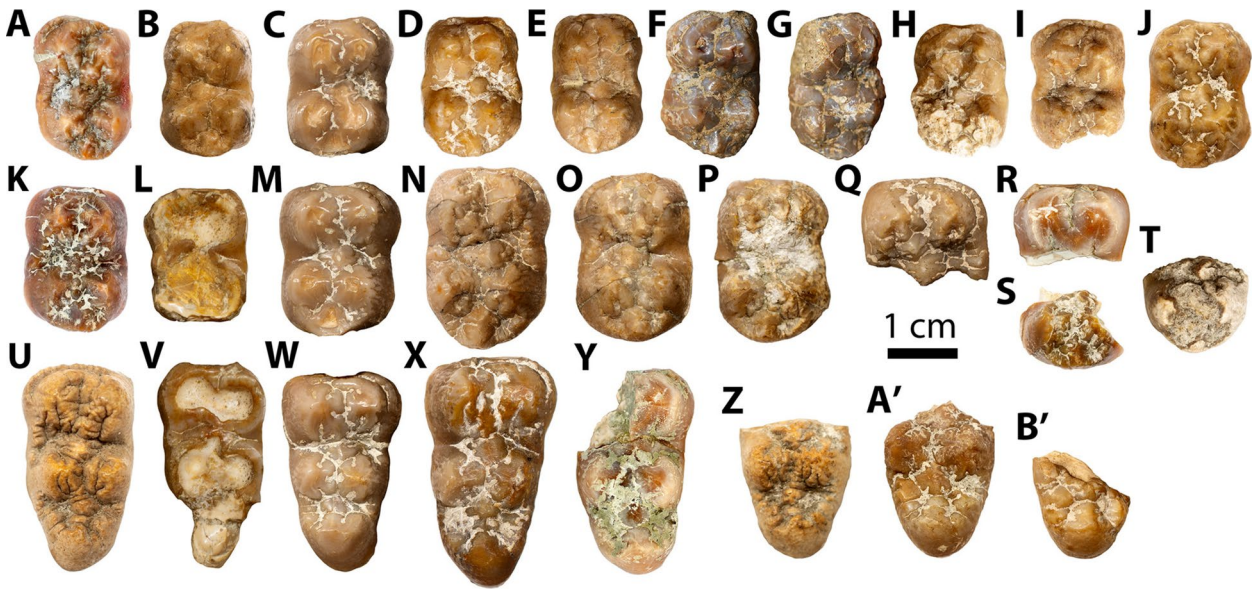

Fig. 10 Permanent lower molars of '*Parachleuastochoerus' valentini* described in this paper: **A** IPS96060 [VP996], L m1 germ; **B** MGSB30489, L m1; **C** MGSB30480, R m1; **D** MGSB48821, R m1; **E** MGSB30475, R m1; **F** IPS27505 [IPS1063], L m1 from SQ-PN; **G** IPS27505 [IPS1063], R m1 from SQ-PN; **H** MGSB48919, L m1 (damaged); **I** MGSB48822, L m1 partial germ; **J** MGSB48873, R m2 germ; **K** IPS96061 [VP997], L m2 germ; **L** MGSB30490, L m2; **M** MGSB30480, R m2; **N** MGSB48818, R m2; **O** MGSB48820, L m2; **P** MGSB48819, R m2; **Q** MGSB48823, R m2 mesial fragment; **R** IPS119090 from SQ-TFC, L m2 mesial fragment; **S** MGSB48840, R m2 distal fragment; **T** MGSB48827, R m2 distal fragment; **U** MGSB30488, L m3 germ; **V** MGSB30490, L m3; **W** MGSB30480, R m3; **X** MGSB48949, R m3; **Y** IPS119091, partial R m3 from SQ-TFC; **Z** MGSB48828, R m3 distal fragment; **A'** MGSB48825, L m3 distal fragment; **B'** MGSB48826, R m3 distal fragment. All specimens come from SQ-TF unless explicitly indicated and are depicted in occlusal view

germs enabling an adequate description of their occlusal morphology. One of the M1s (Fig. 5A) was formerly identified by Golpe-Posse (1971) as an M2.

The M1s and M2s (Fig. 5A–W) show similar proportions and occlusal shape, being characterized by a subrectangular occlusal contour (slightly longer than broad),

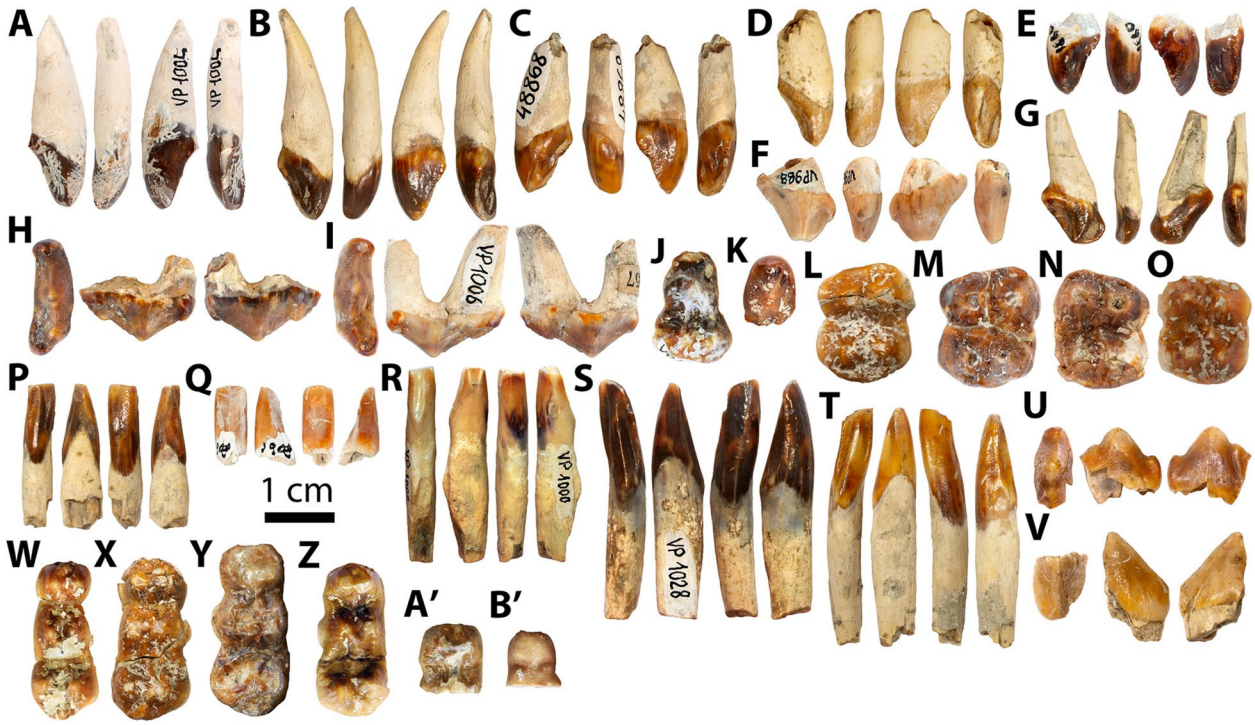

Fig. 11 Deciduous teeth of '*Parachleuastochoerus*' *valentini* described in this paper: **A** IPS94956 [VP1005], L DI1; **B** MGSB48865, L DI1; **C** MGSB48868, R DI1; **D** MGSB48869, L DI1; **E** IPS94954 [IPS1860], R DI1; **F** IPS95997 [VP988], L DI2; **G** MGSB48866, L DI3; **H** IPS95945 [5462], L DP2; **I** IPS96083 [VP1006], R DP2; **J** IPS96070 [VP1011], R DP3; **K** IPS96077, R DP3 mesial fragment; **L** MGSB48839, L DP4; **M** IPS31080 [VP1010], L DP4; **N** IPS95961 [4292], R DP4; **O** IPS96069 [VP1001], R DP4 crown; **P** MGSB48864.1, L di1; **Q** IPS31024 [IPS1908], R di1 from CF2; **R** IPS96085 [VP1000], L di1; **S** IPS96084 [VP1028], R di2; **T** MGSB48864.2, L di2; **U** MGSB48936.2, L dp2 partial germ; **V** MGSB48936.3, R dp3 distal fragment; **W** IPS96075, R dp4; **X** MGSB48838, R dp4; **Y** IPS27505 [IPS1063], L dp4 from SQ-PN; **Z** IPS31073 [VP1012], L dp4; **A'** IPS95965, L dp4 mesial fragment; **B'** IPS96076, R dp4 mesial fragment. All specimens come from SQ-TF unless explicitly indicated. Incisors are depicted, from left to right, in lingual, mesial, labial, and distal views, whereas premolars are depicted, from left to right, in occlusal, lingual, and distal views, except for DP3s, DP4s, and dp4s, which are depicted only in occlusal view

with two biconvex and distinct lobes, a straighter mesial contour, and a slightly protruding distal one. The distal lobe is generally slightly narrower and more asymmetric than the mesial (due to a greater distolingual than distobuccal expansion of the crown base). The four main cusps are pyramidal in shape and display marked crests and Fürchen, with a moderate development of enamel crenulations when unworn. The lingual cusps are slightly more distally located than the mesial. The mesial cingulum is well developed and displays a distinct protopreconule at about its median portion, but is continued neither buccally nor lingually. The transverse valley separating the two lobes is partly interrupted by a centrally located hypopreconule that is more developed than the protopreconule. The buccal metaectoconule is variably developed (generally small, but sometimes double, completely enclosing the transverse valley), whereas the lingual hypoectoconule is small and slightly more distally located at the end of the hypoectocrista. The metaectoconule is sometimes continued distally by a variably developed distolingual cingulum that may merge with the distal one. The latter is at least as well developed as the mesial but more protruding and buccolingually more restricted, displaying some development of secondary enamel cuspules.

The M3s (Fig. 5X–F') are generally lightly to moderately worn, with very restricted dentine exposure (if at all) and conspicuous evidence of Fürchen and some crenulations of the enamel (most evident in the unworn crown germ; Fig. 5E'). Besides the aforementioned likely antimeres (Fig. 5Y–Z), based on occlusal similarities four additional specimens might constitute two additional antimere pairs (Fig. 5A'–B' and Fig. 5C'–D') and be associated with some of the preceding molars, although this cannot be conclusively determined. The M3 is similarly broad to the M2 on the mesial lobe, but much longer, displaying a more elongate and distally tapering, subtriangular, and asymmetric occlusal contour (longer lingually than buccally). The central lobe is narrower than the mesial and separated from it by moderately to marked buccal and lingual constrictions of the occlusal contour. The pentacone-bearing distal lobe is much smaller but generally well distinct from the central, being mostly located on

Table 1 Dentognatic remains and isolated teeth of '*Parachleuastochoerus*' *valentini* described in this paper

Catalog No	Site	Description	Figure	References
IPS96058 [VP1013]	SQ-TF	R I1	Fig. 3A	GP1971[a], PI2014[b]
IPS30986	SQ-TF	R I1	Fig. 3B	–
MGSB48853.1	SQ-TF	L I1 partial germ	Fig. 3C	–
MGSB48853.2	SQ-TF	R I1 partial germ	Fig. 3D	–
MGSB48842	SQ-TF	R I1 germ	Fig. 3E	–
MGSB30487	SQ-TF	L I2	Fig. 3F	BA1924[c]
MGSB48862	SQ-TF	L I2 (damaged)	Fig. 3G	–
MGSB48559	SQ-TF	R I2 crown	Fig. 3H	–
IPS96051 [VP1032]	SQ-TF	R I3	Fig. 3I	GP1971[d]
MGSB48918	SQ-TF	L C1f	Fig. 3J	–
MGSB49727	SQ-TF	R C1m	Fig. 3K	–
IPS31069 [VP1009]	SQ-TF	L C1m	Fig. 3L	GP1971[a], PI2014[b]
IPS95962 [4290]	SQ-TF	R P1	Fig. 4A	–
IPS96073 [VP998]	SQ-TF	R P2	Fig. 4B	GP1971[a], PI2014[b]
IPS96074 [VP999]	SQ-TF	L P2	Fig. 4C	GP1971[a], PI2014[b]
MGSB48854	SQ-TF	R P2	Fig. 4D	–
MGSB48860	SQ-TF	L P2 mesial fragment	Fig. 4E	–
IPS31028 [IPS1980]	CF2	R P2	Fig. 4F	–
IPS96072 [IPS1858]	SQ-TF	R P2 distal fragment	Fig. 4G	GP1971[a], PI2014[b]
MGSB48586	SQ-TF	R P3	Fig. 4H	–
MGSB48587	SQ-TF	R P3	Fig. 4I	–
IPS138283	SQ-TF	R P4 lingual fragment	Fig. 4J	–
MGSB48937	SQ-TF	L P4	Fig. 4K	–
MGSB48836	SQ-TF	L P4	Fig. 4L	–
IPS96056 [IPS1825]	SQ-TF	R P4	Fig. 4M	GP1971[a], PI2014[b]
IPS31065a–d [VP1014]	SQ-TF	L P4 (a) + M1 (b) + M2 (c) + M3 (d)	Figs. 4N, 5L, T, Z	GP1971[a], PI2014[b]
IPS96055 [VP1015]	SQ-TF	L M1 crown	Fig. 5A	GP1971[a], PI2014[b]
IPS31026 [IPS1881]	CF2	L M1	Fig. 5B	GP1971[a]
MGSB48939	SQ-TF	R M1	Fig. 5C	–
MGSB48831	SQ-TF	R M1 (partial)	Fig. 5D	–
IPS96081 [IPS1794]	SQ-TF	R M1	Fig. 5E	PI2014[b]
MGSB48915	SQ-TF	L M1 (damaged)	Fig. 5F	–
MGSB48824	SQ-TF	L M1 (partial)	Fig. 5G	–
MGSB49725	SQ-TF	R M1 mesial fragment	Fig. 5H	–
IPS63283	SQ-TF	R M1 mesial fragment	Fig. 5I	–
IPS30988	SQ-TF	R M1 distal fragment	Fig. 5J	–
IPS31061 [VP1007]	SQ-TF	R maxillary fragment with M1–M2 (a) + M3 (b)	Figs. 5K, S, Y, 6A	GP1971[a], PI2014[b]
MGSB48914	SQ-TF	R M2	Fig. 5M	–
MGSB48832	SQ-TF	L M2	Fig. 5N	–
MGSB48814	SQ-TF	R M2 partial germ	Fig. 5O	–
MGSB48816	SQ-TF	L M2	Fig. 5P	–
MGSB48835	SQ-TF	L maxillary fragment with M2 (damaged)	Fig. 5Q	–
MGSB49726.2	SQ-TF	R M2 buccal fragment	Fig. 5R	–
IPS31078 [55]	SQ-TF	R M2 distal fragment	Fig. 5U	–
MGSB48833	SQ-TF	L M2? (fragmentary)	Fig. 5V	–
MGSB48841	SQ-TF	L M2? mesial fragment	Fig. 5W	–
IPS38614	SQ-PN	R M3 distal fragment	Fig. 5X	–
MGSB48829	SQ-TF	R maxillary fragment with M3	Fig. 5A′	–
MGSB48830	SQ-TF	L maxillary fragment with M3	Fig. 5B′	–

Table 1 (continued)

Catalog No	Site	Description	Figure	References
MGSB48815	SQ-TF	R M3	Fig. 5C′	–
MGSB48813	SQ-TF	L M3	Fig. 5D′	–
IPS95947 [514]	SQ-TF	R M3 germ	Fig. 5E′	–
IPS31027 [IPS1882]	CF2	L M3	Fig. 5F′	GP1971[a,e]
IPS27505 [IPS1063]	SQ-PN	Partial juvenile mandible with L dp4–m1 and R m1	Figs. 6B, 10F–G, 11Y	GP1971[a]
MGSB30480	SQ-TF	R mandibular fragment with m1–m3	Figs. 6C, 10C, M, W	–
MGSB30490	SQ-TF	L mandibular fragment with m2–m3	Figs. 6D, 10L, V	–
IPS96057 [VP1008, 56]	SQ-TF	L i1	Fig. 7A	GP1971[a], PI2014[b]
MGSB48848	SQ-TF	R i1	Fig. 7B	–
MGSB48851	SQ-TF	R i1 crown	Fig. 7C	–
MGSB48853.3	SQ-TF	L i1 germ	Fig. 7D	–
MGSB48853.4	SQ-TF	R i1 germ	Fig. 7E	–
MGSB48913	SQ-TF	L i1	Fig. 7F	–
MGSB48850	SQ-TF	L i2 germ	Fig. 7G	–
MGSB48843	SQ-TF	L i2	Fig. 7H	–
MGSB48936.1	SQ-TF	L i2? partial crown	Fig. 7I	–
MGSB48849	SQ-TF	L i2	Fig. 7J	–
IPS96087 [VP1004, 60]	SQ-TF	R i3	Fig. 7K	GP1971[a], PI2014[b]
IPS95966 [5456]	SQ-TF	L i3	Fig. 7L	–
IPS96086 [IPS1859]	SQ-TF	L i3	Fig. 7M	GP1971[a]
MGSB48863	SQ-TF	L i3 germ (damaged)	Fig. 7N	–
IPS31060 [VP1003]	SQ-TF	L i3	Fig. 7O	GP1971[a], PI2014[b]
MGSB30471 [24]	SQ-TF	R c1m	Fig. 8A	–[c]
MGSB30471 [23]	SQ-TF	L c1m	Fig. 8B	–[c]
MGSB30471 [22]	SQ-TF	L c1m	Fig. 8C	–[c]
MGSB48852	SQ-TF	L c1f	Fig. 8D	–
IPS96063 [VP1002]	SQ-TF	L p1	Fig. 9A	GP1971[a], PI2014[b]
MGSB48856	SQ-TF	L p1	Fig. 9B	–
MGSB48855	SQ-TF	L p2	Fig. 9C	–
MGSB48857	SQ-TF	R p2 partial crown	Fig. 9D	–
MGSB48858	SQ-TF	R p2 mesial fragment	Fig. 9E	–[f]
MGSB48861	SQ-TF	R p2 distal fragment	Fig. 9F	–[f]
MGSB48817	SQ-TF	L p3 (damaged)	Fig. 9G	–
IPS96062 [IPS1857]	SQ-TF	R p3 (partial)	Fig. 9H	GP1971[a], PI2014[b]
MGSB48859	SQ-TF	L p3 mesial fragment	Fig. 9I	–
MGSB48588	SQ-TF	L p4	Fig. 9J	–
MGSB48951	SQ-TF	L p4	Fig. 9K	–
IPS96060 [VP996]	SQ-TF	L m1 germ	Fig. 10A	GP1971[a], PI2014[b]
MGSB30489	SQ-TF	L m1	Fig. 10B	BA1924[g]
MGSB48821	SQ-TF	R m1	Fig. 10D	–
MGSB30475	SQ-TF	R mandibular fragment with m1	Fig. 10E	BA1924[g]
MGSB48919	SQ-TF	L mandibular fragment with m1 (damaged)	Fig. 10H	–
MGSB48822	SQ-TF	L m1 partial germ	Fig. 10I	BA1924[g]
MGSB48873	SQ-TF	R m2 germ	Fig. 10J	BA1924[g]
IPS96061 [VP997]	SQ-TF	L m2 germ	Fig. 10K	GP1971[a], PI2014[b]
MGSB48818	SQ-TF	R m2	Fig. 10N	–
MGSB48820	SQ-TF	L m2	Fig. 10O	–
MGSB48819	SQ-TF	R m2	Fig. 10P	BA1924[g]
MGSB48823	SQ-TF	R m2 mesial fragment	Fig. 10Q	–

Table 1 (continued)

Catalog No	Site	Description	Figure	References
IPS119090	SQ-TFC	L m2 mesial fragment	Fig. 10R	–
MGSB48840	SQ-TF	R m2 distal fragment	Fig. 10S	–
MGSB48827	SQ-TF	R m2 distal fragment	Fig. 10T	–
MGSB30488	SQ-TF	L m3 germ	Fig. 10U	BA1924[g]
MGSB48949	SQ-TF	R mandibular fragment with m3	Fig. 10X	–
IPS119091	SQ-TFC	R m3 (partial)	Fig. 10Y	–
MGSB48828	SQ-TF	R m3 distal fragment	Fig. 10Z	BA1924[g]
MGSB48825	SQ-TF	L m3 distal fragment	Fig. 10A′	–
MGSB48826	SQ-TF	R m3 distal fragment	Fig. 10B′	–
IPS94956 [VP1005]	SQ-TF	L DI1	Fig. 11A	GP1971[a]
MGSB48865	SQ-TF	L DI1	Fig. 11B	–
MGSB48868	SQ-TF	R DI1	Fig. 11C	–
MGSB48869	SQ-TF	L DI1	Fig. 11D	–
IPS94954 [IPS1860]	SQ-TF	R DI1	Fig. 11E	GP1971[a]
IPS95997 [VP988]	SQ-TF	L DI2	Fig. 11F	–
MGSB48866	SQ-TF	L DI3	Fig. 11G	–
IPS95945 [5462]	SQ-TF	L DP2	Fig. 11H	–
IPS96083 [VP1006]	SQ-TF	R DP2	Fig. 11I	GP1971[a], PI2014[b]
IPS96070 [VP1011]	SQ-TF	R DP3	Fig. 11J	GP1971[a], PI2014[b]
IPS96077	SQ-TF	R DP3 mesial fragment	Fig. 11K	–
MGSB48839	SQ-TF	L DP4	Fig. 11L	–
IPS31080 [VP1010]	SQ-TF	L DP4	Fig. 11M	GP1971[a], PI2014[b]
IPS95961 [4292]	SQ-TF	R DP4	Fig. 11N	–
IPS96069 [VP1001]	SQ-TF	R DP4 crown	Fig. 11O	GP1971[a], PI2014[b]
MGSB48864.1	SQ-TF	L di1	Fig. 11P	–
IPS31024 [IPS1908]	CF2	R di1	Fig. 11Q	GP1971[a]
IPS96085 [VP1000]	SQ-TF	L di1	Fig. 11R	GP1971[a]
IPS96084 [VP1028]	SQ-TF	R di2	Fig. 11S	GP1971[a]
MGSB48864.2	SQ-TF	L di2	Fig. 11T	–
MGSB48936.2	SQ-TF	L dp2 partial germ	Fig. 11U	–
MGSB48936.3	SQ-TF	R dp3 distal fragment	Fig. 11V	–
IPS96075	SQ-TF	R dp4	Fig. 11W	PI2014[b]
MGSB48838	SQ-TF	R dp4	Fig. 11X	–
IPS31073 [VP1012]	SQ-TF	L dp4	Fig. 11Z	GP1971[a], PI2014[b]
IPS95965	SQ-TF	L dp4 mesial fragment	Fig. 11A′	–
IPS96076	SQ-TF	R dp4 mesial fragment	Fig. 11B′	–

Old collection numbers are provided within brackets. Abbreviations: BA1924, Bataller (1924); GP71, Golpe-Posse (1971); PI2014, Pickford (2014)

[a] Attributed by Golpe-Posse (1971) to *H. soemmeringi*

[b] Attributed by Pickford (2014) to *Pa. valentini*

[c] Attributed by Bataller (1924) to *L. splendens*

[d] Attributed by Golpe-Posse (1971) to *L. splendens*

[e] Collected in the 1970 according to museum records

[f] These two specimens belong to the same tooth, which was attributed to Carnivora indet. by Bataller (1924)

[g] Attributed by Bataller (1924) to *S. palaeochoerus*

the lingual half of the crown and either distally directed or somewhat buccally tilted. The two mesial cusps are slightly larger and more inflated than the hypocone and the metacone, while the lingual cusps are more distally located than their corresponding buccal counterparts (more clearly so than in the M1 and M2). The mesial cingulum and the centrally located protopreconule are even better developed than in the preceding molars. Only in a

couple of M3s, the mesial cingulum continues along the buccal crown wall forming a buccal cingulum (which is somewhat or totally interrupted at the level of the metacone), whereas there is no distinct lingual cingulum. All the M3s display a distinct hypoectoconule, generally more developed than that of the M2s and that the M3 metaectonocule, which consists of one or more cuspule-like enamel thickenings (integrated in the buccal cingulum when present). The pentacone is located toward the distal end of the crown and generally well developed (albeit smaller than the other main cusps), whereas the pentapreconule is more indistinct and smaller than the other preconules. Only in some specimens the pentacone is smaller and more indistinct (Fig. 5E'), even being preceded by two secondary cusps that might be interpreted as the pentaectoconule and an incipient hexaconule (Fig. 5C'–D').

Lower incisors The lower incisors are represented in the sample by multiple i1s (Fig. 7A–F), i2s (Fig. 7G–J), and i3s (Fig. 7K–O) from SQ-TF, of which only an i1 (Fig. 7A) had previously been figured by Pickford (2014: fig. 13B). The latter specimen was interpreted by Golpe-Posse (1971) as an I1 (which is probably a typo) and by Pickford (2014) as an i2. The latter interpretation was probably influenced by the mesially tilted distal margin; however, as noted by Pickford (2014), the distal margin is worn, while a missing crown portion on the mesial side, close to the apex, further contributes to give this tooth a weird appearance. Based on the vertical endocristid and the apicobasal alignment between the crown and the root, we concur with McKenzie et al. (2023a, 2024) that this incisor is better interpreted as an i1.

Some of the remaining i1s included in the sample more adequately enable the description of the unworn crown shape of this incisor (Fig. 7C–E), which is characterized by a symmetrical incisal edge with subtle serrations and two (mesial and distal) distinct mamelons (preconulid and postconulid, respectively, with no protoconid in between). The crown is tall relative to its basal dimensions, which are broader than long but progressively become labiolingually compressed toward the apex. The labial wall is uniformly convex, whereas the lingual side is concave and displays a well-developed endocristid. The prestylid and poststylid are thick and similarly well developed, whereas the endocristid is very vertically aligned (only minimally mesially tilted), very thick, and lingually protruding, markedly tapering along its apical-most portion until fading away at or close to the unworn incisal edge. The prefossid and endofossid are thus well separated by the endocristid, with the former becoming indistinct slightly farther away from the cervix than the endofossid. The endocristid originates from a moderately developed swelling of the lingual crown base, located above the marked endosynclinid. The preanticlinid and postanticlinid are deep and similarly developed to one another, variously pointed depending on the specimen. However, in all cases they are markedly asymmetric because the ectosynclinid extends much farther rootward than the endosynclinid. The crown base is not markedly waisted at the cervix and the root is vertically aligned with the crown and mesiodistally compressed, although slenderer in the newly reported specimen that partially preserves the crown (Fig. 7B) than in the previously published specimen (Fig. 7A).

The i2s available in the sample are less completely preserved than the i1s (only the basal-most portion of the root is preserved in some specimens; Fig. 7H, J) but appear quite similar in size and proportions, merely being somewhat larger and slightly more mesiodistally compressed at the base, but similarly high-crowned. Despite overall similarities, the i2 can be distinguished from the i1 by the more mesially tilted crown relative to the root. Furthermore, the unworn (Fig. 7G) and slightly worn (Fig. 7J) incisal edge is constituted by two distinct mamelons that, unlike those of the i1, are markedly asymmetrical, with the postconulid being lower than the preconulid. Other differences of the i2 relative to the i1 include a slightly more mesially tilted endocristid and a more curved poststylid—resulting in an overall more asymmetrical crown and a more inclined incisal edge (even when unworn)—and slightly shallower and less asymmetric anticlinids (as the ectosynclinid is less extended onto the root).

The i3 is represented by five specimens (Fig. 7K–O). Three of these incisors (Fig. 7K, M, O) were originally interpreted as I2s by Golpe-Posse (1971), some of them being subsequently identified as an i3 (Fig. 7K) and as an I3 (Fig. 7O) by Pickford (2014). Most recently, McKenzie et al. (2024) concurred with Pickford (2014) that the former specimen is an i3 and mentioned another (previously unpublished) specimen (Fig. 7L) that similarly preserves a lightly worn crown and most of the root. The remaining specimen is severely worn (Fig. 7M) but may be identified as an i3 based on the morphology of the root and basal crown portion, whereas the two crown germs reported here (Fig. 7N–O) are consistent in crown shape and proportions with the more complete specimens, except for being slightly more labiolingually compressed. An alternative identification of these two crown germs as di3s is not impossible, given that this tooth locus is unknown for '*Pa.*' *valentini*, but is unlikely given that they are no more brachyodont or markedly smaller than the remaining i3s. The i3 markedly differs in shape and proportions from the i1 and i2, being smaller overall, generally more mesiodistally compressed, and much lower-crowned, further displaying a more asymmetric and mesially tilted crown.

The short prestylid and the longer poststylid are curved and confluent at the mesially located apex of the crown, which is markedly convex and lacks distinct mamelons. A sharp and thick endocristid originates from a marked and distolingually located basal swelling. The endocristid is only slightly tilted mesially and generally terminates at or close to the apical portion of the postcristid, separating the narrow endofossid from the more spacious prefossid. A less distinct secondary cristid is present in some specimens in the prefossid, running from the prestylid toward the crown apex. The crown is somewhat waisted at the cervix, which shapes a distinct and moderately deep preanticlinid, no discernible postanticlinid, and similarly developed and mesially tilted ectosynclinid and endosynclinid. The root is mesiodistally compressed and progressively tapers toward its apical portion, which is mesially curved.

Lower canines The three c1ms available from the whole sample were all reported by Bataller (1924: pl. 5, figs. 1–3), who attributed them to *L. splendens*. They are registered at the MGSB with a single catalog number despite belonging to more than a single individual, being thus distinguished here by the addition of an old collection number within brackets. Two of these specimens (Fig. 8A–B) are only partially preserved, lacking their apical-most portion, although one of them is only missing the tip and preserves a long and oblique wear facet on the distal face of the tooth along half of its preserved length (Fig. 8A). The third specimen (Fig. 8C) is completely preserved, albeit somewhat damaged at its basal-most portion, further displaying a small wear facet restricted to the apical-most portion of the distal side of the crown. The c1m is very hypsodont (preserved chord length in the best-preserved specimen is 9.7 cm) and ever-growing (thus lacking a distinct root). From base to apex, the crown is very curved distalward and slightly curved labially, only minimally tapering toward the apex, which appears pointed due to wear on the distal side. The cross section is scrofic[1] and very asymmetric, with the labial side being the narrowest, the lingual side being somewhat broader than the distal (10–24%) and much broader than the labial (63–79%), and the distal side being also clearly broader than the labial (33–63%). The distal side is devoid of enamel and rather flat to mildly convex, so that no bump attributable to any cementum ridge can be discerned. The labial side is moderately concave, whereas the lingual is flatter except toward its mesial-most portion, where a shallow but distinct sulcus runs along the whole height of the crown, contributing to delineate a broad and markedly convex mesial precristid. Fine longitudinal striations of the enamel can be discerned along the labial and lingual sides, being particularly evident on the lingual side of one of the specimens (Fig. 8A). Another specimen (Fig. 8B) shows more marked transverse striations at certain portions of the crown that correspond to enamel hypoplasias. The third specimen (Fig. 8C), in contrast, displays narrow, enamel-free bands on the basal-most portion of the lingual side, of which one is apically continued throughout the whole height of the crown; these narrow bands do not appear to result from taphonomical damage, but it is unclear whether they may be qualified as pathological (albeit they are lacking in the other specimens).

The single c1f (Fig. 8D) similarly comes from SQ-TF but remained unpublished until now. It completely preserves the very slightly worn crown as well as most of the root (except for its apical-most portion). Both the crown and the root are markedly compressed labiolingually. The crown is pointed and distally recurved, with its apex being aligned with the distal margin of the crown and the root. The labial and mesial crown walls are markedly convex, whereas the labial crown wall is flatter, being separated from the distal side by a very thick, blunt, and distolingually oriented postcristid that runs from the crown apex toward its base. Together with the more indistinct and distolabially oriented ectocristid, the postcristid delimits a shallow distolabial basin on the lower half of the crown. The root is not markedly waisted at the cervix, which is somewhat irregular labially (with no distinct ectosynclinid) and displays a moderately developed postsynclinid distally, a shallow endoanticlinid lingually, and a moderately developed mesiolabial preanticlinid. The root is labiolingually compressed, distally curved (especially on its mesial side), and moderately apically tapering, and if complete it would have been somewhat higher than the crown.

Lower premolars The available sample of lower premolars is not very abundant but records the four premolar loci, including the p1 (Fig. 9A–B), the p2 (Fig. 9C–F), the p3 (Fig. 9G–I), and the p4 (Fig. 9J–K). Only a single p1 (Fig. 9A) from SQ-TF was previously figured by Pickford (2014: fig. 14D). The p1s preserve the complete and unworn crowns but only the basal-most portion of the two roots (Fig. 9A–B), whereas the p2 is represented by a complete and only slightly worn specimen (Fig. 9C), as well as a partial one (Fig. 9D) and two (mesial and distal) fragments (Fig. 9E–F). The latter specimens currently have two different catalog numbers but originally

[1] Two main morphologies of of c1m are distinguished in suids: in scrofic canines, the lingual side is the broadest and the labial is the narrowest, whereas in verrucosic canines the labial and lingual sides are similarly broad and broader than the distal (Cherin et al., 2020). Therefore, in scrofic canines the narrowest side is the labial, whereas in verrucosic canines it is the distal (Van der Made et al., 1999).

constituted a single, complete tooth that Bataller (1924: pl. 11, fig. 18) attributed to an indeterminate carnivoran.

The two mesial premolar positions are elongate (very buccolingually compressed) and moderately trenchant but low-crowned, with the pointed protoconid being located on the mesial half of the crown. The p1 (Fig. 9A–B) displays a subelliptical contour with a distinct constriction on the lingual side at the level of the protoconid, a markedly convex mesial end, and a slightly distolingually tilted distal portion. The crown walls are moderately convex around the protoconid, which is very buccolingually compressed, and rather concave distally from it. A blunt, slightly lingually tilted, and very steep protoprecristid descends from the protoconid apex toward a low but moderately well-developed mesial stylid. Apically, this protoprecristid displays a moderately convex profile in lingual/buccal views, basally becoming convex before reaching the prestylid. The protopostcrista is less inclined than the protoprecrista and displays some serrations and cuspule-like developments until bifurcating into two distinct cristids. The buccal one progressively curves until reaching the distal end of the crown and, along its midway, displays a buccolingually compressed hypoconid that is slightly higher than the prestylid. In turn, the lingual cristid is directed toward the distolingual crown margin and, together with the former cristid, delimits a distinct but narrow and distally open fossid. A moderately developed buccal cleft is present at the level of the protopostcristid. The cervix displays moderately developed anticlinids and the crown extends farther rootward distally than mesially on both the buccal and lingual sides. Although the roots are not preserved, it can be ascertained that two distinct roots were originally present.

The p2s (Fig. 9C–F) are similar in shape to the p1s (subelliptical and distolingually tilted occlusal contour, buccolingually compressed and mesially located protoconid, steeply inclined protoprecristid ending in a low and moderately developed prestylid, and cervix extending farther rootward distally than mesially on both sides). However, they are larger and further display some occlusal differences: the protoprecristid displays a straighter profile and is more buccally tilted than in the p1; the protopostcristid does not bifurcate and is obliquely oriented toward the distobuccal end of the crown, where it ends on a rather indistinct hypoconid. Like the p1, the p2 displays two distinct roots, the mesial being stouter and more mesially tilted than the distal one.

The distal premolars are represented by a relatively complete p3 that preserves the damaged crown and most of the roots (Fig. 9G), two more partial p3s (Fig. 9H–I), and two slightly worn p4s (Fig. 9J–K) of which one preserves most of the roots. None of these specimens had previously been figured, although Pickford (2014) reported one of the p3s (Fig. 9H). The most complete p3 (Fig. 9G) displays a moderately elongate subelliptical contour, with a mild lingual constriction at about the level of the protoconid as well as markedly convex and slightly lingually tilted mesial and distal ends. One of the partial p3s (Fig. 9I) displays an even narrower occlusal contour on the mesial half of the crown, whereas the other (Fig. 9H) appears broader and suggests an original oval (i.e., distally expanded) rather than subelliptical contour. All the specimens display a thick, straight, and steeply inclined protoprecristid ending on a low and moderately developed mesial prestylid. In the more complete p3, the protopostcristid, albeit considerably worn, is straight and mesiodistally aligned, ending in a rather indistinct hypoconid close to the distal end of the crown. The lingual crown walls are only convex around the protoconid and otherwise concave, with mildly developed lingual and buccal clefts at the protopostcristid level. This premolar displays three roots, the distal ones being slenderer but as mesially tilted as the mesial.

The p4s (Fig. 9J–K) are about as long as the more complete p3 but much stouter (relatively broader), displaying a suboval contour that is only minimally broader distally than mesially and very rounded overall, with only a very subtle lingual constriction at about crown midlength. The protoconid is centrally located, tall, and pointed, with inflated buccal and lingual walls. The protoprecristid is very thick, slightly lingually tilted, and as steeply inclined as in the p3. It descends from the protoconid apex to the mesial stylid, which is somewhat higher and better developed than in the p3. The prestylid is flanked by distinct cingular developments that are restricted to the mesial crown margin, being separated from the base of the protoconid by narrow but marked clefts. In one of the specimens (Fig. 9K), the somewhat worn protopostcristid is distolingually oriented and almost as thick as the protoprecristid, albeit shorter. In the other, almost unworn p4 (Fig. 9J), a smaller but distinct cuspulid (metaconid) can be still distinguished mesiolingually from the protoconid. In both specimens, the short protopostcristid descends distolingually until reaching a trefoil-like structure located at the distal portion of the crown. This structure, which consists of a distal cuspulid-like portion and two transverse (buccal and lingual) cristid-like extensions, may be globally interpreted as the hypoconid. It is higher than the prestylid and separated from the protoconid and metaconid by deep and wide clefts at both sides of the protopostcristid (the buccal one being slightly better developed than the lingual). A marked transverse groove runs along the lowest portion of both clefts, even partially interrupting the connection between the end of the protopostcristid and the hypoconid. These clefts display

no cingulids, which are entirely restricted to the distal crown margin at both sides of the hypoconulid. The p4 also displays three roots, which are similar but larger than those of the p3.

Lower molars Although lower molars are well represented in the sample, only a few are associated. These include those socketed in two mandibular fragments from SQ-TF, one with m1–m3 (Figs. 6C, 10C, M, W) and the other with m2–m3 (Figs. 6D, 10L, V), plus the two m1 antimeres of a juvenile mandible from SQ-PN (Figs. 6B, 10F–G); an m2 mesial fragment (Fig. 10R) and partial m3 (Fig. 10Y) that, according to collection data, come from SQ-TFC, might also belong to the same individual. The remaining lower molars, either complete or partial, come from SQ-TF and consist of isolated specimens, including m1s (Fig. 10A, B, D, E, H, I), m2s (Fig. 10J–K, N–Q, S, T), and m3s (Fig. 10U, X, Z–B')—note that these are our preferred anatomical identifications, but due to size variation among individuals, the smaller isolated m2s might be alternatively identified as m1s of large individuals, or vice versa. Several of the lower molars housed in the MGSB (Figs. 10B, E, I, J, P, U, Z) were figured by Bataller (1924: pl. 6, figs. 1–9, 11), who misidentified some of them as upper molars and assigned them all to *S. palaeochoerus*. In turn, Pickford (2014: fig. 16E–F) figured two of the lower molars (Fig. 10A, K). For all lower molar positions, there are complete unworn and lightly worn specimens enabling the adequate description of their occlusal morphology. The least worn specimens (Fig. 10A, J, K, N, U, Z) display very marked Fürchen and considerable development of enamel wrinkling. The latter becomes easily eroded by wear even at minimal dentine exposure, and enamel appears thick in more worn specimens.

One of the specimens identified here as an m1 (Fig. 10A) was previously identified as an m2 by Golpe-Posse (1972) and Pickford (2014), although this is debatable because these two molar positions display a similar occlusal morphology and considerably overlap in size. As a result, only those molars belonging to mandibular fragments (Fig. 6B–D) can be unambiguously identified as either m1s (Fig. 10C, F, G) or m2s (Fig. 10L–M), indicating that the latter is somewhat longer and broader than the former. This distinction does not apply when interindividual variation is considered, as one of the unequivocal m1s (Fig. 10C) is about the same size as one of the m2s (Fig. 10L). Otherwise, the specimens identified here as m1s (Fig. 10A–I) tend to taper mesially, whereas m2s (Fig. 10J–P) tend to taper distally, although with some exceptions. Both molar positions display a subrectangular occlusal contour with two (mesial and distal lobes), separated by buccolingual constrictions that are more marked buccally than lingually. The four main cuspids are pyramidal in shape and transversely aligned in pairs. The protoprecristid is normally thick and curves along the mesial portion of the crown toward the end of the shorter and lesser developed metaectocristid and metaprecristid, sometimes merging with the former, more rarely with the latter, and in other instances being separated from them both by a groove. A beaded and normally continuous mesial cingulid is present in all the specimens, being more extensive and marked along the mesiobuccal corner of the crown. The protoendocristid bifurcates into two distinct and short cristids, the mesial one being directed toward the similarly developed metaprecristid, partly obliterating the protofossid but being separated from one another by a longitudinal groove. The distal portion of the protoendocristid and the metaendocristid are obliquely oriented and distally enclose the protofossid. The metaendocristid ends in a rather distinct metaendoconulid, which is located mesiolingually from the larger hypopreconulid. The obliquely oriented protopostcristid and the more distally oriented metapostcristid end at the transverse valley that separates the two lobes and that is largely interrupted by a large, centrally located, and often buccolingually expanded hypopreconulid. The transverse valley is lingually open with a single exception (Fig. 10N), in which a small entoendoconulid is present lingually from the hypopreconulid. In contrast, the transverse valley is buccally enclosed by a cingulid that is not continuous with the mesial cingulid and displays a markedly beaded appearance (with multiple enamel thickenings that generally do not constitute a distinct hypoectoconulid). The two distal cuspids are mesiodistally aligned with their mesial counterparts and display a symmetrical cristid pattern, being separated by a very narrow (groove-like) hypofossid. The latter is distally enclosed by a well-developed and distally projecting pentaconid, which partly overlaps the distal cingulid and is slightly tilted lingually relative to the hypopreconulid.

The m3s (Fig. 10U–B') resemble the other lower molars in occlusal morphology but differ in size, occlusal contour, and the greater development of the distal-most (pentaconid-bearing) portion of the crown, which constitutes a distinct third lobe. In the two individuals in which the m3s are associated with other molars (Fig. 6C–D), the m3 is similarly broad but much longer than the m2. As in the other lower molars, the mesial lobe of the m3 is separated from the central lobe by a more marked buccal than lingual constriction of the occlusal contour, whereas this is not the case regarding the distal lobe. There is some variation in the degree of distal tapering: in one of the m3s (Fig. 10U), the central lobe is only moderately narrower than the mesial and the distal tapers more abruptly; in contrast, other specimens (Fig. 10W–X) taper distally more progressively, resulting in a more triangular contour. Otherwise, the occlusal shape of the

mesial and central lobes is entirely comparable to the two lobes of the m1 and m2, and will not be reiterated here. The distal lobe, in contrast, displays a distinct pentapreconulid that is mesiodistally aligned with the larger hypopreconulid, as well as a large pentaconid that is located at the distal end of the crown and smaller than the remaining four main cuspids. The pentaconid is linked to the pentapreconulid by a short and generally thick pentaprecristid, whereas the pentaectocristid displays several enamel thickenings but no distinct pentaectoconulid. One or two secondary cuspulids may also be present lingually from the pentaconid and pentaprecristid. In all the specimens, the distal lobe is distally directed or only buccally tilted very slightly.

Upper deciduous teeth All the upper deciduous tooth positions are represented in the sample. None of the upper deciduous incisors had previously been figured, although two of the ones here identified DI1s (Fig. 11A, E) were formerly reported by Golpe-Posse (1971) as I3s. In total, the described sample includes five DI1s (Fig. 11A–E), a single DI2 (Fig. 11F), and a single DI3 (Fig. 11G); the identification of the two latter incisors is tentative, as they display a similar morphology, although the one identified as a DI2 is larger and higher-crowned than the DI3.

The DI1s (Fig. 11A–E) are smaller but similar in shape to the I1s, except that the former display a more labiolingually compressed crown and a somewhat slenderer root. The mesiolabial crown wall is convex, whereas the lingual portion is slightly concave except at its base. The precrista and postcrista are moderately marked and progressively converge to configure a rounded incisal edge. The lingual cingulum is subtle and crown base below it does not appear swollen. An obliquely oriented endocrista (double in one of the specimens; Fig. 11C) originates from the cingulum and fades away at about crown midheight, thus only partly separating the prefossa from the endofossa. The cervix shapes a moderately deep preanticline mesiolingually and a more indistinct endosyncline distally. The root is much higher than the crown and moderately compressed labiolingually at its base, progressively curving distally and tapering apically, with the apex further being slightly tilted lingually. The crown is only very slightly waisted at the cervix, particularly on the distal end.

The upper incisors interpreted as DI2 (Fig. 11F) and DI3 (Fig. 11G) display a similar morphology, with the crown being much more labiolingually compressed and more mesially and distally protruding from the cervix than in the DI1. The DI2 resembles the I2 in displaying a triangular profile in labial/lingual views, as well as a convex but centrally inflated lingual crown wall that displays an apically tapering but rather indistinct endocrista. However, the DI2 differs from the I2 in being smaller, lower-crowned, and more asymmetrical (with the apex more clearly positioned on the mesial half of the crown, and a much longer and less steeply inclined postcrista that displays a concave rather than convex profile in labial/lingual views), and further displaying a better developed prestyle at the base of the precrista but an even more indistinct lingual cingulum). The DI3 shows essentially the same morphology as the DI2 but is lower-crowned and more mesially protruding from the cervix, and it further displays somewhat more distinct lingual cingulum and endocrista (the latter delimiting a more spacious and concave endofossa). The DI3 preserves most of the root, which is labiolingually compressed, markedly waisted at the cervix, and very distally tilted.

The upper deciduous premolars include two DP2s (Fig. 11H–I), of which one was previously identified as a P2 by Golpe-Posse (1971) and Pickford (2014: fig. 14A); two DP3s, including a complete one (Fig. 11J) previously reported but not figured by Pickford (2014) as well as a mesial crown fragment (Fig. 11K); and four DP4s (Fig. 11L–O), two of them previously reported (and one figured) by Pickford (2014: fig. 16A). The two DP2s are very lightly worn and display an occlusal morphology entirely comparable to one another—somewhat intermediate between those of the P1 and the P2, but differing from these permanent loci in the less mesially located paracone, the more asymmetrical occlusal contour, and the lower occlusal relief. The occlusal contour of the DP2 is elongate and vaguely comma-shaped, owing to the mesiolingually directed prestyle and the lingually tilted distal third of the crown. The prestyle is well developed and surrounded by cingular developments that do not extend either lingually or buccally. The main cusp (paracone) is quite centrally located (albeit slightly toward the mesial half of the crown), pointed, and labiolingually compressed. Two similarly steep crests originate from the paracone apex: the paraprecrista is mesiodistally aligned except on its mesial-most third, which curves toward the prestyle; the parapostcrista, in turn, displays minor cuspule-like thickenings and a greater degree of curvature, being initially distobuccally directed and subsequently distolingually oriented until merging with the moderately well-developed and crest-like metacone. The latter is well distinct in lingual/buccal views and approximately as high as the prestyle. The buccal crown wall is moderately convex, slightly bulging at the paracone level and basally protruding at the level of the metacone. The lingual crown wall, in contrast, is concave except at the level of the paracone, forming a well-developed basin-like structure at the protruding distolingual corner of the crown, which is surrounded by a distinct cingulum. The cervix extends farther rootward on the distal than on

the mesial half of the crown, but less markedly so than in the P1 and P2. This premolar displays two distinct roots that are only merged at the base: the mesial is vertically directed, whereas the distal is stouter and distally tilted.

The DP3 (Fig. 11J–K) displays a subtriangular (longer than wide) occlusal contour with marked buccal and lingual constrictions at about crown midlength, which define two distinct lobes. The mesial lobe is somewhat elongate and markedly convex mesially, whereas the distal lobe is much wider than the mesial and also more asymmetrical, as a result of a more marked distolingual than distobuccal crown expansion. There is a moderately developed prestyle on the mesial end of the crown, continued along the buccal and lingual walls by subtle cingula that fade away before reaching the distal lobe. The paracone is centrally located on the mesial lobe and pyramidal in size. Three main cristids originate from its apex: a marked and mesiolingually directed paraprecrista, which ends at the lingual cingulum, close to the prestyle; and the more tenuous but similarly obliquely oriented paraendocrista and parapostcrista (which are distolingually and distobuccally directed, respectively). A secondary and obliquely oriented cristid is also present mesiobuccally from the paracone, although it is shorter than the paraprecrista and, unlike the latter, does not reach the paracone apex. The paraendocrista and parapostcrista reach the transverse valley and are continued into the distal lobe by the ectoprotocrista and ectometacrista, respectively. The distal cusps are similarly developed and close to one another (i.e., not very peripheral). The distal cristids that originate from them are discernible but shorter and less well-developed than the mesial ones, although the protoendocrista seemingly reaches the moderately developed distal cingulum. The latter is not continued either buccally or lingually. The whole occlusal surface displays moderately abundant enamel wrinkling.

The DP4s (Fig. 11L–O) resemble in general occlusal pattern the M1s and M2s (see above), including a subrectangular occlusal contour that is longer than broad, with two distinct lobes, four main cusps (with the buccal ones being more mesially located than their lingual counterparts), and well-developed mesial and distal cingula. However, besides being smaller and lower-crowned, the DP4s further display some differences characteristic of this tooth locus that enable their distinction from the permanent molars, namely: the straight and markedly oblique mesial contour; the slightly less peripheral distal cusps, which appear closer to one another than the mesial ones; and the lesser developed (almost inconspicuous) protopreconule and metaectoconule (whereas, in contrast, the hypopreconule is as developed as in the permanent upper molars).

Lower deciduous teeth The lower deciduous teeth from the sample record all tooth positions except for the di3 (unless MGSB48863 and IPS31060, here identified as i3s, are indeed deciduous, which we consider unlikely). The di1 is represented by three specimens (Fig. 11P–R), two of which (Fig. 11Q–R) were previously identified as permanent i1s by Golpe-Posse (1971). In turn, the di2 is represented by two specimens (Fig. 11S–T), one of them (Fig. 11S) originally considered a permanent i2 by Golpe-Posse (1971). The shape of the unworn incisal edge of the di1 cannot be ascertained, but the general shape of this deciduous incisor (Fig. 11P–R) resembles that of the i1 at a smaller size (see above), being both characterized by a relatively high crown that is vertically aligned with the root, as well as a distinct endocristid that is only slightly tilted mesially and originates from a moderately developed basal bulge. The most remarkable differences refer to the less marked difference in rootward extension of the ectosynclinid as compared with the endosynclinid, as well as the more marked waisting of the root base below the cervix in the di1. The di2 (Fig. 11S–T) differs from the di1 in the markedly mesial tilting of the crown and endocristid, with the distal margin of the crown displaying a rather continuous curvature with the root across the cervix. In these regards, the differences between di2 and di1 parallel those between their permanent counterparts at a smaller size. Nevertheless, the di2 more markedly differs from the i2 by displaying a slenderer crown as well as a more marked distal curvature of the crown and root. The two di2s from SQ-TF display a similar shape, characterized by a very broad endocristid that originates from a moderately developed basal bulge and progressively tapers apically, narrow prefossid and endofossid, a preanticlinid somewhat deeper than the postanticlinid, and a moderately mesiodistally compressed and lingually curved root. However, these two specimens further denote some variation in this tooth locus, as one of them (Fig. 11S) displays a mildly convex postcristid, whereas the other (Fig. 11T) displays a conspicuously concave poststylid that runs in parallel to the profile of the prestylid in lingual/labial views.

With regard to the deciduous lower premolars, the dp2 and the dp3 are only represented by a partial germ (Fig. 11U) and a distal crown fragment (Fig. 11V), respectively, whereas the dp4 is represented by three complete crowns (Fig. 11W–X, Z) and two mesial fragments (Fig. 11A'–B') from SQ-TF, plus the socketed specimen of the juvenile mandible (Figs. 6B, 11Y) from SQ-PN. The distal end of the dp2 is broken away (Fig. 11U) but it would have originally displayed a subelliptical or suboval occlusal contour. The protoconid is centrally located and, despite the apparent lack of wear, displays a rounded morphology, owing to the convex profile of both the

protoprecristid and protopostcristid in buccal/lingual views. The protoprecristid is long, steeply inclined, blunt, and sinuous, as it originates from the mesiolingual aspect of the protoconid apex and then progressively curves in mesiobuccal direction until reaching a well-developed prestylid at the mesial end of the crown. The protopostcristid is as developed and inclined as the protoprecristid but shorter, ending at a well-developed hypoconid that is much higher than the prestylid, mesiodistally aligned with the protoconid, and distally continued by a straight cristid aligned with but less steeply inclined than the protopostcristid. There is no metaconid distally from the protoconid. The buccal crown wall is mildly convex and the lingual a bit flatter, except at the level of the prestylid and, especially, the protopostcristid, where a marked buccal cleft and a shallower lingual one flank the mesial aspect of the hypoconulid. No buccal or lingual cingulids can be discerned on the preserved portion of the crown.

The dp3 (Fig. 11V) is more incompletely preserved than the dp2. It resembles the morphology of the p3 at a smaller size, being either interpretable as a L mesial fragment or a R distal fragment, although the lack of a distinct stylid on the preserved end of the crown favors the latter option. The dp3 appears larger and higher crowned than the dp2, with a steeply inclined and only slightly distobuccally curved protopostcristid that reaches the distal end of the crown without displaying a distinct metaconid or hypoconid. The crown base appears distolingually protruding, while the crown walls appear convex at the protoconid level and concave along the protopostcristid, particularly on the buccal side, although no conspicuous cleft can be discerned.

The dp4 (Fig. 11W–B') has the trilobate morphology characteristic of this tooth locus, with an elongate and slightly mesially tapering occlusal contour, a moderately rounded mesial end, and a slightly projecting distal margin. The buccal crown base configures more conspicuous convexities (and, hence, deeper constrictions between consecutive lobes) than the lingual. The six main cuspids are pyramidal in shape, with sharp cristids and deep Fürchen, and are transversely aligned in pairs. On the mesial end of the crown, a thick and obliquely oriented paraprecristid is directed toward the primoprecristid, terminating in some specimens in a small and indistinct parapreconulid. Mesially from it, a buccolingually restricted and non-projecting mesial cingulid may be discerned. The paraendoconulid, protoendoconulid, and hypopreconulid are poorly developed and smaller than the pentaconid. The latter is distinct but lower and less extensive than the six main cuspids, being centrally located (even if slightly buccally tilted) on the projecting and rounded distal cingulid. Buccal and lingual cingulids are only mildly developed along the distal lobe. Minor crenulations of the enamel can still be discerned in some specimens, particularly on the cristids and cingulids.

Comparisons

Upper incisors The size variation displayed by the I1s from SQ-TF largely encompasses that displayed by the I1s from CB attributed to the same taxon (Additional file 1: Table S2). In contrast, they are larger on average than the I1s of *V. steinheimensis* (albeit with considerable overlap) and more clearly larger than those of *C. simorrensis* and *R. matritensis*. In terms of shape (Additional file 1: Table S3), comparisons of the lingual morphology to other I1s of '*Pa.*' *valentini* are restricted to a single specimen from CB reported by McKenzie et al. (2024), which displays a less distinct endocrista—however, an unambiguous assignment of this incisor (IPS1749) to '*Pa.*' *valentini* is not possible, as *V. steinheimensis* is also recorded there. The figured I1 of *V. steinheimensis* from Gratkorn is also too worn to ascertain the lingual morphology, although overall it appears lower-crowned than those of '*Pa.*' *valentini* at comparable wear stages. The I1s from Göriach and elsewhere attributed to *R. matritensis* display a more lingually tilted crown than those of '*Pa.*' *valentini*, but otherwise are similar in terms of crown height and endocrista development.

The I2s from SQ-TF superficially resemble those of *L. splendens*, which display overlapping dimensions (even though the latter are larger on average; Van der Made, 1996b: pl. 36, figs. 9–10, 13). However, the described specimens display multiple morphological details that discount this alternative attribution: the higher, more labiolingually compressed, and less lingually recurved crown; the more asymmetrical profile in labial/lingual views (the tip is more mesially located); and the more diffuse endocrista and much fainter lingual cingulum. Accordingly, they are assigned to '*Pa.*' *valentini*. These I2s are larger, more elongate, and lower-crowned than two incisors from CB (IPS92710 and IPS92857) identified by McKenzie et al. (2023a: fig. 3i–j) as I2s but here reinterpreted as DI1s of '*Pa.*' *valentini* (see below). We therefore conclude that the specimens described here are the first I2s reported for '*Pa.*' *valentini.* They closely resemble in size and proportions (Additional file 1: Table S2) the I2s of *V. steinheimensis*, whereas those of *R. matritensis* from Göriach are somewhat smaller (albeit with some overlap). In occlusal shape (Additional file 1: Table S3), the described specimens of '*Pa.*' *valentini* differ from those of *V. steinheimensis* in the less marked lingual cingulum and more labiolingually compressed root, as well as from those of *R. matritensis* in the more indistinct endocrista and lingual cingulum. The I2s from SQ-TF are also similar in size and proportions to the incisor from the same site tentatively identified here as an I3, being larger on

average than the I3s of *V. steinheimensis* and *R. matritensis* (Additional file 1: Table S2). It is noteworthy that the moderately worn I3 of *V. steinheimensis* from Gratkorn displays a moderately distinct endocrista, more similar to that displayed by the I2s of '*Pa.*' *valentini* (not ascertainable in the I3 due to wear) and the I3 from Göriach than the I2s from the latter site (Additional file 1: Table S3).

Upper canines One of the C1ms from SQ-TF described here (Fig. 3L) was previously reported by Pickford (2014: p. 187), who qualified it as "extraordinary". The new specimen described here (Fig. 3K) shows some minor differences (it is relatively broader labiolingually, no clear labial or lingual grooves can be discerned on the cementum surface, and the mesial wear facet against the c1m is more steeply inclined). However, it generally agrees in morphology, confirming the main features highlighted by Pickford (2014): oval cross section, marked mesial and distal crests overhanging the small root, and deep lingual and labial anticlines. The C1ms from SQ-TF overlap in mesiodistal length with two specimens from Kleineisenbach attributed to '*Pa.*' *valentini* by Pickford (2016) but are labiolingually less compressed, unlike those of *V. steinheimensis* and *R. matritensis*, which display similar proportions but are comparatively smaller (more markedly so those of the latter species; Additional file 1: Table S2). In terms of shape (Additional file 1: Table S3), the two C1ms from SQ-TF closely resemble those from Kleineisenbach attributed to '*Pa.*' *valentini*. They differ from those of *V. steinheimensis* and *R. matritensis* in displaying a shorter crown with a more distinct (albeit short) root and marked mesial and distal protrusions of the crown base, as well as a more marked distal keel.

The specimen from SQ-TF identified as a C1f of '*Pa.*' *valentini* markedly differs from the C1fs from CCN20 (IPS106329) and CB (IPS1715 and IPS93150) that were attributed to this species by McKenzie et al. (2023a: fig. 3d, 2024: fig. 4e–f). The latter are much higher-crowned and display a single and stouter root, thus more closely resembling the C1fs of *Pr. palaeochoerus* from CB (McKenzie et al., 2024: fig. 4a–d) and elsewhere (Van der Made et al., 1999: pl. 2, fig. 4; McKenzie et al., 2023a: fig. 3b–c; Alba et al., 2024: fig. 6b). In contrast, the C1f from SQ-TF displays tetraconodontine affinities (see below). For this reason, the aforementioned specimens from CCN20 and CB are here reassigned to *Pr. palaeochoerus*, implying that the SQ-TF specimen is the first described C1f of '*Pa.*' *valentini*. In size and proportions, this specimen resembles the C1fs of *C. simorrensis* from Przeworno (which are only slightly longer) as well as those of *R. matritensis* from Göriach—the C1f of *V. steinheimensis* being, to our knowledge, unknown (unless the Przeworno sample is assigned to this species). In occlusal shape, the C1f from SQ-TF resembles those of *C. simorrensis* and *R. matritensis* in being double-rooted and displaying a premolar-like crown, i.e., elongate (relative to breadth) and lower-crowned (relative to length). The specimen described here more closely resembles the C1f of *C. simorrensis* from Przeworno in displaying strong mesial and distal styles, although further similarities are difficult to ascertain because these specimens were only figured in labial view. However, the C1f from SQ-TF appears to display a more mesially tilted apex, with the precrista and postcrista being straighter in labial view (instead of moderately convex and concave, respectively), as well as a deeper ectoanticline. The crown base also appears more protruding mesially and distally, and the degree of fusion of the two roots might have been greater (as suggested by the more vertical orientation of the fused basal portions of the roots), although the latter cannot be conclusively ascertained due to incomplete preservation. In the C1f of *R. matritensis*, the styles are much weaker and the occlusal contour is different from that of the SQ-TF specimen (more uniformly convex labially and less flat lingually, being swollen at the level of the main cusp).

Upper premolars The single P1 from SQ-TF is similar in size and proportions to those of '*Pa.*' *valentini* from CB (Fig. 12A; Additional file 1: Table S2), whereas those of *V. steinheimensis* and, especially, *C. simorrensis* and *R. matritensis* are larger and relatively broader on average. The shape of the SQ-TF specimen also most closely resembles the two P1s of '*Pa.*' *valentini* previously reported by McKenzie et al. (2024) from CB, except for a few minor occlusal details (fainter prestyle and less distinct metacone in the former). In contrast, the P1s of '*Pa.*' *valentini* more extensively differ from those of *V. steinheimensis, C. simorrensis*, and *R. matritensis* in being more trenchant and higher-crowned, and displaying a more mesially located paracone, milder constrictions of the crown wall, a more indistinct metacone, and a longer and more curved parapostcrista, further lacking a distinct lingual cingulum. The P1s of *V. steinheimensis* more markedly differ by displaying a more developed prestyle, as well as a more inflated paracone with deep buccal and lingual clefts both mesially and distally from it. However, the specimens attributed to *C. simorrensis* and *R. matritensis* from Göriach are also distinguishable from those of '*Pa.*' *valentini* based on the features listed above—although the P1s from Simorre attributed to *R. matritensis* by Pickford and Laurent (2014) display a somewhat more mesially located metacone and a less developed lingual cingulum than the Göriach specimens.

The P2s from SQ-TF and CF2 display very similar proportions to the P1 of the same taxon at a larger size (Additional file 1: Table S2), but are much slenderer than the P2 from CCN20 (IPS124328; BLI = 54%) previously

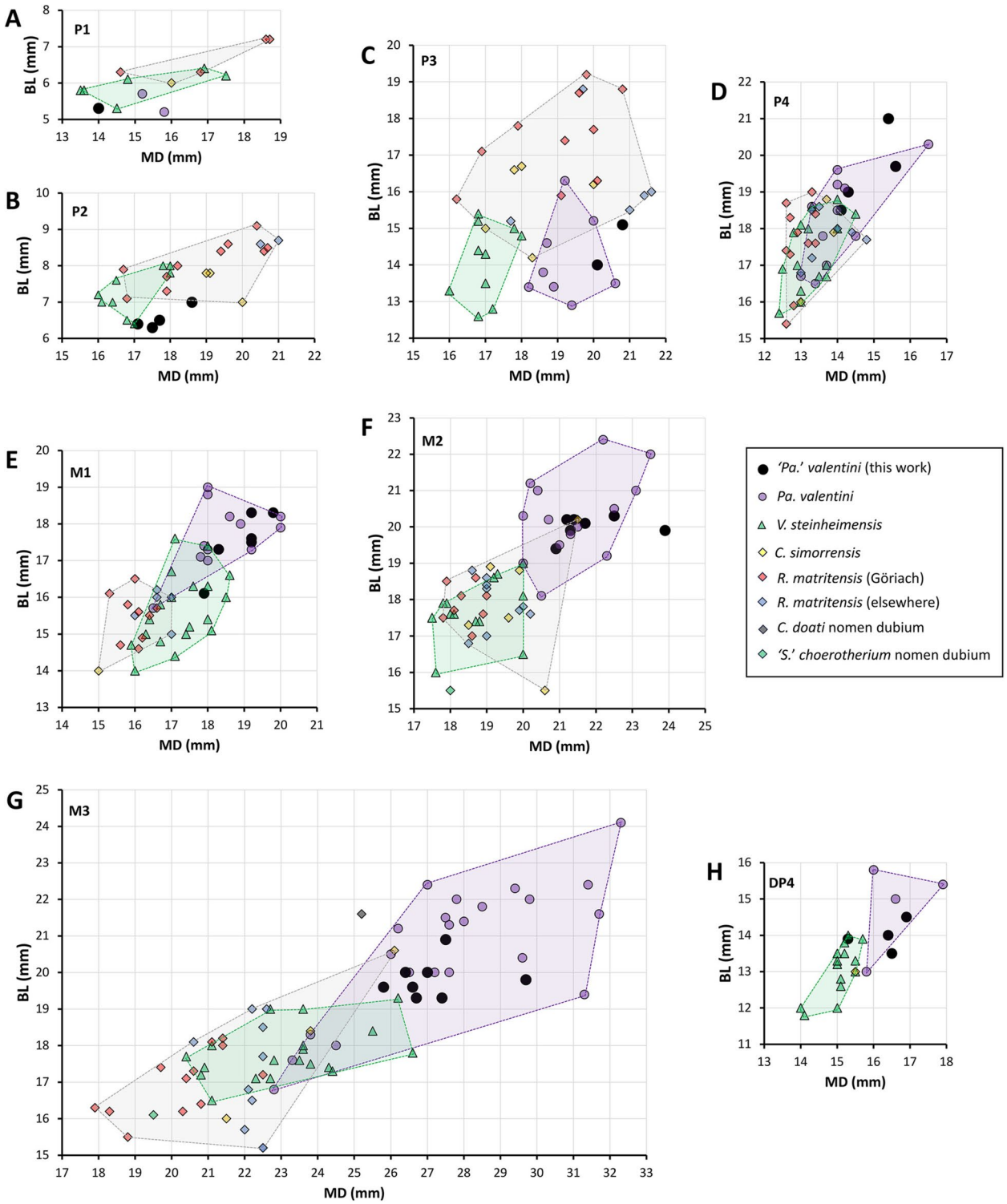

Fig. 12 Bivariate plots of BL vs. MD for the upper cheek teeth of '*Parachleuastochoerus*' *valentini* from Sant Quirze localities as compared with those of this species and other tetraconodontines from elsewhere: **A** P1; **B** P2; **C** P3; **D** P4; **E** M1; **F** M2; **G** M3; **H** DP4. Metrical data for the material from Sant Quirze localities are reported in Table 1, while those for the comparative sample have been taken from the literature (see Materials and methods for details on the published sources). Convex hulls outlining the variation of several species (without considering the remains from Sant Quirze localities) are depicted

attributed to '*Pa.*' *valentini* by McKenzie et al. (2023a: fig. 4e). The latter specimen displays a somewhat trenchant appearance, but its overall morphology is not particularly tetraconodontine-like, and its wide proportions and marked distolingual extension of the crown are much more consistent with being a large P2 of *Pr. palaeochoerus* (cf. McKenzie et al., 2024: fig. 14e), to which it is reassigned here. The specimens described herein thus represent the first P2s reported for '*Pa.*' *valentini*. They are similar in size to but slenderer on average than those of *V. steinheimensis*, whereas the P2s of *C. steinheimensis* and *R. matritensis* are generally both larger and relatively broader than those of '*Pa.*' *valentini* (Fig. 12B; Additional file 1: Table S2). The described P2s further differ from those of the other tetraconodontines included in the comparative sample in the same features as the P1s. Thus, compared with *V. steinheimensis*, '*Pa.*' *valentini* displays a higher-crowned P2 with a more mesially located paracone and less marked constrictions of the crown walls, a more obliquely oriented parapostcrista, a more indistinct metacone, and lack of lingual cingulum. The same differences apply as compared with *R. matritensis* from Göriach and Villefranche d'Astarac and, as far as it can be ascertained, *C. simorrensis*, even though such differences appear more marked in the case of *V. steinheimensis* (as it is also the case for the P1). Some P2s from Simorre and Elgg attributed to *R. matritensis* by Pickford and Laurent (2014) and Pickford (2016), respectively, display a somewhat more mesially placed paracone and lesser developed lingual cingulum, but also differ from those of '*Pa.*' *valentini* in the lower occlusal relief and better developed metacone.

The two P3s from SQ-TF largely overlap in size and proportions (Fig. 12C; Additional file 1: Table S2) with those of '*Pa.*' *valentini* previously reported from multiple sites, being in contrast longer and relatively slenderer than those of *V. steinheimensis*, and generally narrower in absolute and especially relative terms than in *C. simorrensis* and *R. matritensis*. In terms of occlusal shape (Additional file 1: Table S3), the P3s from SQ-TF appear more mesially tapering than those of '*Pa.*' *valentini* from CB (McKenzie et al., 2024), but cannot be adequately compared with them because they are too worn and somewhat damaged. The SQ-TF specimens are more similar to the single P3 of '*Pa.*' *valentini* from CCN20 (McKenzie et al., 2023b), which displays a well-developed prestyle, an inflated paracone, and an almost continuous lingual cingulum that bears a low and crest-like protocone, but which differs by possessing a stouter occlusal contour (with a more convex buccal side and a more distolingual expansion). Similar variation in occlusal contour and proportions is displayed by the P3s of '*Pa.*' *valentini* from elsewhere (Pickford, 2014)—including the P3 from Keineisenbach (Pickford, 2016)—overall fitting well with the variation of this species. The P3s of *V. steinheimensis* display a similar morphology but differ from those of '*Pa.*' *valentini* in the possession of more indistinct metacone and protocone, so that the distolingual extension of the cingulum is less accentuated. In turn, the P3s of *C. simorrensis* as well as *R. matritensis* from Göriach and elsewhere display a variably developed distobuccal extension of the crown, with specimens of *C. simorrensis* generally displaying a less developed lingual cingulum and a more indistinct protocone than in '*Pa.*' *valentini*. However, *C. simorrensis* and *R. matritensis* differ from both '*Pa.*' *valentini* and *V. steinheimensis* in displaying a stouter and higher-crowned P3 at comparable wear stages, which is conspicuously hypertrophied relative to the P4 and the upper molars. In most specimens, the development of the metacone cannot be adequately ascertained because this cusp is rapidly obliterated by wear (constituting a confluent oblique wear facet with the distal aspect of the paracone). However, the P3s from SQ-TF suggest that the metacone would have been less developed in '*Pa.*' *valentini* than in the other taxa, at least based on two lightly worn specimens from Simorre. These two specimens were attributed to different species (*R. matritensis* and *C. simorrensis*) by Pickford and Laurent (2014) despite showing comparable occlusal proportions and shape, including a stout contour, high relief, a moderately developed distolingual extension, and a tall metacone that is located closer to the paracone and appears better developed than in '*Pa.*' *valentini*.

The P4s from SQ-TF match relatively well the P4 size and proportions of '*Pa.*' *valentini* from the Vallès-Penedès Basin and elsewhere (Fig. 12D; Additional file 1: Table S2), only extending slightly its upper breadth range. Those of *V. steinheimensis*, despite differences in occlusal contour (see below), display similar proportions but are overall smaller (albeit with some overlap). The P4s of *C. simorrensis* and *R. matritensis* considerably overlap in proportions with '*Pa.*' *valentini* but tend to be stouter on average and are also generally smaller. In occlusal shape (Additional file 1: Table S3), the P4s from SQ-TF resemble the more worn specimens from CB attributed to '*Pa.*' *valentini* by McKenzie et al. (2024)—characterized by a very lingually tapering contour, a protocone less peripheral than the buccal cusps, a metacone subequal in size to the paracone and separated from it by a vertical groove on the buccal crown wall, moderately well-developed prestyle and poststyle, and an absent to poorly developed and discontinuous buccal cingulum—except that the newly reported specimens display a mesially tilted lingual crown half. Other specimens attributed to '*Pa.*' *valentini* further display additional variation in occlusal contour (more or less lingually tapering or variably

mesiobuccally protruding) and/or other minor details (slightly developed buccal and lingual cingula or less mesially located protocone), but otherwise display a similar morphology. Overall, the P4s of '*Pa.*' *valentini* from SQ-TF and elsewhere differ from those of *V. steinheimensis* in the less mesially located protocone (not completely aligned transversely with the paracone), the larger metacone less closely packed with the paracone and separated from it by a buccal groove, the more marked distal cingulum, and the generally more lingually tapering occlusal contour. In both '*Pa.*' *valentini* and *V. steinheimensis*, the P4 is almost as high and much broader than the P3, whereas in *R. matritensis* the P4 is higher than in these species but comparatively less hypertrophied (i.e., much lower-crowned and only slightly wider) than the P3. The P4s of *C. simorrensis* and *R. matritensis* further differ from those of both '*Pa.*' *valentini* and *V. steinheimensis* in several occlusal details, including the more or less constricted buccal contour (only insinuated in some specimens of '*Pa.*' *valentini*) and the generally somewhat better developed lingual cingulum. They further differ from *V. steinheimensis* (thus more closely resembling '*Pa.*' *valentini*) in the less mesial position of the protocone (generally not completely aligned with the paracone) and the presence of a vertical groove separating the apices of paracone and metacone on the buccal crown wall. As in '*Pa.*' *valentini*, the P4 samples available for *C. simorrensis* and *R. matritensis* show some variation in occlusal contour (degree of lingual tapering), position of the protocone (more or less peripheral and/or aligned with the paracone), size and position of the metacone (more or less vestigial and/or closely packed to the paracone), and development of the lingual cingulum. However, no consistent differences can be discerned between the P4s attributed to *C. simorrensis* and *R. matritensis* by Pickford and Laurent (2014). Only the P4s of *R. matritensis* from the type locality (Puente Vallecas) and Paşalar stand out by displaying a protocone completely aligned with the paracone and virtually lacking a metacone. Even if it is assumed that the apices of both cusps would have been distinct when unworn (Golpe-Posse, 1972; Pickford & Laurent, 2014), the case is that they are distinct at comparable wear stages (including the remains of a buccal groove) in other P4s variously attributed to *C. simorrensis* or *R. matritensis*, including the large sample from Göriach.

Upper molars The M1s from SQ-TF and CF2 fit well in size and proportions with those previously reported from the Vallès-Penedès Basin and elsewhere (Fig. 12E; Additional file 1: Table S2). In turn, the M2s are larger and sometimes slenderer than the M1s, and further agree in dimensions and proportions with previously reported specimens of *'Pa.' valentini* (Fig. 12F; Additional file 1: Table S2). In contrast, the M1s and M2s of the studied sample are larger than those of *V. steinheimensis* (more markedly so in the case of the M2), with no relevant differences in proportions. The same applies when compared with the samples of *R. matritensis* and *C. simorrensis*, only with some overlap, particularly in the case of the Mira specimen (Golpe-Posse, 1971, 1972; Pickford, 2014), which is the largest M2 attributed to *C. simorrensis*. The M2 from the Sansan tetraconodontine, here provisionally identified as '*S.*' *choerotherium* (*nomen dubium*), is smaller than those of *C. simorrensis* and, especially, '*Pa.*' *valentini* but overlaps in length with those of *R. matritensis* and *V. steinheimensis* (despite being slightly narrower). In occlusal shape (Additional file 1: Table S3), the described M1s and M2s from SQ-TF and CF2 resemble those of '*Pa.*' *valentini* previously figured in the literature, but also those of *V. steinheimensis*. In contrast, the M1s and M2s attributed to *R. matritensis* and *C. simorrensis*, leaving aside size differences, generally display better developed preconules and a more distinct conule on the distal cingulum, as well as a more distally tapering distal lobe (particularly the M2), although there is considerable variation in these regards.

The M3s from SQ-TF and CF2 largely overlap in size and proportions with those of '*Pa.*' *valentini* from the same basin and elsewhere (Fig. 12G; Additional file 1: Table S2), being similar in proportions to but generally larger than the M3s of *V. steinheimensis* (albeit with some overlap). The described M3s are also larger and slenderer than those attributed to *R. matritensis* (albeit with some overlap in proportions) and *C. simorrensis* (albeit with some overlap in size, especially as a result of the inclusion of the Mira specimen in *C. simorrensis*; see McKenzie et al., 2024). The lectotype M3 of *C. doati* from Bonnefond, a nominal species here considered a *nomen dubium* following McKenzie et al. (2024), falls close to the variation of '*Pa.*' *valentini* but is slightly broader and is also closer in dimensions to the M3 from Mira (Fig. 12G; Additional file 1: Table S2). The M3 from Kleineisenbach attributed by Pickford (2016) to '*Pa.*' *valentini* is the smallest currently recorded for this species and overlaps in size and proportions with those of *V. steinheimensis*, further falling close to the metrical variation of the other tetraconodontines included in the comparative sample but not far from other small M3s of '*Pa.*' *valentini*. The M3 from Sansan tetraconodontine—i.e., '*S.*' *choerotherium* (*nomen dubium*)—is smaller than all the tetraconodontines included in the studied and comparative samples except *R. matritensis*. In occlusal shape (Additional file 1: Table S3), the described M3s are consistent with the attribution to a single species and more closely resemble those previously attributed to '*Pa.*' *valentini*—despite some variation in occlusal proportions

and contour, as previously noted by McKenzie et al. (2023a, 2024). In contrast, the M3s of '*Pa.*' *valentini* differ from those of *V. steinheimensis* in the possession of a less tapering central lobe and a generally better developed and more distinct distal lobe, which bears a lesser developed pentapreconule but a better developed and distally directed or buccally tilted pentacone. The M3s of '*Pa.*' *valentini* also differ from those attributed to *R. matritensis*, *C. simorrensis* (including the Mira specimen), and '*S.*' *choerotherium* (*nomen dubium*) from Sansan in the lesser developed pentaconules (including the pentapreconule), the less marked constriction between the mesial and central lobes (contrasting with the more distinct distal lobe), and the lack of lingual tilting of the central and distal lobes relative to the mesial. Compared with these species, '*Pa.*' *valentini* also displays a narrower but more distinct and distally protruding distal lobe, which generally bears a lesser developed distal cingulum and displays a much more developed, distinct, and not lingually tilted pentacone—albeit there is also considerable variation in the development of the M3 distal lobe in these taxa, from very poorly developed to moderately protruding distolingually. The M3s of '*Pa.*' *valentini* markedly differ from the lectotype of *C. doati* (Additional file 1: Table S3), as previously remarked by McKenzie et al. (2024), who considered that the latter is a *nomen dubium*—potentially synonymous with either *C. simorrensis* or *V. steinheimensis*—although the broad proportions and metrical similarities with the Mira specimen are more consistent with an attribution to *C. simorrensis*.

Lower incisors The i1s described here cannot be compared with any previously known specimen of '*Pa.*' *valentini*, given that the incisor identified as such by Pickford (2014) from the SQ-TF sample is here considered an i2. Nevertheless, our metrical comparisons (Additional file 1: Table S2) indicate that the described i1s are larger and, on average, more mesiodistally compressed than those of *V. steinheimensis*. The former are also generally larger than the few specimens attributed to *R. matritensis* and *C. simorrensis*, which nevertheless appear more similar in proportions to those of '*Pa.*' *valentini* than to those of *V. steinheimensis*. In terms of occlusal shape (Additional file 1: Table S3), no differences can be noticed compared with the previously figured i1s of *V. steinheimensis* and *C. simorrensis* from Mira, all of which are nevertheless too worn to ascertain the apical morphology of the crown. Nevertheless, the root of the single completely preserved i1 from TF-SQ appears much more tapering on its apical half than the CB specimen figured by McKenzie et al. (2024).

The i2s from SQ-TF appear larger and relatively much broader than the i2 from Wartenberg bei Erding (MD = 8.5 mm, BL > 9.6 mm) attributed to '*Pa.*' *valentini* by Pickford (2016); however, this is largely because this specimen is broken and does not preserve the base of the crown on the lingual side. Yet the i2s described herein are also somewhat larger than those from CCN20 and CB previously attributed to '*Pa.*' *valentini* by McKenzie et al. (2023a, 2024), which also overlap to a large extent in both size and proportions with the few i2s available for *R. matritensis* and *C. simorrensis*, and the more extensive sample of *V. steinheimensis*—excluding an incisor from Steinheim (GPIT MA 1178–42; MD = 5.0 mm, BL = 7.4 mm) that was identified as an i2 by Pickford (2016), but which appears too small and is here considered a di2 following Hünermann (1968). Comparisons of occlusal shape (Additional file 1: Table S3) with the i2s of *R. matritensis* and *C. simorrensis* are hindered by their advanced wear, as it is also the case of various figured i2s of '*Pa.*' *valentini* and *V. steinheimensis*. Nevertheless, compared with the least worn i2s of *V. steinheimensis* figured by Chen (1984) and Pickford (2016), those from SQ-TF display a more asymmetrical crown, due to the more curved poststylid, which is also more distinct (as marked as the prestylid). In these regards, the described specimens most closely resemble the lightly worn i2s of '*Pa.*' *valentini* from CB (McKenzie et al., 2024), which are slightly smaller and display an even more asymmetrical crown (with a more curved poststylid and a more mesially tilted endocristid).

In dimensions and proportions (Additional file 1: Table S2), the described i3s considerably overlap with those previously attributed to '*Pa.*' *valentini* as well as *V. steinheimensis*, even though the latter are somewhat narrower labiolingually on average. In terms of shape (Additional file 1: Table S3), the i3s from SQ-TF also more closely resemble those of '*Pa.*' *valentini*, which display a higher (relative to basal dimensions), slenderer (less labiolingually inflated), and more mesially tilted crown than the figured i3s of *V. steinheimensis*. The single available i3 of *R. matritensis* from Göriach is even more distinctive by displaying a more labiolingually elongate (mesiodistally compressed) crown and root.

Lower canines. The c1ms from SQ-TF allow us, for the first time, to describe the morphology of this tooth locus for '*Pa.*' *valentini* (see Discussion for further considerations in this regard). Although these specimens were originally attributed to *L. splendens* by Bataller (1924), their marked scrofic morphology does not fit with the c1m proportions of the latter species, which generally displays verrucosic or mildly scrofic canines (Van der Made, 1996a). In particular, 56% (39/70) of the c1ms of *L. splendens* measured by Van der Made (1996b: fig. 48) display verrucosic proportions (with the distal side narrower than the labial), whereas the remaining 44% have moderate scrofic proportions (with a La/Di ratio above 80%

in 30 specimens and a single specimen with a La/Di ratio around 75%). In contrast, the three described c1ms display lower La/Di ratios (61%, 70%, and 75%), and indeed they display a narrower labial side than all the c1ms of *L. splendens* measured by Van der Made (1996b: fig. 48). These differences are even more marked regarding the seven c1ms of *L. splendens* from Sant Quirze measured by Van der Made (1996b: fig. 48), which display La/Di ratios between 110 and 140% and a labial side more than twice wider than the specimens here attributed to '*Pa.*' *valentini*. The latter, like those of other tetraconodontines included in the comparative sample, display a clearly scrofic morphology, with a very asymmetric cross section characterized by a narrowest labial side and a broadest lingual side, which is 64–79% broader than the labial (Additional file 1: Table S2). In cross-sectional dimensions and proportions (Additional file 1: Table S2), they extensively overlap with the c1ms of *V. steinheimensis*, which display a lingual side 46–111% broader than the labial, albeit being on their upper size range. Compared with the SQ-TF specimens, a c1m of *R. matritensis* from Göriach is slightly smaller and displays a greater asymmetry between the lingual and the labial sides (the former about twice the latter), but the latter is not the case for an apical fragment from the same site, whereas no comparable measurements are available for other specimens attributed to either *C. simorrensis* or *R. matritensis*. Despite overall similarities in c1m shape among the aforementioned taxa (Additional file 1: Table S3), the c1ms of *V. steinheimensis* and *C. simorrensis* display a more marked concavity along the labial side than the SQ-TF specimens, and at least the most complete specimen of *V. steinheimensis* from CB (McKenzie et al., 2024) further differs by a more markedly labial curvature toward the tip. No suitable c1m pictures of *R. matritensis* from Göriach are available—as the specimen depicted by Hofmann (1893) only preserves the tip—but it may be ascertained based on a c1m from Simorre attributed to this species by Pickford and Laurent (2014). The c1ms of *C. simorrensis* differ from all other taxa considered here, including *R. matritensis*, by the presence of a longitudinal ridge of cementum along the distal side, which mostly relies on the comparison between the *C. simorrensis* specimens from Carpetana (Pickford, 2013b) and the aforementioned specimen from Simorre. However, as noted by Pickford and Laurent (2014) based on Stehlin (1900), this feature can also be ascertained in a c1m from the type locality of *C. doati* (see Discussion for additional remarks in this regard).

The single c1f from SQ-TF displays similar size and proportions (Additional file 1: Table S2) than those previously attributed to '*Pa.*' *valentini* except for being slightly narrower in absolute terms. Taken overall, despite overlapping in proportions, the c1fs of '*Pa.*' *valentini* are larger than the few c1fs reported for *V. steinheimensis* and *C. simorrensis*. On morphological grounds, the described specimen is the first c1f of '*Pa.*' *valentini* enabling an adequate description of the occlusal shape of this tooth locus, because those previously described by McKenzie et al. (2023a, 2024) from CCN20 and CB are heavily worn. These specimens display a somewhat stouter root than the SQ-TF c1f but, as far as it can be ascertained, are consistent in shape. Although root development cannot be properly evaluated in the few available specimens of *V. steinheimensis*, the latter display a very different crown shape, being somewhat lower-crowned and possessing along the distal facet a much deeper fossid flanked by sharper and more distinct ectocristid and postcristid. This is difficult to evaluate based on the available pictures of the c1fs of *C. simorrensis* from Przeworno 2 and *R. matritensis* from Göriach, which appear higher-crowned than those of *V. steinheimensis* but differ from those of '*Pa.*' *valentini* by being less labiolingually compressed and, in the case of the Przeworno 2 specimens, by displaying a much slenderer root.

Lower premolars The newly reported p1 from SQ-TF closely resembles in size and shape that previously described by Pickford (2014) from the same site, except for the slightly developed prestylid and better developed cuspule-like developments along the protopostcristid. When considered together, these two p1s are slightly longer than but display similar proportions to those from CB attributed to the same taxon (McKenzie et al., 2024; Fig. 13A; Additional file 1: Table S2). McKenzie et al. (2023a: fig. 9e) further identified a lower premolar from CCN20 (IPS95813) as a p1 of '*Pa.*' *valentini*, but this specimen is most likely a dp2 of *Pr. palaeochoerus* and hence excluded from the comparative sample. The p1s of *V. steinheimensis* are shorter and generally also relatively stouter (albeit with some overlap) than those of '*Pa.*' *valentini*. In turn, the single p1 of *C. simorrensis* resembles in size and proportions the more abundant p1 sample of *R. matritensis* from Göriach, which overlap in length with both *V. steinheimensis* and '*Pa.*' *valentini* but are relatively stouter (and, with a single exception, also broader in absolute terms). In terms of occlusal shape (Additional file 1: Table S3), the two p1s from SQ-TF most closely resemble those of '*Pa.*' *valentini* from CB (McKenzie et al., 2024), despite some variation in the inclination of the protopostcristid in both samples. Furthermore, the bifurcation of the protopostcristid at the level of hypoconid can only be ascertained, even if less clearly than in the SQ-TF specimens, in some but not all of the premolars from CB identified as p1s of '*Pa.*' *valentini*. However, an alternative identification of the latter as p2s of '*Pa.*' *valentini* is not supported based on size, suggesting

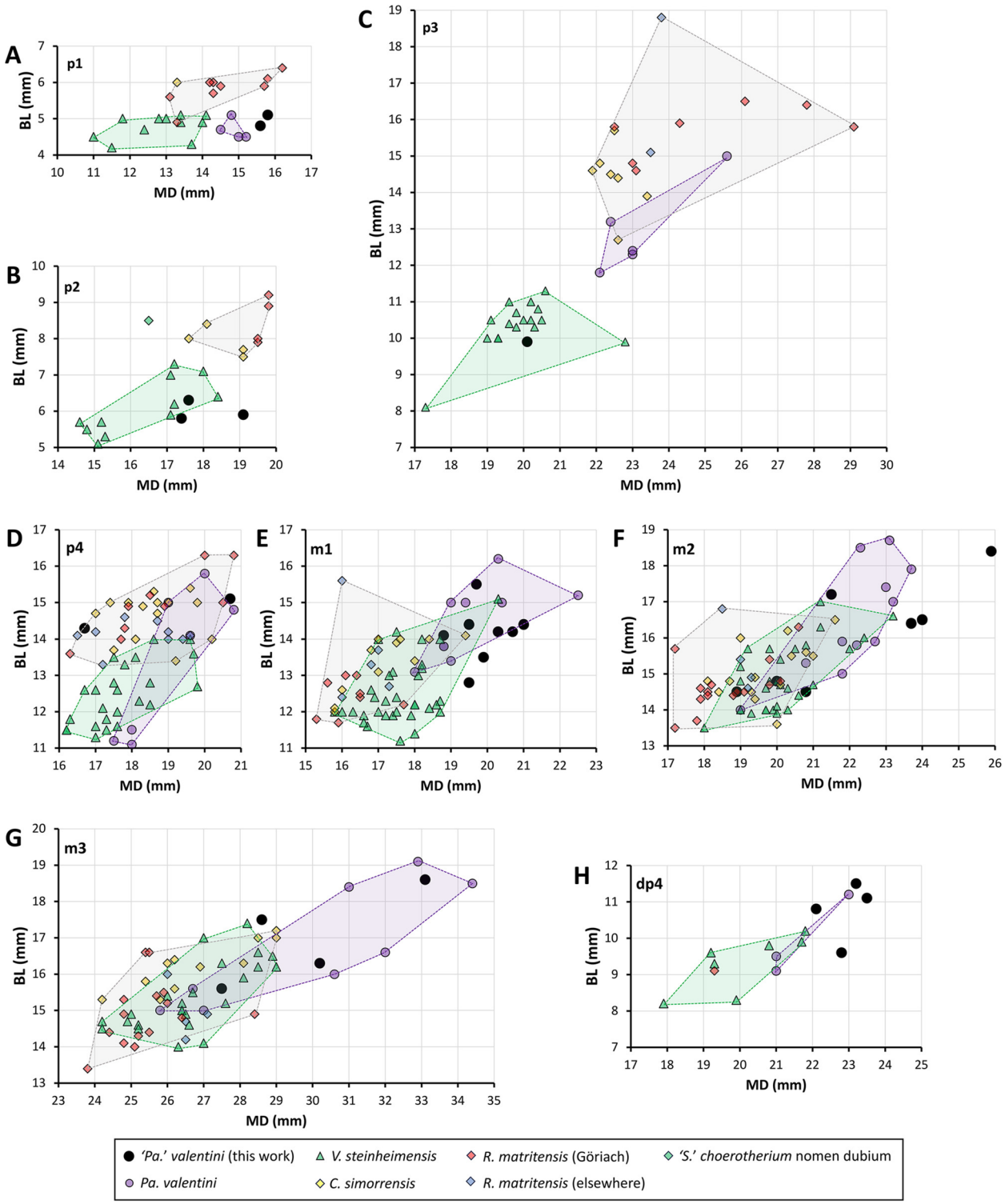

Fig. 13 Bivariate plots of BL vs. MD for the lower cheek teeth of '*Parachleuastochoerus*' *valentini* from Sant Quirze localities as compared with those of this species and other tetraconodontines from elsewhere: **A** p1; **B** p2; **C** p3; **D** p4; **E** m1; **F** m2; **G** m3; **H** dp4. Metrical data for the material from Sant Quirze localities are reported in Table 1, while those for the comparative sample have been taken from the literature (see Materials and methods for details on the published sources). Convex hulls outlining the variation of various species (without considering the remains from Sant Quirze localities) are depicted

that the distal shape of the p1 is intraspecifically variable in '*Pa.*' *valentini*. Indeed, similar variation can be ascertained in *V. steinheimensis*, with some p1s from Steinheim and Gratkorn displaying a bifurcated protopostcristid with a distolingually placed hypoconid and others from Steinheim and CB displaying an undivided or less clearly divided protopostcristid with a generally more centrally located hypoconid. Taken overall, this tooth locus is not very diagnostic between '*Pa.*' *valentini* and *V. steinheimensis*, although the former tends to display a more elongate p1 crown with a less steeply inclined protopostcristid. The p1s of *R. matritensis* from Göriach and *C. simorrensis* from Carpetana display a morphology reminiscent of that of '*Pa.*' *valentini*, with a distally bifurcated protopostcristid, except for the partial fusion of the roots, the apparent lack of a distinct hypoconid, and the above-mentioned less elongate occlusal contour. The differences are more marked in the case of the *C. simorrensis* p1s, which further differ because the protopostcristid bifurcates more mesially (closer to the protoconid) and the crown displays a more oval contour (with the distal half being much wider than the mesial).

The p2s from SQ-TF can be compared with that of the Fonte do Pinheiro mandible, here attributed to '*Pa.*' *valentini*, which overlaps in length (MD = 19.0 mm; Van der Made, 1989 provided no BL measurement). The p2s from SQ-TF further overlap considerably in dimensions, but minimally in proportions (Fig. 13B; Additional file 1: Table S2), with those of *V. steinheimensis*—excluding IPS92720 from CB (McKenzie et al., 2024), which was originally interpreted as a p2 (on the grounds of its small size) but is probably best interpreted as a p3 based on occlusal shape and proportions (see below). Despite the overlap in dimensions, the p2s of '*Pa.*' *valentini* tend to be relatively more elongate than those of *V. steinheimensis*. The p2s of *C. simorrensis* and *R. matritensis* from Göriach are relatively broader (and also absolutely broader in the case of *R. matritensis*) than those of '*Pa.*' *valentini* and *V. steinheimensis*. The p2 from Sansan, probably attributable to the same species represented by the type maxilla of '*S.*' *choerotherium* (*nomen dubium*), is smaller than those of *C. simorrensis* and, especially, *R. matritensis* from Göriach, but stouter than all the other specimens and broader in absolute terms than those of *V. steinheimensis* and '*Pa.*' *valentini*. With regard to occlusal morphology (Additional file 1: Table S3), the p2s from SQ-TF appear comparable in occlusal contour and general morphology with the single p2 previously available for '*Pa.*' *valentini* from Fonte do Pinheiro. In contrast, the p2s of *V. steinheimensis* differ from those of '*Pa.*' *valentini* in the presence of more or less marked buccal and lingual constrictions of the occlusal contour at the protoconid level, as well as the generally bifurcated protopostcristid with a sometimes better-developed hypoconid—although there is variation in these features. The p2s of *R. matritensis* from Göriach resemble those of '*Pa.*' *valentini* in the morphology of the protopostcristid and distinctiveness of the hypoconid, but differ in their less elongate and more distally expanded occlusal contour. These differences further apply to the two p2s from Villefranche d'Astarac figured by Pickford and Laurent (2014), including the lectotype mandible of *C. simorrensis* and another mandible assigned to *R. matritensis*, which further insinuate an incipient bifurcation of the protoprecristid. In contrast, the p2s from the mandibles of *C. simorrensis* from Carpetana resemble those of '*Pa.*' *valentini* in protopostcristid and hypoconid development. However, they more clearly differ from the latter than the above-mentioned specimens from Göriach and Villefranche d'Astarac in the more buccally tilted and less steeply inclined protoprecristid, the more marked buccolingual constriction of the occlusal contour at the protoconid level, and the greater expansion of the distal portion of the crown. A p2 from Sansan—originally identified as a P1 of *C. simorrensis* by Ginsburg (1977), subsequently identified as a p2 of the same species by Pickford (2012), and most recently attributed to *Retroporcus sindiensis* (Lydekker, 1878) by Van der Made (2020)—is too worn to allow for meaningful comparisons with '*Pa.*' *valentini* other than illustrating the much stouter occlusal contour of Sansan specimen (see the Discussion for further comments about its taxonomic attribution).

The single p3 from SQ-TF that is complete enough to take all measurements (MGSB48817) and the p3 mesial fragment (MGSB48859) newly reported here appear narrower than the other incomplete specimen (IPS96062 [IPS1857]) from the same site (Table 2), previously reported (but not figured) by Pickford (2014), as well as other p3s of '*Pa.*' *valentini* previously reported from elsewhere (Fig. 13C; Additional file 1: Table S2). The SQ-TF complete specimen falls instead within the p3 variation range of *V. steinheimensis*, which is characterized by a narrower crown in both absolute and relative terms. The above-mentioned lower premolar IPS92720 from CB, previously identified as a p2, is smaller than both species but fits well with the p3 proportions of *V. steinheimensis*. These comparisons suggest the size and proportions of the p3 are quite variable in both species, so that other occlusal details are probably more reliable to distinguish between them (see below). In turn, the p3s of *C. simorrensis* and *R. matritensis* considerably overlap in dimensions with those of '*Pa.*' *valentini* (except for the SQ-TF specimen reported here) but are broader on average, although differences in both size and proportions are more marked as compared with *V. steinheimensis*. It is noteworthy that the p3 sample of *R. matritensis* from

Table 2 Dental measurements (in mm) and indices (in %) of '*Parachleuastochoerus' valentini* from Sant Quirze[a]

Catalog No.	Tooth	MD/Li	BL/La	BLm/Di	BLd	BLI
IPS96058 [VP1013]	R I1	14.2	11.5			81.0
IPS30986	R I1	16.4	11.5			70.1
MGSB48853.1	L I1	>9.2	>8.7			–
MGSB48853.2	R I1	>7.6	>5.5			–
MGSB48842	R I1	17.7	10.4			58.8
MGSB30487	L I2	14.4	6.0			41.7
MGSB48862	L I2	13.6	7.2			52.9
MGSB48559	R I2	14.3	8.0			55.9
IPS96051 [VP1032]	R I3	14.3	7.5			52.4
MGSB48918	L C1f	16.1	7.9			49.1
MGSB49727	R C1m	25.1	21.8			86.9
IPS31069 [VP1009]	L C1m	32.5	22.2			68.3
IPS95962 [4290]	R P1	14.0	5.3			37.9
IPS96073 [VP998]	R P2	17.5	6.3			36.0
IPS96074 [VP999]	L P2	17.7	6.5			36.7
MGSB48854	R P2	17.1	6.4			37.4
MGSB48860	L P2	–	>6.0			–
IPS31028 [IPS1980]	R P2	18.6	7.0			37.6
IPS96072 [IPS1858]	R P2	>15.6	6.2			–
MGSB48586	R P3	20.1	14			69.7
MGSB48587	R P3	20.8	15.1			72.6
IPS138283	R P4	>13.9	>11.2			–
MGSB48937	L P4	15.4	21.0			136.4
MGSB48836	L P4	15.6	19.7			126.3
IPS96056 [IPS1825]	R P4	14.1	18.5			131.2
IPS31065a [VP1014]	L P4	14.3	19.0			132.9
IPS31065b [VP1014]	L M1	18.3	17.3	17.3	16.9	94.5
IPS31065c [VP1014]	L M2	21.7	20.1	20.1	(19.1)	92.6
IPS31065d [VP1014]	L M3	29.7	19.8	19.8	16.6	66.7
IPS96055 [VP1015]	L M1	19.8	18.3	18.3	18.0	92.4
IPS31026 [IPS1881]	L M1	19.2	17.5	17.5	17.0	91.1
MGSB48939	R M1	19.2	18.3	18.3	(18.1)	95.3
MGSB48831	R M1	19.2	(17.6)	17.6	–	(91.7)
IPS96081 [IPS1794]	R M1	17.9	16.1	15.6	16.1	89.9
MGSB48915	L M1	17.2	>15.7	–	>15.7	–
MGSB48824	L M1	>15.5	>15.3	–	15.3	–
MGSB49725	R M1	–	(15.5)	15.5	–	–
IPS63283	R M1	–	(17.6)	17.6	–	–
IPS30988	R M1	–	(17.8)	–	17.8	–
IPS31061a [VP1007]	R M1	18.3	17.3	17.3	16.8	94.5
IPS31061a [VP1007]	R M2	21.3	19.9	19.9	19.9	93.4
IPS31061b [VP1007]	R M3	26.7	19.3	19.3	16.6	72.3
MGSB48914	R M2	20.9	19.4	19.4	17.5	92.8
MGSB48832	L M2	21.2	20.2	20.2	19.7	95.3
MGSB48814	R M2	23.9	(19.9)	–	19.9	(83.3)
MGSB48816	L M2	22.5	20.3	20.3	18.9	90.2
MGSB48835	L M2	21.4	20.2	20.1	20.2	94.4
MGSB49726.2	R M2	>21.4	–	–	–	–
IPS31078 [55]	R M2	>15.8	>20.3	>20.3	18.4	–

Table 2 (continued)

Catalog No.	Tooth	MD/Li	BL/La	BLm/Di	BLd	BLI
MGSB48833	L M2?	(23.9)	<21.9	–	–	–
MGSB48841	L M2?	–	>18.8	>18.8	–	–
IPS38614	R M3	>16.7	>19.3	–	17.2	–
MGSB48829	R M3	26.6	19.6	19.6	15.9	73.7
MGSB48830	L M3	25.8	19.6	19.6	15.6	76.0
MGSB48815	R M3	27.4	19.3	19.3	15.8	70.4
MGSB48813	L M3	26.4	20.0	20.0	16.6	75.8
IPS95947 [514]	R M3	(27.0)	20.0	20.0	16.6	(74.1)
IPS31027 [IPS1882]	L M3	27.5	20.9	20.9	18.3	76.0
IPS27505 [IPS1063]	L dp4	23.5	11.1			47.2
IPS27505 [IPS1063]	L m1	20.3	14.2	14.2	13.5	70.0
IPS27505 [IPS1063]	R m1	21.0	14.4	14.4	12.6	68.6
MGSB30480	R m1	19.7	15.5	15.5	15.1	78.7
MGSB30480	R m2	21.5	17.2	17.2	16.3	80.0
MGSB30480	R m3	28.6	17.5	17.5	14.5	61.2
MGSB30490	L m2	18.9	14.5	14.5	(13.7)	76.7
MGSB30490	L m3	(27.5)	15.6	15.6	14.2	(56.7)
IPS96057 [VP1008, 56]	L i1	8.6	11.8			137.2
MGSB48848	R i1	8.2	12.4			151.2
MGSB48851	R i1	7.9	11.8			149.4
MGSB48853.3	L i1	(7.4)	>8.6			–
MGSB48853.4	R i1	(7.1)	>7.6			–
MGSB48913	L i1	7.5	11.7			156.0
MGSB48850	L i2	>8.4	>6.8			–
MGSB48843	L i2	8.9	14.1			158.4
MGSB48936.1	L i2?	–	>6.9			–
MGSB48849	L i2	9.5	14.8			155.8
IPS96087 [VP1004, 60]	R i3	7.1	10.5			147.9
IPS95966 [5456]	L i3	7.0	10.8			154.3
IPS96086 [IPS1859]	L i3	6.6	9.9			150.0
MGSB48863	L i3	6.4	12.6			196.9
IPS31060 [VP1003]	L i3	6.4	12.4			193.8
MGSB30471 [24]	R c1m	18.9	11.4	15.2		
MGSB30471 [23]	L c1m	17.5	10.7	15.1		
MGSB30471 [22]	L c1m	17.7	9.9	16.1		
MGSB48852	L c1f	14.2	8.0			56.3
IPS96063 [VP1002]	L p1	15.6	4.8			30.8
MGSB48856	L p1	15.8	5.1			32.3
MGSB48855	L p2	17.6	6.3			35.8
MGSB48857	R p2	17.4	(5.8)			(33.3)
MGSB48858 + MGSB48861	R p2	(19.1)	5.9			(30.9)
MGSB48817	L p3	20.1	9.9			49.3
IPS96062 [IPS1857]	R p3	>16.8	>10.0			–
MGSB48859	L p3	–	>8.5			–
MGSB48588	L p4	20.7	15.1			72.9
MGSB48951	L p4	16.7	14.3			85.6
IPS96060 [VP996]	L m1	20.7	14.2	14.2	14.1	68.6
MGSB30489	L m1	19.5	12.8	12.8	12.4	65.6
MGSB48821	R m1	19.5	14.4	13.7	14.4	73.8

Table 2 (continued)

Catalog No.	Tooth	MD/Li	BL/La	BLm/Di	BLd	BLI
MGSB30475	R m1	19.9	13.5	13.0	13.5	67.8
MGSB48919	L m1	(18.8)	(14.1)	12.8	(14.1)	(75.0)
MGSB48822	L m1	>18.0	13.6	13.6	13.4	–
MGSB48873	R m2	20.8	14.5	14.3	14.5	69.7
IPS96061 [VP997]	L m2	20.0	14.8	14.6	14.8	74.0
MGSB48818	R m2	25.9	18.4	18.4	17.5	71.0
MGSB48820	L m2	24.0	16.5	16.5	16.3	68.8
MGSB48819	R m2	23.7	16.4	16.4	15.9	69.2
MGSB48823	R m2	>15.2	17.8	17.8	–	–
IPS119090	L m2	>12.2	17.0	17.0	–	–
MGSB48840	R m2	–	>14.3	–	>14.3	–
MGSB48827	R m2	>13.7	>14.6	–	>14.6	–
MGSB30488	L m3	30.2	16.3	16.3	15.5	54.0
MGSB48949	R m3	33.1	18.6	18.6	15.6	56.2
IPS119091	R m3	(28.3)	>15.0	–	15.0	–
MGSB48828	R m3	>19.9	>16.1	–	16.1	
MGSB48825	L m3	>21.9	>15.6	–	15.6	–
MGSB48826	R m3	>15.5	–	–	–	–
IPS94956 [VP1005]	L DI1	8.7	5.7			65.5
MGSB48865	L DI1	8.3	5.6			67.5
MGSB48868	R DI1	8.2	5.5			67.1
MGSB48869	L DI1	9.6	5.4			56.3
IPS94954 [IPS1860]	R DI1	7.9	5.3			67.1
IPS95997 [VP988]	L DI2	12.2	5.0			41.0
MGSB48866	L DI3	10.1	3.8			37.6
IPS95945 [5462]	L DP2	16.7	6.0			35.9
IPS96083 [VP1006]	R DP2	16.8	6.2			36.9
IPS96070 [VP1011]	R DP3	15.9	11.4			71.7
IPS96077	R DP3	>10.5	>7.7			–
MGSB48839	L DP4	16.5	13.5			81.8
IPS31080 [VP1010]	L DP4	16.9	14.5			85.8
IPS95961 [4292]	R DP4	16.4	14.0			85.4
IPS96069 [VP1001]	R DP4	15.3	13.9			90.8
MGSB48864.1	L di1	4.6	5.5			119.6
IPS31024 [IPS1908]	R di1	4.6	5.9			128.3
IPS96085 [VP1000]	L di1	4.6	5.6			121.7
IPS96084 [VP1028]	R di2	5.2	7.7			148.1
MGSB48864.2	L di2	4.7	6.3			134.0
MGSB48936.2	L dp2	>12.0	(5.5)			–
MGSB48936.3	R dp3	–	>8.0			–
IPS96075	R dp4	22.8	9.6			42.1
MGSB48838	R dp4	23.2	11.5			49.6
IPS31073 [VP1012]	L dp4	22.1	10.8			48.9
IPS95965	L dp4	–	>9.3			–
IPS96076	R dp4	–	>7.9			–

See Table 1 for provenance. Measurements within parentheses are estimates, whereas a 'greater than' (>) symbol denotes that the actual measurement would have been higher than that provided due to damage, and an 'en dash' (–) indicates that no meaningful measurement can be taken owing to incomplete preservation

[a] For measurement abbreviations, see Materials and methods

Göriach displays considerable variation (particularly in length and, hence, proportions), in agreement with the condition displayed by *V. steinheimensis* as well as '*Pa.*' *valentini* (especially when the SQ-TF specimen is considered). Regarding occlusal shape (Additional file 1: Table S3), the previously figured p3s of '*Pa.*' *valentini* vary considerably in occlusal contour (elliptical to oval, and variably constricted lingually at the protoconid level)—in further agreement with their aforementioned metrical variation. However, they otherwise display a consistent occlusal shape, characterized by: a pointed, centrally located, and distally tilted protoconid; a thick, blunt, straight, and moderately steep protoprecristid that ends in a low and mildly developed prestylid; and a similarly developed protopostcristid, which is flanked by shallow buccal and lingual clefts and usually bifurcates, giving rise to a very restricted, shallow, and distally open fossid with a poorly-developed and distobuccally located hypoconid. The p3s from SQ-TF fit well with this morphological pattern, except that the protopostcristid does not bifurcate (only ascertainable in the more complete specimen) and that the protoprecristid appears more steeply inclined; the occlusal contour of the complete p3 is most similar to that of the Fonte do Pinheiro mandible figured by Roman (1907). The p3s of *V. steinheimensis* also show some variation in occlusal contour (more or less elongate, subelliptical to suboval, with or without lingual constriction) and distal development of the protopostcristid and hypoconulid (non-bifurcated and centrally located vs. bifurcated and distobuccally placed). However, they are generally slenderer than those of '*Pa.*' *valentini*, from which they further differ in possessing a better developed prestylid, more concave crown walls along the protoprecristid, much deeper buccal and lingual clefts at the level of the protopostcristid, generally a more distinct (albeit poorly developed) metaconid just distally or distolingually from the protocristid (only ascertainable on unworn to lightly worn specimens), and a more rootwardly extended cervix on the distal crown portion. The p3s of both *R. matritensis* and *C. simorrensis* are somewhat variable in occlusal contour but more closely resemble those of '*Pa.*' *valentini* in most of the aforementioned features. The only exception is the greater distal than mesial rootward extension of the cervix in the specimens of *R. matritensis* and *C. simorrensis*. In this regard, the p3 from Kleineisenbach attributed to '*Pa.*' *valentini* by Pickford (2016) is most compatible with this species, differing from *C. simorrensis* and *R. matritensis* in the less pronounced rootward extension of the cervix distally. Furthermore, *R. matritensis* and *C. simorrensis* differ from both '*Pa.*' *valentini* and *V. steinheimensis* by displaying a hypertrophied (longer, broader, and much higher) p3 as compared with the remaining premolars (including the p4), thus paralleling the hypertrophy of the P3 in the upper dentition.

The two p4s from SQ-TF considerably but not completely overlap in size and proportions with the small sample of p4s previously available for '*Pa.*' *valentini* (Fig. 13D; Additional file 1: Table S2). In particular, one of the described specimens fits well in both size and proportions, whereas the other is shorter and relatively broader. Compared with the larger sample available for *V. steinheimensis*, one of the SQ-TF specimens is larger (both longer and broader) but displays similar proportions, whereas the smaller p4 from SQ-TF is broader in both absolute and relative terms—overall suggesting that the SQ-TF specimens fit worse with the variation of *V. steinheimensis* than that of '*Pa.*' *valentini*. The p4s of *R. matritensis* and *C. simorrensis* show very similar size and proportions, being broader on average (with substantial overlap) than those of *V. steinheimensis*, but generally showing broader proportions at comparable p4 length. In contrast, *'Pa.' valentini* shows a broader range of variation, with some p4s (including those from SQ-TF) more closely resembling the proportions of *R. matritensis* and *C. simorrensis*, and others (from Saint-Gaudens and CB) being slenderer (even more so than those of *V. steinheimensis*). This illustrates that the p4 proportions of '*Pa.*' *valentini* (and the associated occlusal contour) are not particularly diagnostic, unlike other details of its occlusal morphology. In the latter regard (Additional file 1: Table S3), the two p4s from SQ-TF resemble those of '*Pa.*' *valentini* from elsewhere in multiple features, including the presence of a distinct metaconid apex just distolingually from the protoconid (in some of the least worn specimens, such as mandible from El Buste, attributed by Pickford & Laurent, 2014 to *C. doati*), the distolingually oriented protopostcristid, and the distally and centrally located hypoconid. The p4s of *V. steinheimensis* similarly display a metaconid distolingually placed from the protoconid (in unworn specimens) and a well-developed and centrally located hypoconid, but they differ from those of '*Pa.*' *valentini* in the generally more oval (distally broader) occlusal contour (although it is variable in '*Pa.*' *valentini*, as illustrated by the Fonte do Pinheiro specimen), the stronger and usually higher prestylid (associated to better developed cingular developments and/or deeper clefts along the protoprecristid), and the more concave crown walls along the protopostcristid (usually with a broader and/or deeper buccal cleft). The p4s of *R. matritensis* from Göriach and elsewhere, as well as those attributed to *C. simorrensis*, are somewhat variable in occlusal contour (generally subrectangular to suboval) but nevertheless stouter and less elongate than in the two aforementioned taxa, differing from the generally elliptical p4 occlusal contour of '*Pa.*' *valentini*

(but see the Fonte do Pinheiro specimen). Furthermore, in *R. matritensis* and *C. simorrensis* the prestylid is less well developed, the crown walls along the protoprecristid are more inflated (less concave), and the buccal cleft along the protopostcristid is shallower than in *V. steinheimensis*, most closely resembling '*Pa.*' *valentini* in these regards. Nevertheless, although in *R. matritensis* and *C. simorrensis* the p4 appears much smaller than the p3, the former tooth is much broader than the m1, differing from the condition of both '*Pa.*' *valentini* and *V. steinheimensis*, where the p4 is similar in breadth to the m1.

Lower molars The described m1s and m2s display similar proportions and overlap to some extent with one another in breadth and, particularly, length, although the m2s are larger on average. The studied sample almost completely overlaps in m1 (Fig. 13E) and m2 (Fig. 13F) size and proportions (Additional file 1: Table S2) with '*Pa.*' *valentini* from elsewhere, only minimally expanding the range of variation previously recorded for this species (including those attributed to *C. doati* by Pickford, 2016). The described sample further overlaps to a large extent with the m1 and m2 size and proportions recorded for *V. steinheimensis*, but surpasses the upper size range of the latter, thereby indicating a better fit with the metrical variation of '*Pa.*' *valentini*. Size differences are more clear-cut as compared with *R. matritensis* and *C. simorrensis*, which generally display smaller m1s and m2s than '*Pa.*' *valentini*, although with some overlap. In contrast, there seem to be no noticeable differences in m1 and m2 proportions among the species included in the comparative sample. The described m1s and m2s display a generalized tetraconodontine occlusal morphology—with marked Fürchen and profuse but moderately developed enamel wrinkling when unworn or lightly worn, and a generally more conspicuous (but not abrupt) buccal than lingual constriction between the mesial and the distal lobes. In these regards (Additional file 1: Table S3), they are fully comparable to the variation displayed by '*Pa.*' *valentini* but also *V. steinheimensis* or even (leaving proportions aside) *R. matritensis* and *C. simorrensis*.

The four m3s from the studied sample almost overlap completely with the previously documented variation of '*Pa.*' *valentini* in size and proportions (Fig. 13G; Additional file 1: Table S2), except for extending slightly the upper range of occlusal proportions. In contrast, despite a considerable overlap, the m3s of '*Pa.*' *valentini* are larger on average than those of *V. steinheimensis* (despite considerable overlap), with the latter species almost completely overlapping the joint range of variation in m3 dimensions and proportions of *C. simorrensis* and *R. matritensis* (with the latter tending to fall on the lower size range of *C. simorrensis* and *V. steinheimensis*). In occlusal shape (Additional file 1: Table S3), the described m3s show some variation in occlusal contour—ranging from those with a central lobe subequal to the mesial one and an abruptly tapering distal lobe (Fig. 10U) to a more triangular contour that progressively tapers distalward (Fig. 10W–X)—although in all instances they display an only slightly buccally tilted distal lobe. This variation can be accommodated within that previously recorded for the m3s of '*Pa.*' *valentini*, which even include some specimens in which the distal lobe is more distinct from the central one or more markedly tilted buccally. The m3s of *V. steinheimensis* also show variation in occlusal contour and degree of distal tapering, but are generally more clearly subtriangular and uniformly tapering, so that the distal lobe tends to be less developed, less distinct from the central lobe, and more markedly oriented distobuccally. The m3s of *R. matritensis* from Göriach and *C. simorrensis* generally taper distally less markedly than in *V. steinheimensis* and some specimens of '*Pa.*' *valentini*, with the central lobe being subequal in size to the mesial one, as in other specimens of '*Pa.*' *valentini*. Furthermore, although in *R. matritensis* from Göriach and *C. simorrensis* the buccal tilting and breadth of the distal lobe is variable, the latter is generally broader than in *V. steinheimensis* and less distinct than in '*Pa.*' *valentini*. A similar morphology is displayed by other m3s attributed to *R. matritensis*, where the buccal tilting of the distal lobe is very variable and also ranges from almost non-existent to very marked (even when considering specimens from the type locality).

Upper deciduous teeth The described DI1s (Fig. 11A–E) are slightly longer and relatively narrower (Additional file 1: Table S2) than those from CB previously attributed to '*Pa.*' *valentini* by McKenzie et al. (2024). However, as explained above, we consider that two upper incisors from this site—previously identified as I2s of '*Pa.*' *valentini* by McKenzie et al. (2024) but which strikingly differ from the I2s from SQ-TF—are indeed larger DI1s of the same species. The possibility remains that the smallest tetraconodontine DI1s from CB belong instead to *V. steinheimensis*, also recorded there, but the largest specimens fit sufficiently well in size and shape (Additional file 1: Table S3) with those described herein so as to be attributed to the same species (i.e., '*Pa.*' *valentini*). The lack of additional deciduous incisors reported from the literature for the species included in the comparative sample precludes more detailed comparisons. If correctly identified, the DI2 and DI3 from SQ-TF reported herein represent the first description of these tooth loci for '*Pa.*' *valentini*, suggesting that they display similar shape and proportions, only differing in the slightly larger and higher crown of the DI2.

The two DP2s from SQ-TF are slightly larger than but resemble in proportions those from CB previously

attributed to '*Pa.*' *valentini*, being more clearly larger and slenderer than those from the same site assigned to *V. steinheimensis* (Additional file 1: Table S2). The SQ-TF specimens also fit better in occlusal morphology (Additional file 1: Table S3) with previously figured DP2s of '*Pa.*' *valentini*, whereas those of *V. steinheimensis* display an even more asymmetrical contour and a more buccolingually expanded distal crown portion, a better developed metacone (much higher than the prestyle), a concave buccal crown wall along the paraprecrista, and more marked buccal and lingual clefts at the level of the parapostcrista. In turn, the single complete DP3 from SQ-TF closely resembles in size and proportions the specimens previously attributed to *'Pa.' valentini* and is, in contrast, slightly broader than those of *V. steinheimensis* (Additional file 1: Table S2). Besides these slight metrical differences, the DP3 described herein more closely resembles those of '*Pa.*' *valentini* than those of *V. steinheimensis* in the more marked constriction between the mesial and distal lobes (resulting in a rather pear-shaped, less subtriangular occlusal contour). Finally, the described DP4s overlap to a large extent in size and proportions with those of '*Pa.*' *valentini* but are in contrast larger than those of *V. steinheimensis* (Fig. 13H; Additional file 1: Table S2), albeit with some overlap. A DP4 of *C. simorrensis* from Villefranche d'Astarac overlaps with both taxa. In occlusal shape (Additional file 1: Table S3), the described DP4s also fit better with those previously attributed to '*Pa.*' *valentini* than to those of *V. steinheimensis*. As previously noted by McKenzie et al. (2024), the DP4s of these species differ in the generally straighter and more uniformly inclined mesial contour as well as the less transversely aligned distal cusps of '*Pa.*' *valentini*. A DP4 from Villefranche d'Astarac attributed to *R. matritensis* by Pickford and Laurent (2014) displays an intermediate morphology, more closely resembling '*Pa.*' *valentini* in the mesial contour but *V. steinheimensis* in the alignment of the distal cusps.

Lower deciduous teeth The di1s described herein (Fig. 11P–R) resemble in size and proportions the few specimens previously attributed to '*Pa.*' *valentini* and *V. steinheimensis* in the literature (Additional file 1: Table S2). In terms of occlusal shape (Additional file 1: Table S3), the di1s from SQ-TF fit well with those previously attributed to '*Pa.*' *valentini*, whereas those assigned to *V. steinheimensis* are similar but seemingly display a more labiolingually compressed apical portion of the crown. A lower deciduous incisor of *R. matritensis* from Göriach, originally interpreted as a possible di2 or di3 (Hofmann, 1893), is morphologically similar (as far as it can be appreciated from the figure) to both species, being thus interpreted as a di1. In turn, the di2s from SQ-TF are also similar in dimensions to those previously assigned to '*Pa.*' *valentini* and *V. steinheimensis* (Additional file 1: Table S2), although the small sample sizes preclude more meaningful comparisons. In terms of shape (Additional file 1: Table S3), the described di2s agree well with a previously reported specimen of '*Pa.*' *valentini* from CB, overall differing from those of *V. steinheimensis* from the same site in the more marked mesial tilting of the crown. Nevertheless, the new specimens reported here differ from the CB ones in displaying a thicker endocristid (more similar to specimens previously assigned to *V. steinheimensis*). As noted by McKenzie et al. (2024), the identifications of the CB di2s must be considered tentative as currently available samples are too scarce to adequately assess intra- and interspecific variation. Despite of this, the SQ-TF sample shows that differences in di2 endocristid thickness are probably intraspecifically variable within '*Pa.*' *valentini*, as it is also the case of other features such as the lingual contour of the poststylid.

The partial dp2 from SQ-TF (BL > 6.9 mm) is much broader than that attributed to *V. steinheimensis* (Additional file 1: Table S2), further differing from the latter in occlusal shape (Additional file 1: Table S3) by displaying a stouter contour, a better developed prestylid, a less pointed protoconid, and a larger hypoconid flanked by more marked buccal and lingual clefts. McKenzie et al. (2023a: fig. 11p) tentatively identified a lower premolar from CCN20 (IPS114102) as a dp2 of '*Pa.*' *valentini*, but its morphology fits better with a large dp2 of *Pr. palaeochoerus*. Given that the SQ-TF partial specimen vaguely resembles the p2s and p3s of '*Pa.*' *valentini*, but differs from them in several occlusal details, the smaller size, and the lower crown, the most reasonable option is to identify it as the actual dp2 of this species and reassign the CCN20 specimen to *Pr. palaeochoerus*. Something similar occurs with the dp3, as McKenzie et al. (2024: fig. 13s–v) identified several partial lower premolars from CB (IPS92881, IPS92779, IPS93153, and IPS92388) as tetraconodontine but, based on the higher occlusal relief of the dp3s of *V. steinheimensis*, *C. simorrensis*, and *R. matritensis* (Additional file 1: Table S3), the CB specimens most likely correspond to dp2s and dp3s of *Pr. palaeochoerus*. In contrast, the distal crown fragment from SQ-TF (BL > 8.0 mm) more closely resembles the distal morphology of the p3 of '*Pa.*' *valentini* at a smaller size, being thus interpreted as a dp3 of this taxon, even though it is slightly broader than previously reported specimens of both *'Pa.' valentini* and *V. steinheimensis* (Additional file 1: Table S2). Finally, the dp4s from SQ-TF and SQ-PN closely resemble in size and proportions the dp4s from elsewhere attributed to '*Pa.*' *valentini* and are larger than those attributed to *V. steinheimensis*, even though the two species overlap to a large extent (Fig. 13H; Additional file 1: Table S2). A dp4 of *R. matritensis* from Göriach is

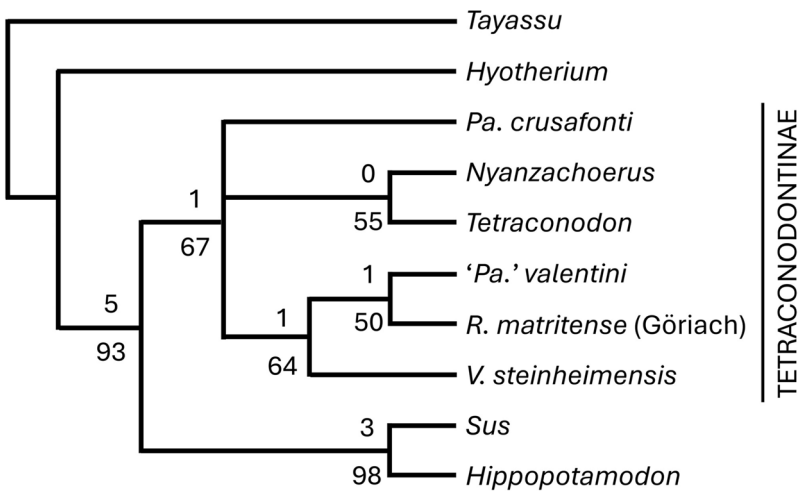

Fig. 14 Bootstrap 50% majority-rule consensus tree. Those ingroup clades with bootstrap support ≥ 50% are depicted, with bootstrap support indicated below nodes and Bremer's indices above. The analysis found five most parsimonious trees, whose strict consensus (see Additional file 1: Fig. S1) failed to recover one of the clades weakly supported by bootstrap (Bremer's index = 0)

smaller than those of '*Pa.*' valentini but overlaps in proportions, more closely resembling in size those of *V. steinheimensis*. In terms of occlusal morphology (Additional file 1: Table S3), the described specimens also closely resemble previously reported specimens of '*Pa.*' *valentini* from elsewhere while differing from those of *V. steinheimensis* in a few details, such as the less protruding mesial cingulid, the more distally protruding distal cingulid (less rounded distal contour), and the more transversely aligned pairs of crests. Although a dp4 of *R. matritensis* is also available from Göriach, the only available published picture does not allow us to compare it with the described specimens.

Cladistic analysis

Our parsimony analysis recovered five most parsimonious cladograms with a tree length of 52 steps (CI = 0.642, HI = 0.359, RI = 0.672, RCI = 0.431). They all retrieved *Hyotherium* as the basal-most ingroup taxon and recovered the monophyly of both the analyzed suines and tetraconodontines. Among tetraconodontines, the bootstrap 50% majority-rule consensus yielded a polytomy between *Parachleuastochoerus* s.s. (i.e., based on the type species of the genus), a clade including *Tetraconodon* + *Nyanzachoerus*, and another clade including the three taxa newly coded in this paper (Fig. 14). The strict consensus yielded the same results for the latter taxa but collapsed the clade of *Tetraconodon* + *Nyanzachoerus* (Additional file 1: Fig. S1). Among the newly coded tetraconodontines, '*Pa.*' *valentini* clustered with the Göriach sample (variously attributed to *R. matritensis* or *C. simorrensis* s.l.) exclusive of *V. steinheimensis*, indicating that the former are more closely related to one another, but also more so to *V. steinheimensis* than to *Parachleuastochoerus* s.s. This topology is not very robust, as it only took an additional step to entirely collapse the tetraconodontine clade with suines—whose monophyly appears in contrast much more robust, like that of tetraconodontines + suines to the exclusion of *Hyotherium*. Tetraconodontines + suines are defined by 10 synapomorphies (of which seven unambiguous), suines by six (four unambiguous), tetraconodontines by eight (four unambiguous), and the clade including the three tetraconodontines newly coded here by seven (although only three unambiguous; Additional file 1: Table S6). In contrast, '*Pa.*' *valentini* and the Göriach sample are united by a single unambiguous synapomorphy.

Discussion

Taxonomic attribution of the described material

Based on dental morphology (size, proportions, and occlusal shape), the described tetraconodontine sample from SQ-TF—which considerably enlarges that previously described by Pickford (2014) from the same site—as well as SQ-PN and CF2 is attributable to a single species. This sample most closely resembles the hypodigm of '*Pa.*' *valentini* sensu McKenzie et al. (2024), only slightly expanding its known metrical and shape variation. In contrast, the described sample differs in multiple tooth loci from both *V. steinheimensis* sensu McKenzie et al. (2024)—i.e., including *V. grivensis* as its junior synonym (contra Pickford, 2014, 2016)—and both *R. matritensis* and *C. simorrensis* s.s., being accordingly attributed to '*Pa.*' *valentini*. It is noteworthy that this species generally more closely resembles *R. matritensis* and *C. simorrensis* than *V. steinheimensis* in tooth shape,

despite more closely resembling the latter in the reduced size of the distal premolars as compared with the molars. It is also remarkable that, among the SQ-TF tetraconodontine sample, there are no remains attributable to *Pa. huenermanni*, with previous reports (e.g., Pickford, 2014) being demonstrably based—as attested by Golpe-Posse (1971)—on mislabeled specimens from other sites housed at the ICP.

Our comparisons between the described material and that previously included in '*Pa.*' *valentini* supports the hypodigm composition favored by McKenzie et al. (2024)—with the single exception of some specimens from CCN20 and CB (such as C1fs) that are here reassigned to *Pr. palaeochoerus*. The hypodigm composition of '*Pa.*' *valentini* considered here, following McKenzie et al. (2024), includes most specimens previously attributed to *C. doati* by Pickford and colleagues (Pickford & Laurent, 2014; Pickford, 2013a, 2014, 2016) but excludes the material from Mira (including the holotype of *C. melendezi*, here included in *C. simorrensis*). Particular mention deserves in this regard the restricted tetraconodontine dental sample from Kleineisenbach—including a C1m, a P3, an M3, and p3 (Pickford, 2016)—which was formerly attributed to *C. simorrensis* (e.g., Fortelius et al. 1996) and subsequently reassigned to '*Pa.*' *valentini* by Pickford (2016). This M3 is the smallest one attributed to '*Pa.*' *valentini* and, as noted by McKenzie et al. (2024), it seems to fit better in size and proportions with those of *V. steinheimensis*. However, an attribution to the latter species is not supported by the C1m and P3 morphology from the same site, which support instead an attribution to '*Pa.*' *valentini*. As noted by Pickford (2014, 2016), the C1m morphology of '*Pa.*' *valentini* is quite distinctive, so that the somewhat more labiolingually compressed crown of the Kleineisenbach C1ms could merely reflect intraspecific variation. An alternative attribution of the Kleineisenbach sample to *C. simorrensis* s.s.—not represented in the C1m comparative sample—is not particularly favored by the age of the site (MN7+8 or MN9; Pickford, 2016), albeit not impossible given the persistence of *C. simorrensis* until MN7+8 (Kubiak, 1981; Pickford, 2016). Nevertheless, the p3 from Kleineisenbach is also most similar to that of '*Pa.*' *valentini* and differs in various regards from those of *C. simorrensis*, leading us to concur with Pickford (2016) that the Kleineisenbach tetraconodontine is best attributed to '*Pa.*' *valentini*.

The described sample from SQ-TF allows us to describe for the first time several tooth loci that were previously unknown for '*Pa.*' *valentini* (I2, C1f, c1m, p2, DI2, DI3, and dp2, even though some were described based on erroneous anatomical and/or taxonomic identifications; McKenzie et al., 2023a, 2024), as well as the unworn morphology of the c1f. These tooth positions generally confirm the distinctiveness of '*Pa.*' *valentini* relative to other tetraconodontines included in the comparative sample, which is most clear in the case of the canines. Thus, the C1f shows similarities with those of *R. matritensis* and *C. simorrensis*, but appears distinct in several regards, supporting the view that '*Pa.*' *valentini* is not a junior synonym of *C. simorrensis* (contra Van der Made, 2020). In turn, the unworn c1f from SQ-TF is generally consistent with the heavily worn specimens previously attributed to '*Pa.*' *valentini* by McKenzie et al. (2023a, 2024), and most clearly differs from the morphology displayed by *V. steinheimensis* in being higher-crowned, displaying a much better developed postcristid relative to the ectocristid, and lacking a well-developed and deep fossid on the distal side. The type species of *Parachleuastochoerus* (Pickford, 1981: fig. 5) displays an intermediate c1f morphology that resembles '*Pa.*' *valentini* in crown height but differs in the less developed postcristid and better developed distal fossid (albeit shallower than in *V. steinheimensis*). Coupled with differences for many other tooth loci (see McKenzie et al., 2024), the c1f reported here reinforces the view that the tetraconodontine sample from SQ-TF is attributable to '*Pa.*' *valentini*—instead of *V. steinheimensis* as traditionally assumed (e.g., Van der Made, 1990, 1997). However, it neither supports nor contradicts the inclusion of '*Pa.*' *valentini* in *Parachleuastochoerus* supported by Pickford (2014, 2016), nor the synonymy between *Versoporcus* and *Parachleuastochoerus* advocated by Van der Made (2020).

In any event, the most taxonomically relevant information is that provided by the c1m because, as remarked by McKenzie et al. (2024), an unambiguous classification of '*Pa.*' *valentini* in *Parachleuastochoerus* instead of *Conohyus* was hindered by the lack of information about this tooth locus. Ironically, these c1ms were already published by Bataller (1924), who attributed them to *L. splendens*. The lack of multiple views might have hindered determining from the published plates the tetraconodontine affinities of these canines, which were not listed by Van der Made (1996a, 1996b) among the listriodontine material housed in the MGSB. In contrast, Pickford (2014) reported (but did not describe) a c1m fragment from SQ-TF housed in the ICP (IPS31067, incorrectly attributed to old number [VP1113]) as belonging to '*Pa.*' *valentini*. However, this specimen corresponds in fact to [IPS1113], attributed by Golpe-Posse (1971) to *L. splendens* and identified by McKenzie et al. (2024) as a fragmentary c1f of the latter species. In any event, the three c1ms from SQ-TF attributed herein display a scrofic morphology similar to that of other tetraconodontine c1ms included in the comparative sample—particularly those of *V. steinheimensis*, which only differ in minor

details—and can be thus confidently attributed to '*Pa.*' *valentini*. They differ from the c1ms of *C. simorrensis* in the lack of a longitudinal cementum ridge on the distal face of the tooth (see in particular Pickford, 2013b: fig. 6E), which has been considered a diagnostic feature of *Conohyus* to the exclusion of *Retroporcus* and other tetraconodontines (Pickford, 2016; Pickford & Laurent, 2014).

The lack of a distinct ridge on the distal face of the c1ms from SQ-TF supports the view that '*Pa.*' *valentini* is not a junior synonym of *C. simorrensis* (Pickford, 2013a, 2014, 2016; Pickford & Laurent, 2014; McKenzie et al., 2023a, 2024; Alba et al., 2024; contra Van der Made, 2020)—albeit the purported diagnostic value of this feature at the genus and species rank remains to be better ascertained. If Pickford and Laurent's (2014) diagnosis of genus *Conohyus* were to be strictly followed, it would support the inclusion of '*Pa.*' *valentini* in *Parachleuastochoerus* rather than *Conohyus*, as further suggested by distal premolar proportions (Pickford, 2014, 2016). Ironically, this would be at odds with Pickford's (2014: p. 171, 2016: p. 181) own diagnosis of *Parachleuastochoerus*, according to which the section of the c1m would be verrucosic. This assertion is probably based on Pickford's (1981: fig. 5) description of a specimen from Can Llobateres (IPS1698 [IPS1517]) that was interpreted by him as a c1m but is arguably the I1 of a hyracoid (authors' pers. obs.)—probably *Pliohyrax rossignoli*—previously identified at this site based on other material (Arranz et al., 2023; Golpe-Posse & Crusafont-Pairó, 1981; Pickford et al., 1997). In contrast, c1ms from Can Llobateres unambiguously attributable to *Pa. crusafonti*, such as IPS39510e (associated with postcanine teeth, including an m3 figured by Pickford, 2014: fig. 7B) or IPS94913 [IPS1595] (reported in Golpe-Posse, 1971 but not in Pickford, 1981) display a scrofic morphology similar to that of both '*Pa.*' *valentini* and *V. steinheimensis* (authors' unpublished data), despite the narrower proportions of the c1m in the type species of the genus. When this is considered, the c1m morphology of '*Pa.*' *valentini* appears more consistent with its inclusion in *Parachleuastochoerus* (or *Versoporcus*) than *Conohyus*. Nevertheless, this should not be taken as conclusive evidence without a sound phylogenetic framework to interpret the differences between these taxa. In other words, no genus diagnosis should be taken at face value to justify the exclusion of '*Pa.*' *valentini* from *Conohyus* or any other genus unless based on an explicit phylogeny. This is best illustrated by the fact that Van der Made (2020) considered *R. matritensis* a junior synonym of *C. simorrensis*, thus implicitly interpreting the aforementioned differences in c1m morphology as intraspecific variation. Therefore, the genus ascription of '*Pa.*' *valentini* is further discussed below in relation to the results of our phylogenetic analysis.

Taxonomic implications for other tetraconodontines

McKenzie et al. (2024) considered that the nominal species *C. doati* is a *nomen dubium* because the holotype M3 could potentially fit with the variation of both *C. simorrensis* and *V. steinheimensis*. However, the broader proportions of the M3 from the type locality of *C. doati* as compared with those of *V. steinheimensis*, together with metrical similarities between the former and the Mira M3 (here attributed to *C. simorrensis* following McKenzie et al., 2024), favor considering *C. doati* a junior subjective synonym of *C. simorrensis*—as previously supported by Van der Made (2020) and McKenzie et al. (2023a). This is further supported by the morphology of the c1m from the type locality of *C. doati*, which displays the longitudinal ridge of cementum on the distal face that was considered diagnostic of genus *Conohyus* by Pickford and Laurent (2014) and Pickford (2016). Accordingly, *C. doati* is here considered a junior subjective synonym of *C. simorrensis*, and the aforementioned morphology of the c1m is considered to be diagnostic (at most) to the species rank.

As noted above, the c1m morphology also has implications for the purported synonymy between *R. matritensis* and *C. simorrensis* supported by Van der Made (2020), as the lack of the distal cementum band in *R. matritensis* is arguably the most diagnostic feature between these two species. Besides the possession of a distal ridge of cementum along the c1m, Pickford and Laurent (2014) and Pickford (2016) considered that *Conohyus* further differs from *Retroporcus* by the possession of more sectorial mesial premolars set at the same level as the distal premolars (instead of vertically offset), as well as its less symmetrical m3 talonid with a buccally flaring distal root. Determining the distinctiveness of *Retroporcus* relative to *Conohyus* is outside the scope of this paper, but it is noteworthy that our comparisons with samples attributed to *R. matritensis* and *C. simorrensis* (both included in the comparative sample; see Materials and methods for further details) suggest that differences in the mesial premolar morphology or m3 occlusal contour among these taxa are not very consistent, in agreement with Van der Made's (2020) opinion that *R. matritensis* is a junior subjective synonym of *C. simorrensis*. In contrast, both species can be generally distinguished from *V. steinheimensis* and '*Pa.*' *valentini* based on m3 morphology (among many other features), even if differences are more subtle and less consistent than in the case of the lower premolars. Only the P4 morphology from the type locality of *R. matritensis* appears somewhat distinctive, indicating—coupled with differences in c1m morphology—that

it might be preliminary to formally synonymize it with *C. simorrensis*.

Alternatively, both species might be distinct, and the problem could be the hypodigm distribution proposed by Pickford and Laurent (2014), especially for localities such as Simorre and Villefranche d'Astarac, where both species were considered to co-occur (Pickford, 2016; Pickford & Laurent, 2014). After all, the purportedly diagnostic c1m morphology of *C. simorrensis* is only based on the specimens from Carpetana (Pickford, 2013b) and the specimen from Bonnefond (Stehlin, 1900) used by Pickford and Laurent (2014) to justify the inclusion of *C. doati* in the genus, which can be only compared with those from Göriach (Hofmann, 1893) and a single specimen from Simorre (Pickford & Laurent, 2014) attributed by the latter authors to *R. matritensis*. Additional specimens from other localities would be required to further substantiate the consistency of this diagnostic feature, but even if this were the case, the possession of a cementum ridge along the distal face of the c1m must not necessarily imply a distinction at the genus rank between *R. matritensis* and *C. simorrensis*. Such a distinction is, in our opinion, difficult to reconcile with their close similarities in size and shape for postcanine tooth loci. Pending an in-depth revision of the tetraconodontine material from the type locality of *R. matritensis* (Puente Vallecas) and its comparison to other samples attributed to the same species—including the more abundant sample from Göriach, which was used to erect *C. simorrensis goeriachensis* by Van der Made (1989)—and to *C. simorrensis*, we refrain from providing a new combination for *R. matritensis*. This is further advisable given that only the sample from Göriach has been included in the cladistic analysis performed in this paper. From a nomenclatural viewpoint, it is relevant to stress that *R. matritensis* is not the type species of *Retroporcus*, as Pickford and Laurent (2014) designated *Retroporcus complutensis* Pickford and Laurent (2014) instead. The latter was erected by these authors based on material from Somosaguas, previously assigned to *C. simorrensis* by Van der Made and Salesa (2004) and most recently synonymized with *R. sindiensis*, also known from Asia, by Van der Made (2020). This species, not included in the comparative sample and in the phylogenetic analysis of the present article, is the main reason why Van der Made (2020) kept *Retroporcus* as a distinct genus rather than considering it a junior synonym of *Conohyus*. The latter author, in particular, hypothesized that *R. sindiensis* might be ancestral to European *Conohyus* s.l. as well as other Asian tetraconodontines. However, a cladistic analysis including a wider representation of both European and Asian tetraconodontines would be required to confirm this hypothetical cladogenetic event from an ancestral stock represented by *R. sindiensis*.

Our comparisons also shed some light on the taxonomic attribution of the Sansan tetraconodontine, recently discussed based on a premolar interpreted as a P1 (Ginsburg, 1977) or p2 Pickford (2012) of *C. simorrensis*, and most recently reassigned to *R. sindiensis* by Van der Made (2020). As noted by Pickford (2017), the Sansan tetraconodontine is also represented by a lost maxilla with M2–M3 (reproduced in Pickford, 2017: fig. 6A) that is the holotype of '*S.*' *choerotherium*, here considered a *nomen dubium*. Van der Made (2020) interpreted that this nominal species is no longer a *nomen oblitum*—because Pickford (2017) used it as a valid name to illustrate the specimen—and remarked that it was a potential senior subjective synonym of *C. simorrensis* as well as all *Retroporcus* species. Nevertheless, it is clear from Pickford's (2017: p. 46) explanations ("most probably a species of tetraconodont […] close in morphology and dimensions to *Conohyus simorrensis* and *Retroporcus matritensis*") that he did not consider this name to represent a taxonomically valid species. Based on our metrical comparisons, the scarce tetraconodontine sample from Sansan does not fit well with '*Pa.*' *valentini*, *V. steinheimensis*, *C. simorrensis*, or even, except for the M3, *R. matritensis* (shorter p2 and narrower M2). However, contra Van der Made (2020), the Sansan specimens do not fit particularly well with those from Somosaguas (Van der Made & Salesa, 2004), or even '*C.*' *olujici* (based on the p2, because the upper molars of the latter are unknown; Bernor et al., 2004). Until the taxonomy of early Middle Miocene (MN5 and MN6) tetraconodontines is further clarified, or additional specimens from Sansan become available, we consider that the taxonomic identity of '*S.*' *choerotherium* must remain uncertain.

Phylogenetic relationships and systematic implications

Our cladistic analysis does not resolve the phylogenetic relationships of all the investigated tetraconodontines and, when it does, the various subclades are not robustly supported. As such, we do not feel compelled to translate our phylogenetic results into an updated systematic scheme for European tetraconodontines. On the other hand, our results are arguably the most comprehensive attempt to tackle the phylogenetic relationships of European tetraconodontines since Bernor et al.'s (2004) pioneering efforts in this regard. Therefore, the implications of our results, even if preliminary, deserve further discussion, as they outline future directions of work required to more conclusively settle European tetraconodontine systematics and evolution.

Our results do not particularly support Van der Made's (1999) systematic arrangement of tetraconodontines into three tribes (Tetraconodontini, Nyanzachoerini, and Parachleuastochoerini), as the three taxa newly coded

here do not join with any of their type genera and rather appear to constitute a distinct clade of their own. Our cladistic results are also at odds in several respects with Pickford's (2014: fig. 38 and p. 215) phylogenetic tree of the Tetraconodontinae, which was not sustained by any formal cladistic analysis. Pickford's (2014) hypothesis was mostly based on the hypertrophy of the distal premolars, the morphology of the c1m, and the position of the zygomatic arch. It contemplated the possibility that hypertrophied distal premolars relative to the mesial ones might be homologous for tetraconodontines as a whole, in which case the reduced distal premolars of *Parachleuastochoerus* and *Versoporcus* would have been independently acquired. Mostly based on zygomatic morphology, Pickford (2014) proposed a deep dichotomous split of two distinct tetraconodontine clades, maybe even implying a polyphyletic origin from a hyotheriine ancestor different from that of suines: one clade including the European genera *Conohyus* and *Versoporcus*, *Retroporcus* from Eurasia, and *Tetraconodon* from Asia; and the other including *Parachleuastochoerus* together with other genera such as *Sivachoerus* from Asia and *Nyanzachoerus* from Africa. The hypothesis further envisaged an early divergence between *Conohyus* and *Retroporcus* in the first clade, whereas *Parachleuastochoerus* (including '*Pa.*' *valentini*, *Pa. huenermanni*, *Pa. crusafonti*, and '*C.*' *olujici*) was placed in the other clade—mostly based on the cranial morphology of '*Pa.*' *valentini*, as it is unknown from all other species of the genus. This second clade would further include more derived Asian (e.g., *Sivachoerus*) and African (e.g., *Nyanzachoerus*) genera, characterized not only by the diverging morphology of the zygomatic arch but also (at least in taxa less basal than *Parachleuastochoerus*) a verrucosic cross section of the c1m.

Our cladistic results depart from Pickford's (2014) hypothesis by supporting a sister-taxon relationship between tetraconodontines and suines, as well as the monophyly of the former (Hou & Deng, 2014; Orliac et al., 2010), and also by tentatively placing *Tetraconodon* in the same clade as *Nyanzachoerus*. Furthermore, our results are consistent with a more basal position for *Pa. crusafonti*, as retrieved by previous cladistic analyses (Bernor et al., 2004; Hou & Deng, 2014; Orliac et al., 2010), while further supporting a more derived status for '*Pa.*' *valentini*, which is recovered as the sister taxon of *R. matritensis* within a clade that also includes *V. steinheimensis*. Our results thus support the view that '*Pa.*' *valentini* and *Pa. crusafonti* are not closely related, which has obvious systematic implications for '*Pa.*' *valentini*, as *Pa. crusafonti* is the type species of *Parachleuastochoerus*—thereby contradicting Pickford's (2014, 2016) inclusion of '*Pa.*' *valentini* in *Parachleuastochoerus* and suggesting that *Parachleuastochoerus* sensu Pickford (2014, 2016) is polyphyletic. At the same time, our results further contradict the inclusion of *V. steinheimensis* in *Parachleuastochoerus* (contra e.g., Van der Made, 2020; Van der Made et al., 2014), thus supporting its inclusion in a different genus (McKenzie et al., 2023b, 2024; Pickford, 2014, 2016).

Unlike with Pickford's (2014) hypothesis, our cladistic results are in general agreement with those previously retrieved by Bernor et al. (2004), even though only a few species were simultaneously analyzed by both studies. Bernor et al. (2004) recovered the Late Miocene *Pa. crusafonti* and *Parachleuastochoerus kretzoii* Fortelius et al., 2005 as successive sister taxa of a clade including four species that they classified in *Conohyus* but which are currently included in multiple genera, namely: '*C.*' *olujici* (currently considered a junior synonym of *Pa. huenermanni* or a subspecies of *V. steinheimensis*, depending on the authors; see above) as the basal-most species, followed by *R. sindiensis*; and *C. simorrensis* s.l. (the latter based on the Göriach and Paşalar samples, i.e., *R. matritensis* instead of *C. simorrensis* s.s.) and *V. steinheimensis* as sister taxa. Our analysis did not include '*C.*' *olujici*, *Pa. huenermanni*, or *R. sindiensis*, and, in contrast, included '*Pa.*' *valentini*. However, when only the three taxa in common (*Pa. crusafonti*, *R. matritensis*, and *V. steinheimensis*) are considered, the results are in good agreement, as both analyses support a closer relationship between *V. steinheimensis* and *R. matritensis* to the exclusion of *Pa. crusafonti*. This topology contrasts with Pickford's (2014) informal phylogeny, which is difficult to reconcile with our most parsimonious trees. Furthermore, as noted above, the derived systematic position of '*Pa.*' *valentini* supported by our results, as compared with the more basal status of *Pa. crusafonti* (contra Pickford, 2014), favors the view that '*Pa.*' *valentini* should be reallocated to another genus.

Our topology would be consistent with various systematic arrangements for '*Pa.*' *valentini*: (1) this species might represent a new, currently unnamed genus; (2) it might belong to *Retroporcus* or *Conohyus* s.s. (assuming they are distinct); or (3) it might be included in *Conohyus* s.l. (together with *R. matritensis*). The first option is not advisable because a monotypic genus would not adequately reflect the closer phylogenetic relationships with other species, as indicated by our cladistic results, and does not seem justified either on disparity grounds. The second option appears more reasonable but, in fact, there is no good reason to favor the inclusion of '*Pa.*' *valentini* into either *Retroporcus* or *Conohyus* s.s. Indeed, before providing a new combination for '*Pa.*' *valentini*, it would be necessary to evaluate further the purported congeneric or even conspecific status (Van der Made,

2020) of *R. matritensis* and *C. simorrensis*. Finally, the third option above evokes the former views by Bernor et al. (2004)—who favored a two-genus distinction (*Parachleuastochoerus* and *Conohyus*) and excluded *V. steinheimensis* from the former—except that these authors did not consider '*Pa.*' *valentini* because it had not been resurrected yet. In agreement with Bernor et al. (2004), our most parsimonious topology supports the exclusion of *V. steinheimensis* from *Parachleuastochoerus* and, thus, yields additional support to Pickford's (2014, 2016) contention that *Versoporcus* is distinct from *Parachleuastochoerus*—albeit for different reasons, as he based his opinion on the assumption that the cranial differences between '*Pa.*' *valentini* and *V. steinheimensis* cannot be accommodated within a single genus (apparently contra Van der Made, 2020). If '*Pa.*' *valentini* is excluded from *Parachleuastochoerus*, cranial morphology (unknown from *Pa. crusafonti*) no longer plays a role in the distinction of *Versoporcus* from the former, although we concur with Pickford (2014) that they advise against including both '*Pa.*' *valentini* and *V. steinheimensis* in the same genus (which, according to our topology, should be *Conohyus* rather than *Parachleuastochoerus*).

In other words, a very broad definition of *Conohyus*, so as to encompass both '*Pa.*' *valentini* and *V. steinheimensis*, might be a practical solution until the taxonomy and phylogeny of the group is clarified further, and would further be consistent with the topology favored by our analysis. However, it would arguably fail short to reflect the disparity of the included species in terms of craniodental morphology. A compromise would be to reallocate '*Pa.*' *valentini* (and *R. matritensis*) but not *V. steinheimensis* in *Conohyus*, but in our opinion it would be necessary to include *C. simorrensis* s.s. (and ideally other tetraconodontines) in the cladistic analyses so as to derive a more robust and comprehensive phylogeny of the subfamily. Particular emphasis should be put on the revision and coding of *Parachleuastochoerus* species, as well as the clarification of whether '*C.*' *olujici* is a junior synonym of *Pa. huenermanni* or a *Versoporcus* (sub)species, to determine whether *Parachleuastochoerus* s.s. is monophyletic—rather than paraphyletic as in Bernor et al.'s (2004) most parsimonious cladogram. As noted above, the purported synonymy between *R. matritensis* and *C. simorrensis* should also be assessed in greater detail—and, if considered to be distinct at least at the species rank, *C. simorrensis* s.s. should be included in the analyses. All in all, given the multiple ongoing uncertainties about the alpha-taxonomy and evolutionary history of the group, we prefer to refrain from providing a new combination for '*Pa.*' *valentini*, while advising to use the genus name within quotes—in agreement with the open nomenclature convention that denotes the use of a genus name that is obsolete for a given species (Bengtson, 1988; Jeppsson & Merrill, 1982), in the lack of a better alternative.

Biochronology and evolutionary implications

As far as European tetraconodontines are considered, and leaving aside the systematic status of '*Pa.*' *valentini*, Pickford's (2014) hypothesis is consistent with part of our cladistic results, in the sense that *Pa. crusafonti* might belong to a different clade than *Retroporcus* and *Versoporcus*. Based on a different systematic scheme, Van der Made (2020) hypothesized that *R. sindiensis* might have dispersed from Asia into Anatolia and Europe ~14.6–14.2 Ma and subsequently given rise there to *C. simorrensis* s.l. (i.e., including both *R. matritensis* and '*Pa.*' *valentini*) ~14.1–13.8 Ma, i.e., during the early Middle Miocene (MN5). Our comparisons contradict the purported synonymy between '*Pa.*' *valentini* and *C. simorrensis* favored by Van der Made (2020) and suggest that a broad concept of *C. simorrensis* should encompass at most *R. matritensis*—in which case, the generic distinction with *R. sindiensis* would also be debatable.

From a biochronological viewpoint, confirming the identification of '*Pa.*' *valentini* at SQ-TF merely attests to the presence of this species in the Iberian Peninsula during the pre-Vallesian (MN7+8) earliest Late Miocene (11.6–11.2 Ma), whereas the remains from CF2 and SQ-PN are best correlated to the earliest Vallesian ($\leq$11.2 Ma). This agrees well with the chronostratigraphic range of this species in the Vallès-Penedès Basin and elsewhere in Europe, where it ranges from MN7+8 to MN9 (Alba et al., 2024; McKenzie et al., 2023a, 2024; Pickford, 2014, 2016). If the tetraconodontine remains from Przeworno 2 are correctly identified as *C. simorrensis* (Kubiak, 1981; Pickford, 2016; this work) instead of *V. steinheimensis* (Van der Made, 2020; Van der Made et al., 2014), this would indicate a possible chronostratigraphic overlap between the former and '*Pa.*' *valentini* during MN7+8, although the lack of a precise dating for most localities does not allow us to conclude this with certainty. Nevertheless, the sister-taxon relationship recovered by our cladistic analysis between *R. matritensis* and '*Pa.*' *valentini* supports the view that the latter could have evolved from a *Conohyus* s.l.-like ancestor characterized by hypertrophied distal premolars. As discussed in the previous subsection, this would justify the inclusion of '*Pa.*' *valentini* in *Conohyus*—as long as *R. matritensis* but not *V. steinheimensis* is also included in the latter genus.

Our cladistic results further suggest that *V. steinheimensis* might belong to a more basal lineage of European tetraconodontines (contra Pickford, 2014). This lineage might share a European last common ancestor with *Conohyus* s.l. or represent an independent dispersal event from Asia during MN5. Van der Made (2020) traced back

the *V. steinheimensis* lineage (included by him in *Parachleuastochoerus*), which is recorded from MN6 until the earliest MN9 (McKenzie et al., 2023b, 2024), to the Lučane tetraconodontine (Bernor et al., 2004). The latter is dated to 15.0 Ma (MN5) and predates the earliest record of *R. sindiensis* in Europe (Van der Made, 2020). The Lučane tetraconodontine is here designated as '*C.*' *olujici* following the original genus ascription, which is put within quotation marks to denote taxonomic uncertainty. This taxon has alternatively been considered a *Parachleuastochoerus* by other authors (Pickford, 2016; Van der Made, 2020; Van der Made et al., 2014), albeit under strongly diverging taxonomic opinions. Thus, Pickford (2016) considered it a junior synonym of *Pa. huenermanni*, whereas Van der Made et al. (2014) classified it as a subspecies of *V. steinheimensis* within *Parachleuastochoerus*. Further research is required to clarify the systematic position of this (sub)species, as its distal premolar proportions are consistent with both *Versoporcus* and *Parachleuastochoerus* s.s. Our cladistic results suggest that, in contrast to Van der Made's (2020) systematic scheme, *Versoporcus* and *Parachleuastochoerus* might represent different lineages. As a result, given its old age, '*C.*' *olujici* should play a key role in more conclusively resolving the phylogeny of European tetraconodontines in years to come.

From a purely biochronological viewpoint, a close relationship between '*C.*' *olujici* and *V. steinheimensis* is indirectly supported by a critical re-evaluation of the chronostratigraphic range of *Pa. huenermanni*. In this regard, it is noteworthy that the latter species is not recorded at SQ-TF (as demonstrated in this work). This implies that, in the Iberian Peninsula, *Pa. huenermanni* is restricted to MN9 (Pickford, 2016; Van der Made, 1997), slightly preceding the record of *Pa. crusafonti*. The range of *Pa. huenermanni* elsewhere in Europe, even when '*C.*' *olujici* from MN5 is considered a different taxon (contra Pickford, 2014, 2016), is debatable because of several reasons. First, the age of the type locality of *Pa. huenermanni* (Breitenbrunn) is uncertain. It was originally correlated to either MN7+8 or MN9 (Heissig, 1989) and further considered late MN7+8 or MN9 by Fortelius et al. (1996). In contrast, Pickford (2016) correlated it to MN6 or else as early MN7+8, based on his interpretation of the deinotheriids and in further agreement with some other authors (Böhme et al., 2012), who estimated it age at ~14–13 Ma. However, there are no deinothere remains from Breitenbrunn (Seehuber, 2008), so Pickford's (2016) assertion might stem from a confusion with the homonymous locality from Austria, which is the only one that, according to the NOW database (The NOW Community, 2024), has yielded deinotheriid remains. Considering that Breitenbrunn is located on the uppermost portion of the Upper Freshwater Molasse (Heissig, 1989), which spans from 13.8 to 11.1 Ma (Kirsher et al., 2016), a latest MN7+8 age similar to that of SQ-TF or even an earliest MN9 age (i.e., ~12–11 Ma), seem likely. Second, other than Breitenbrunn, the only other purported MN7+8 record of *Pa. huenermanni* corresponds to La Grive-Saint-Alban (~12.4–11.2 Ma; Casanovas-Vilar et al., 2011), based on some specimens that were reported with measurements but not figured by Pickford (2014). As one of the oldest records of *Pa. huenermanni*, this identification should be better substantiated based on detailed descriptions and iconography, particularly given that previous authors (e.g., Mein & Ginsburg, 2002) recognized a single tetraconodontine (*V. steinheimensis*) at La Grive. The specimens from La Grive attributed to *Pa. huenermanni* by Pickford (2014) frequently overlap with the lower size range of *V. steinheimensis* but are larger than those of *Pa. huenermanni* from the Vallès-Penedès (Pickford, 1981), thus being potentially attributable instead to small specimens of *V. steinheimensis*.

We therefore consider that the MN7+8 records of *Pa. huenermanni* are debatable and that the possibility remains that this species is not recorded until the Vallesian, as supported by the lack of this species in the sample from SQ-TF as well as other sites from the Vallès-Penedès Basin dated to the late Aragonian and earliest Vallesian (Alba et al., 2006, 2017, 2022; McKenzie et al., 2023a, 2024; Van der Made, 1990, 1997). In Asia, *Parachleuastochoerus* has also been reported from the Vallesian (~10 Ma) of China (Pickford & Liu, 2001) and the early Late Miocene (~12–11 Ma) of Thailand and Myanmar (Pickford et al., 2004; Thaung-Htike, 2009), being represented by *Parachleuastochoerus sinensis* Pickford & Liu, 2001 and some remains unassigned to species, which are larger than European *Parachleuastochoerus* s.s. Given the general view that *Parachleuastochoerus* was already recorded at least by MN7+8 (if not earlier) in Europe, it has generally been assumed that this genus dispersed from Europe into Asia (Liu & Pickford, 2007; Thaung-Htike, 2009). However, given current uncertainties about the chronostratigraphic range of the genus, its place of origin cannot be determined with certainty. *Parachleuastochoerus* attests at least to an intercontinental dispersal event of tetraconodontines not later than the early Vallesian (MN9) but, based on currently available information, the possibility that it dispersed from Asia into Europe (rather than the reverse) cannot be ruled out, as it was the case of hipparionin horses and other large

mammals, including the suine *Propotamochoerus* (see discussion in Alba et al., 2022).

Conclusions

All the tetraconodontine dentognathic material available from the early Late Miocene localities of Sant Quirze (SQ-TF, SQ-PN, and CF2)—which remained largely unpublished—is described herein. The comparisons performed with other medium- to large-size tetraconodontines from Europe confirm the presence of a single species. The described sample is assigned to '*Pa.*' *valentini*, in agreement with some previous studies based on part of the SQ-TF sample but contrary to others that attributed this sample to *V. steinheimensis*. Our examination of the SQ-TF suid sample further enables discounting the presence of the smaller tetraconodontine *Pa. huenermanni*, which was repeatedly cited from the site based on incorrectly labeled material from other sites. The age of the described remains (late MN7+8 to earliest MN9) is consistent with the previously known chronostratigraphic range of '*Pa.*' *valentini*.

Our results further strengthen the view that '*Pa.*' *valentini* is distinct from both *C. simorrensis* and *V. steinheimensis* at least at the species rank, as attested by multiple tooth loci. The morphology of several tooth loci described herein for '*Pa.*' *valentini* for the first time, such as the I2, C1f, and c1m, strengthens further this view. It is particularly noteworthy that '*Pa.*' *valentini* lacks the c1m morphology characteristic of *Conohyus*. However, the diagnostic value of these differences at the species and genus ranks should be assessed further, as it has implicitly been questioned by some authors that synonymized *R. matritensis* with *C. simorrensis*. Indeed, the generic (and even specific) distinction between the two latter species appears questionable, given their great similarities in dental morphology. Overall, '*Pa.*' *valentini* generally more closely resembles *V. steinheimensis* in dental size and proportions (including the lack of hypertrophied distal premolars), but differs from it and approaches instead both *R. matritensis* and *C. simorrensis* in occlusal shape, overall not fitting well with any of the genera represented by these species.

The similarities in premolar proportions with both *Pa. crusafonti* and *V. steinheimensis*, coupled with cranial differences relative to the latter, justified the inclusion of '*Pa.*' *valentini* within *Parachleuastochoerus* when this nominal species was resurrected about a decade ago. Nevertheless, our cladistic results support a more basal status for the type species of *Parachleuastochoerus*, while '*Pa.*' *valentini* appears instead more closely related to *R. matritensis* and, to a lesser extent, *V. steinheimensis*. This suggests that the reduction of distal premolars shown by '*Pa.*' *valentini* is likely homoplastic relative to both *Pa. crusafonti* and *V. steinheimensis*, and that *Parachleuastochoerus*—as currently conceived by all authors (including either '*Pa.*' *valentini* or *V. steinheimensis*)—is likely polyphyletic. We nonetheless refrain from providing a new combination for this species, pending an in-depth revision of other tetraconodontine taxa from Europe.

Further research is necessary to clarify the evolutionary history of European tetraconodontines from a phylogenetic, biochronologic, and paleobiogeographic perspective. Nevertheless, currently available evidence is consistent with the existence of at least two different tetraconodontine lineages in Europe from MN5 onward. The lineage of *Versoporcus* might have been characterized by reduced distal premolars already from MN5, as '*C.*' *olujici* appears more likely ancestral to *V. steinheimensis* than to *Parachleuastochoerus* s.s. In turn, the *Conohyus* s.l. lineage (further including *R. matritensis* and '*Pa.*' *valentini*) would have been originally characterized by hypertrophied distal premolars. Under this scenario, the distal premolars would have been independently reduced in '*Pa.*' *valentini*. It is uncertain whether these two purported lineages would have evolved from a single European ancestor, as tentatively supported by our phylogenetic results, following the dispersal of an Asian tetraconodontine into Europe sometime before 15 Ma. Alternatively, they might have originated from two different (and not necessarily synchronous) dispersal events from Asia during MN5. Clarifying further the systematic status of '*C.*' *olujici* seems key to discerning between the two aforementioned alternatives. If all these taxa were eventually confirmed to constitute a European clade of European tetraconodontines originated during MN5, they would not fit well into any of the previously proposed tetraconodontine tribes. The possibility that *Parachleuastochoerus* s.s. derived from one of these taxa is not completely impossible but is not supported by currently available phylogenetic and biochronological evidence, which suggests instead that it might have originated from a later dispersal event from Asia during the early Vallesian.

Our study enables highlighting future directions of work that would contribute to better resolving the systematics of European tetraconodontines. First, a revision of the type species of *Parachleuastochoerus* (based on the partly unpublished material from Can Llobateres), together with a critical re-assessment of '*C.*' *olujici*, and their comparison with other *Parachleuastochoerus* s.s. from Europe (*Pa. huenermanni*) and Asia (*Pa. sinensis*) seem unavoidable to better determine the phylogenetic, geographic, and

temporal origin of the purported tribe Parachleuastochoerini. Second, a critical reassessment of the purported synonymy between *R. matritensis* and *C. simorrensis*, taking the most abundant sample from Göriach as a starting point but further including comparisons with *R. sindiensis*, would also be required to better determine the closest phylogenetic relationships and the most suitable genus ascription of '*Pa.*' *valentini*. Finally, the detailed description and analysis of the abundant but unpublished tetraconodontine material from Abocador de Can Mata (encompassing the whole MN7+8 and earliest MN9), currently underway by several authors of this paper, will hopefully contribute to clarifying the phylogeny of medium- to large-bodied tetraconodontines species from the Vallès-Penedès Basin (both '*Pa.*' *valentini* and *V. steinheimensis*) based on more complete cranial material.

Supplementary Information

The online version contains supplementary material available at https://doi.org/10.1186/s13358-024-00344-3.

Additional file 1. Supplemental tables and figure with comparative measurements and descriptive statistics, literature citations of comparative iconography, and cladistic matrices and results.

Acknowledgements
We thank J. Galindo (ICP) for discussion about the geology; J.M. Robles (ICP) for collection assistance; F. Carrasco and J. Barrull (MGSB) for access to and assistance with the MGSB collections; M. Gross from Universalmuseum Joanneum in Graz, for access to comparative fossil suid material; Teresa Requena (ICP) for assistance with the literature; and two anonymous reviewers for helpful comments and suggestions. We further acknowledge the collaboration of the MGSB at an institutional level. Finally, this work is part of the PhD dissertation of S.S., in the framework of the PhD Programme in Biodiversity of the Universitat Autònoma de Barcelona.

Author contributions
DMA designed the research; DMA, SS, SGA, and SM collected data (measurements and/or photographs); DMA and SS analyzed metrical data; DMA, SS, and SGA performed the cladistic analysis; DMA, SS, SGA, and ICV prepared the figures; DMA wrote the manuscript with input from the remaining authors.

Funding
This publication is part of R+D+I project PID2020-117289GB-I00/AEI/10.13039/501100011033, funded by the Agencia Estatal de Investigación of the Ministerio de Ciencia e Innovación from Spain. Research has also been funded by the Generalitat de Catalunya/CERCA Programme; the Agència de Gestió d'Ajuts Universitaris i de Recerca of the Generalitat de Catalunya (Consolidated Research Group 2022 SGR 00620); the Departament de Cultura of the Generalitat de Catalunya (CLT0009_22_000018); a predoctoral Joan Oró-FI fellowship (2023 FI-1 00396) to S.S., cofunded by the Agència de Gestió d'Ajuts Universitaris i de Recerca (Departament de Recerca i Universitats, Generalitat de Catalunya) and the European Social Fund Plus (FSE+); a technician contract of the INVESTIGO Program 2022 (reference 100027TC1) financed by the European Union, Next Generation EU to S.G.A.; and a predoctoral fellowship from the Confederated Tribes of Grand Ronde (CTGR) to S.M.

Availability of data and materials
All data supporting the findings of this study are available within the paper and its additional file. The described original fossils are available for study from the ICP and MGSB, which are registered museums recognized by the Generalitat de Catalunya.

Declarations

Ethics approval and consent to participate
Not applicable.

Competing interests
The authors declare no competing interests.

Received: 11 July 2024 Accepted: 18 December 2024
Published online: 17 February 2025

References

Agustí, J. (1981). *Roedores miomorfos del Neógeno de Cataluña.* [Unpublished doctoral dissertation]. Universidad de Barcelona.
Agustí, J. (1982). Biozonación del neogeno continental de Cataluña mediante roedores (Mammalia). *Acta Geológica Hispánica, 17*, 21–26.
Agustí, J. (1990). The Miocene rodent succession in Eastern Spain: A zoogeographical appraisal. In E. H. Lindsay, V. Fahlbusch, & P. Mein (Eds.), *European Neogene mammal chronology* (pp. 375–404). New York: Plenum Press.
Agustí, J. (1999). A critical re-evaluation of the Miocene mammal units in Western Europe: Dispersal events and problems of correlation. In J. Agustí, L. Rook, & P. Andrews (Eds.), *The evolution of Neogene terrestrial ecosystems in Europe* (pp. 84–112). Cambridge: Cambridge University Press.
Agustí Ballester, J. (1977a). Descripción de *Cricetodon lavocati* Freud, 1966 de St. Quirze (Trinxera). *Paleontología y Evolución, 12*, 65–67.
Agustí Ballester, J. (1977b). Contribución al conocimiento del género *Hispanomys* (Cricetidae, Rod., Mamm.) en la cuenca miocénica del Vallès-Penedès (Resumen de Tesina de Licenciatura). *Boletín Informativo del Instituto de Paleontología de Sabadell, 9*, 30–32.
Agustí Ballester, J. (1980). La asociación de *Hispanomys* y *Cricetodon* (Rodentia, Mammalia) en el Mioceno Superior del Vallès-Penedès (Cataluña, España). *Acta Geológica Hispánica, 15*, 51–60.
Agustí, J., Cabrera, L., Garcés, M., Krijgsman, W., Oms, O., & Parés, J. M. (2001). A calibrated mammal scale for the Neogene of Western Europe. State of the art. *Earth-Science Reviews, 52*, 247–260.
Agustí, J., Cabrera, L., Garcés, M., & Parés, J. M. (1997). The Vallesian mammal succession in the Vallès-Penedès basin (northeast Spain): Paleomagnetic calibration and correlation with global events. *Palaeogeography, Palaeoclimatology, Palaeoecology, 133*, 149–180.
Agustí, J., Cabrera, L., & Moyà-Solà, S. (1985). Sinopsis estratigráfica del Neógeno de la fosa del Vallés-Penedés. *Paleontologia i Evolució, 18*, 57–81.
Agustí, J., Casanovas-Vilar, I., & Furió, M. (2005). Rodents, insectivores and chiropterans (Mammalia) from the late Aragonian of Can Missert (Middle Miocene, Vallès-Penedès basin, Spain). *Geobios, 38*, 575–583.
Agustí, J., & Moyà-Solà, S. (1990). Mammal extinctions in the Vallesian (Upper Miocene). *Lecture Notes in Earth Sciences, 30*, 425–432.
Agustí, J., & Moyà-Solà, S. (1991). Spanish Neogene Mammal succession and its bearing on continental biochronology. *Newsletters on Stratigraphy, 25*, 91–114.
Alba, D. M., Casanovas-Vilar, I., Furió, M., García-Paredes, I., Angelone, C., Jovells-Vaqué, S., Luján, À. H., Almécija, S., & Moyà-Solà, S. (2018). Can Pallars i Llobateres: A new hominoid-bearing locality from the late Miocene of the Vallès-Penedès Basin (NE Iberian Peninsula). *Journal of Human Evolution, 121*, 193–203.
Alba, D. M., Casanovas-Vilar, I., Garcés, M., & Robles, J. M. (2017). Ten years in the dump: An updated review of the Miocene primate-bearing localities from Abocador de Can Mata (NE Iberian Peninsula). *Journal of Human Evolution, 102*, 12–20.
Alba, D. M., Garcés, M., Casanovas-Vilar, I., Robles, J. M., Pina, M., Moyà-Solà, S., & Almécija, S. (2019). Bio- and magnetostratigraphic correlation of the Miocene primate-bearing site of Castell de Barberà to the earliest Vallesian. *Journal of Human Evolution, 132*, 32–46.
Alba, D. M., Moyà-Solà, S., Casanovas-Vilar, I., Galindo, J., Robles, J. M., Rotgers, C., Furió, M., Angelone, C., Köhler, M., Garcés, M., Cabrera, L., Almécija, S., & Obradó, P. (2006). Los vertebrados fósiles del Abocador

de Can Mata (els Hostalets de Pierola, l'Anoia, Cataluña), una sucesión de localidades del Aragoniense superior (MN6 y MN7+8) de la cuenca del Vallès-Penedès. Campañas 2002–2003, 2004 y 2005. *Estudios Geológicos, 62*, 295–312.

Alba, D. M., & Moyà-Solà, S. (2012). A new pliopithecid genus (Primates: Pliopithecoidea) from Castell de Barberà (Vallès-Penedès Basin, Catalonia, Spain). *American Journal of Physical Anthropology, 147*, 88–112.

Alba, D. M., Moyà-Solà, S., Malgosa, A., Casanovas-Vilar, I., Robles, J. M., Almécija, S., Galindo, J., Rotgers, C., & Bertó Mengual, J. V. (2010). A new species of *Pliopithecus* Gervais, 1849 (Primates: Pliopithecidae) from the Middle Miocene (MN8) of Abocador de Can Mata (els Hostalets de Pierola, Catalonia, Spain). *American Journal of Physical Anthropology, 141*, 52–75.

Alba, D. M., Robles, J. M., Casanovas-Vilar, I., Beamud, E., Bernor, R. L., Cirilli, O., DeMiguel, D., Galindo, J., Llopart, I., Pons-Monjo, G., Sánchez, I. M., Vinuesa, V., & Garcés, M. (2022). A revised (earliest Vallesian) age for the hominoid-bearing locality of Can Mata 1 based on new magnetostratigraphic and biostratigraphic data from Abocador de Can Mata (Vallès-Penedès Basin, NE Iberian Peninsula). *Journal of Human Evolution, 170*, 103237.

Alba, D. M., Siarabi, S., Arranz, S. G., Galindo, J., McKenzie, S., Vinuesa, V., Robles, J. M., & Casanovas-Vilar, I. (2024). New suid remains from the early Vallesian (Late Miocene) site of Can Missert (Vallès-Penedès Basin). *Journal of Mammalian Evolution, 31*, 19.

Aldana Carrasco, E. J. (1992a). Los Sciurinae (Rodentia, Mammalia) del Mioceno de la Cuenca del Vallès-Penedès (Cataluña, España). *Treballs del Museu de Geologia de Barcelona, 2*, 69–97.

Aldana Carrasco, E. J. (1992b). Los Castoridae (Rodentia, Mammalia) del Neógeno de Cataluña (España). *Treballs del Museu de Geologia de Barcelona, 2*, 99–141.

Almera, J., & Bofill y Poch, A. (1887). Descubrimiento de grandes mamíferos fósiles en Cataluña. *Crónica Científica, 10*, 1–4.

Andrews, P., Harrison, T., Delson, E., Bernor, R. L., & Martin, L. (1996). Distribution and biochronology of European and Southwest Asian Miocene catarrhines. In R. L. Bernor, V. Fahlbusch, & H.-W. Mittmann (Eds.), *The evolution of Western Eurasian Neogene mammal faunas* (pp. 168–207). New York: Columbia University Press.

Arranz, S. G., Casanovas-Vilar, I., Žliobaitė, I., Abella, J., Angelone, C., Azanza, B., Bernor, R. L., Cirilli, O., DeMiguel, D., Furió, M., Pandolfi, L., Robles, J. M., Sánchez, I. M., Van den Hoek Ostende, L., & Alba, D. M. (2023). Paleoenvironmental inferences on the Late Miocene hominoid-bearing site of Can Llobateres (NE Iberian Peninsula): An ecometric approach based on functional dental traits. *Journal of Human Evolution, 103*, 103441.

Azanza, B. (1986). Estudio geológico y paleontológico del Mioceno del sector oeste de la Comarca de Borja. *Cuaderno de Estudios Borjanos, 17–18*, 63–126.

Bataller Calatayud, J. R. (1938). *Els ratadors fòssils de Catalunya*. Barcelona: Impremta de la Casa d'Assistència President Macià.

Bataller, J. R. (1918). Mamífers fòssils de Catalunya. *Treballs de la Institució Catalana d'Història Natural, 4*, 111–272.

Bataller, J. R. (1924). Contribució a l'estudi de nous mamífers fòssils de Catalunya. *Arxiu de l'Institut de Ciències, 12*, 1–53.

Bataller, J. R. (1926). Estudio de restos fósiles de tortuga recientemente encontrados en Cataluña. *Boletín del Instituto Geológico de España, 46*, 145–162.

Begun, D. R. (2002). The Pliopithecoidea. In W. C. Hartwig (Ed.), *The primate fossil record* (pp. 221–240). Cambridge: Cambridge University Press.

Bengtson, P. (1988). Open nomenclature. *Palaeontology, 31*, 223–227.

Bergounioux, F.-M. (1938). Chéloniens fossiles d'Espagne. *Bulletin de la Société d'Histoire Naturelle de Toulouse, 72*, 257–288.

Bergounioux, F. M. (1958). Les Reptiles fossiles du Tertiaire de la Catalogne. *Estudios Geológicos, 14*, 129–219.

Bergounioux, F. M., & Crouzel, F. (1958). Les mastodontes d'Espagne. *Estudios Geológicos, 14*, 224–345.

Bergounioux, F.-M., & Crouzel, F. (1962). Les Deinothéridés d'Espagne. *Bulletin de la Société Geologique de France, 4*, 394–404.

Bernor, R. L., Bi, S., & Radovčić, J. (2004). A contribution to the evolutionary biology of *Conohyus olujici* n. sp. (Mammalia, Suidae, Tetraconodontinae) from the early Miocene of Lučane, Croatia. *Geodiversitas, 26*, 509–534.

Bishop, L. C. (2010). Suoidea. In L. Werdelin & W. J. Sanders (Eds.), *Cenozoic mammals of Africa* (pp. 821–842). Berkeley: University of California Press.

Böhme, M., Aiglstorfer, M., Uhl, D., & Kullmer, O. (2012). The antiquity of the Rhine river: Stratigraphic coverage of the Dinotheriensande (Eppelsheim Formation) of the Mainz basin (Germany). *PLoS ONE, 7*, e36817.

Casanovas-Vilar, I., Alba, D. M., Garcés, M., Robles, J. M., & Moyà-Solà, S. (2011). Updated chronology for the Miocene hominoid radiation in Western Eurasia. *Proceedings of the National Academy of Sciences USA, 108*, 5554–5559.

Casanovas-Vilar, I., Garcés, M., Van Dam, J., García-Paredes, I., Robles, J. M., & Alba, D. M. (2016a). An updated biostratigraphy for the late Aragonian and the Vallesian of the Vallès-Penedès Basin (Catalonia). *Geologica Acta, 14*, 195–217.

Casanovas-Vilar, I., Jovells-Vaqué, S., & Alba, D.M. (2022). The Miocene high-resolution record of the Vallès-Penedès Basin (Catalonia). In I. Casanovas-Vilar, & D.M. Alba (Eds.), NOW 25th Anniversary Meeting. Sabadell (Barcelona), 16–18 November 2022. Abstract Book & Fieldtrip Guide. *Paleontologia i Evolució, memòria especial 9,* 79–122.

Casanovas-Vilar, I., Madern, A., Alba, D. M., Cabrera, L., García-Paredes, I., Van den Hoek Ostende, L. W., DeMiguel, D., Robles, J. M., Furió, M., Van Dam, J., Garcés, M., Angelone, C., & Moyà-Solà, S. (2016b). The Miocene mammal record of the Vallès-Penedès Basin (Catalonia). *Comptes Rendus Palevol, 15*, 791–812.

Chen, G. (1984). Suidae and Tayassuidae (Artiodactyla, Mammalia) from the Miocene of Steinheim a. A. (Germany). *Palaeontographica Abteilung A, 184*, 79–93.

Cherin, M., Alba, D. M., Crotti, M., Menconero, S., Moullé, P.-E., Sorbelli, L., & Madurell-Malapeira, J. (2020). The post-Jaramillo persistence of *Sus strozzii* (Suidae, Mammalia) in Europe: New evidence from the Vallparadís Section (NE Iberian Peninsula) and other coeval sites. *Quaternary Science Reviews, 233*, 106234.

Crusafont, M., & Truyols, J. (1954). *Catálogo paleomastológico del Mioceno del Vallés-Penedés y de Calatayud-Teruel. Segundo Cursillo Internacional de Paleontología*. Sabadell: Museo de la Ciudad de Sabadell.

Crusafont, M., Truyols, J. (1956). *Catálogos paleomastológicos. A) Cuenca del Vallés-Penedés (adiciones). B) Cuenca de Calatayud-Teruel (adiciones). C) Cuenca de La Cerdaña. D) Cuenca de la Seu d'Urgell. E) Cuenca de Tremp. F) Tipos de la fauna española. III Cursillo Internacional de Paleontología.* Sabadell: Museo de la Ciudad de Sabadell.

Crusafont-Pairó, M. (1935). La colección paleontológica del Museo de Sabadell. *Reseñas Científicas de la Real Sociedad Española de Historia Natural, 10*, 131–133.

Crusafont-Pairó, M. (1944). La sección de paleontología del Museo de Sabadell. *Publicaciones del Museo de Sabadell, 2*, 7–19.

Crusafont-Pairó, M. (1950). La cuestión del llamado Meótico español. *Arrahona, 1950*, 41–48.

Crusafont-Pairó, M. (1951). El sistema miocénico en la depresión española del Vallés-Penedés. In *International Geological Congress "Report of the Eighteenth Session, Great Britain, 1948", Part XI*. (pp. 33–42).

Crusafont-Pairó, M. (1953). El sistema miocénico en la depresión española del Vallés-Penedés. *Memorias y Comunicaciones del Instituto Geológico Provincial, 10*, 13–23.

Crusafont-Pairó, M. (1962). Las especies transientes en paleomastología: Su importancia en España. *Notas y Comunicaciones del Instituto Geológico y Minero de España, 65*, 49–60.

Crusafont-Pairó, M. (1965). El desarrollo de los caninos en algunos Driopitécidos del Vallesiense en Cataluña. *Notas y Comunicaciones del Instituto Geológico y Minero de España, 80*, 179–191.

Crusafont-Pairó, M. (1969). *Història de la Paleontologia a Sabadell*. Sabadell: Joan Sallent.

Crusafont-Pairó, M. (1975a). Transición Vindoboniense-Vallesiense en los alrededores de Sabadell. *Boletín Informativo del Instituto de Paleontología de Sabadell, 7*, 33–35.

Crusafont-Pairó, M. (1975b). El gibón fósil (*Pliopithecus*) del Vindoboniense terminal del Vallès. *Boletín Informativo del Instituto de Paleontología de Sabadell, 7*, 36–38.

Crusafont-Pairó, M. (1975c). Topografia paleontològica del Vallès. In Institut d'Estudis Catalans, Societat Catalana de Geografia (Ed.), *Miscel·lània Pau Vila: Biografia, bibliografia, treballs d'homenatge* (pp. 249–254). Granollers: Editorial Montblanc-Martin.

Crusafont-Pairó, M., Villalta, J. F. de, & Bataller, J. R. (1948). Los castores fósiles de España. I. Parte general y descriptiva. *Boletín del Instituto Geológico y Minero de España, 61*, 321–423.

Crusafont-Pairó, M., & Casanovas Cladellas, L. (1973). *Fossilium catalogus. I: Animalia. Pars 121. Mammalia Tertiaria Hispaniae*. The Hague: Dr. W. Junk B.V.

Crusafont-Pairó, M., & Villalta, J. F. de (1948). El Mioceno continental del Vallés y sus yacimientos de vertebrados. *Publicaciones de la Fundación Bosch y Cardellach, Sabadell, 3*, 7–30.

Crusafont-Pairó, M., & Golpe, J. M. (1972). Dos nuevos yacimientos del Vindoboniense en el Vallés. *Acta Geológica Hispánica, 7*, 71–72.

Crusafont-Pairó, M., & Golpe-Posse, J. M. (1972). Los yacimientos de mamíferos fósiles del Vallès. *Boletín Informativo del Instituto Provincial de Paleontología de Sabadell, 4*, 20–24.

Crusafont-Pairó, M., & Golpe-Posse, J. M. (1973). Nuevos hallazgos de *Progenetta montadai* en el Mioceno de Cataluña. *Boletín Geológico y Minero, 84*, 105–113.

Crusafont-Pairó, M., & Golpe-Posse, J.M. (1974). Biozonation des Mammifères néogènes d'Espagne. In G. Demarcq, & G Carbonnel (Eds.), Ve Congrès du Néogène Méditerranéen, Lyon, septembre 1971. *Mémoires du Bureau de Recherches Géologiques et Minières, 78*, 121–129.

Crusafont-Pairó, M., & Golpe-Posse, J. M. (1981). Estudio de la dentición inferior del primer pliopitécido hallado en España (Vindoboniense terminal de Castell de Barberà, Cataluña, España). *Butlletí Informatiu De L'institut De Paleontologia De Sabadell, 13*, 25–38.

Crusafont-Pairó, M., & Golpe-Posse, J. M. (1982). Los Pliopitécidos en España. *Coloquios de Paleontología, 37*, 41–46.

Crusafont-Pairó, M., & Truyols Santonja, J. (1960). Sobre la caracterización del Vallesiense. *Notas y Comunicaciones del Instituto Geológico y Minero de España, 60*, 109–125.

Daams, R., Freudenthal, M., & Van de Weerd, A. (1977). Aragonian, a new stage for continental deposits of Miocene age. *Newsletters on Stratigraphy, 6*, 42–55.

Daams, R., Van der Meulen, A. J., Álvarez Sierra, M. A., Peláez-Campomanes, P., Calvo, J. P., Alonso Zarza, M. A., & Krijgsman, W. (1999). Stratigraphy and sedimentology of the Aragonian (Early to Middle Miocene) in its type area (North-Central Spain). *Newsletters on Stratigraphy, 37*, 103–139.

de Blainville, H.M.D. (1847). *Ostéographie ou description iconographique comparée du squelette et du système dentaire des cinq classes d'animaux vertébrés récents et fossiles, pour servir de base à la Zoologie et à la Géologie. Fascicule 22. Sur les Hippopotames (Buffon), (*Hippopotamus*, L.) et les Cochons (Buffon), (*Sus*, L.)*. Paris: Arthus Bertrand.

de Bruijn, H., Daams, R., Daxner-Höck, G., Fahlbusch, V., Ginsburg, L., Mein, P., Morales, J., Heinzmann, E., Mayhew, D. F., Van der Meulen, A. J., Schmidt-Kittler, N., & Telles Antunes, M. (1992). Report of the RCMNS working group on fossil mammals, Reisensburg 1990. *Newsletters on Stratigraphy, 26*, 65–118.

Depéret, C. (1892). La faune de Mammifères Miocènes de La Grive-Saint-Alban (Isère) et de quelques autres localités du bassin du Rhone. *Archives du Muséum d'histoire Naturelle de Lyon, 5*, 1–95.

Falconer, H. (1868). Description of a fragment of a jaw of an unknown extinct pachydermatous animal from the Valley of the Murkunda. In C. Murchison (Ed.), *Palaeontological memoirs and notes of the late Hugh Falconer. Vol. 1. Fauna antiqua sivalensis* (pp. 149–157). London: Robert Hardwicke.

Filhol, H. (1882). Note relative à une nouvelle espèce de *Sus* fossile trouvée dans les argiles à *Dinotherium* de Valentine (Haute-Garonne). *Bulletin de la Société Philomathique de Paris, 6*, 123–124.

Fischer, G. (1814). *Zoognosia tabulis synopticis illustrata. Volumen tertium. Quadrupedum reliquorum, Cetorum et Monotrymatum descriptionem continens*. Moscow: Nikolai Sergei Vsevolozsky.

Fortelius, M., Armour-Chelu, M., Bernor, R.L., & Fessaha, N. (2005). Systematics and palaeobiology of the Rudabánya Suidae. In R.L. Bernor, L. Kordos, & L. Rook (Eds.), Multidisciplinary research at Rudabánya. *Palaeontographia Italica, 90*, 259–278.

Fortelius, M., Van der Made, J., & Bernor, R.L. (1996). Middle and Late Miocene Suoidea of Central Europe and the Eastern Mediterranean: Evolution, Biogeography, and Paleoecology. In R.L. Bernor, V. Fahlbusch, & H.-W. Mittmann, H.-W. (Eds.), *The evolution of Western Eurasian Neogene faunas* (pp. 348–377). New York: Columbia University Press.

Fraas, O. (1870). Die Fauna von Steinheim. Mit Rücksicht auf die miocänen Säugethier- und Vogelreste des Steinheimer Beckens. *Jahreshefte des Vereins für vaterländische Naturkunde in Württemberg, 26*, 145–306.

Freudenthal, M. (1966). On the mammalian fauna of the *Hipparion*-beds in the Calatayud-Teruel Basin (Prov. Zaragoza, Spain). Part I. The genera *Cricetodon* and *Ruscinomys* (Rodentia). *Proceedings Koninklijke Nederlandse Akademie van Wetenschappen B, 69*, 296–317.

Gaillard, C. (1899). Mammifères miocènes nouveaux ou peu connus de La Grive-Saint-Alban (Isère). *Archives du Muséum d'histoire Naturelle de Lyon, 7*, 1–78.

Galindo i Torres, J., Casanovas i Petanas, J., Navarro, O., Cabrera Pérez, L., Llenas i Avellaneda, M., Agustí i Ballester, J., & Picart i Boira, J. (2001). *Mapa geològic de Catalunya 1:25 000. Sabadell 392–2–2 (72–30)*. Barcelona: Institut Cartogràfic de Catalunya.

Garcés Crespo, M. (1995). *Magnetoestratigrafía de las sucesiones del Mioceno Medio y Superior del Vallès Occidental (Depresión del Vallès-Penedès, N.E. de España): Implicaciones biocronológicas y cronoestratigráficas*. [Unpublished doctoral dissertation]. Universitat de Barcelona.

Garcés, M., Agustí, J., Cabrera, L., & Parés, J. M. (1996). Magnetostratigraphy of the Vallesian (late Miocene) in the Vallès-Penedès Basin (northeast Spain). *Earth and Planetary Science Letters, 142*, 381–396.

Gervais, P. (1850 [1848–1852]). *Zoologie et Paléontologie françaises. Tome I*. Paris: Arthus Bertrand.

Ginsburg, L. (1974). Les faunes de Mammifères burdigaliens et vindoboniens des bassins de la Loire et de la Garonne. *Mémoires du Bureau des Recherches Géologiques et Minières, 78*, 153–167.

Ginsburg, L. (1977). Sur la répartition stratigraphique de *Conohyus simorrensis* (Suidae, Artiodactyla, Mammalia) dans le Miocène européen. *Comptes Rendus Sommaires de la Société Géologique de France, 4*, 203–205.

Ginsburg, L. (1986). Chronology of the European pliopithecids. In J. G. Else & P. C. Lee (Eds.), *Primate evolution* (pp. 47–57). Cambridge: Cambridge University Press.

Glazek, J., Oberc, J., & Sulimski, A. (1971). Miocene vertebrate faunas from Przeworno (Lower Silesia) and their geological setting. *Acta Geologica Polonica, 21*, 473–516.

Golpe-Posse, J.M. (1971). *Suiformes del Terciario español y sus yacimientos*. [Unpublished doctoral dissertation]. Universidad de Barcelona.

Golpe-Posse, J. M. (1972). Suiformes del Terciario español y sus yacimientos (Tesis doctoral-Resumen) (revisado y reimprimido en Diciembre de 1972). *Paleontología y Evolución, 2*, 1–197.

Golpe-Posse, J. M. (1974). Faunas de yacimientos con suiformes en el Terciario español. *Paleontología y Evolución, 8*, 1–87.

Golpe-Posse, J. M. (1982). Un pliopitécido persistente en el Vallesiense Medio-Superior de los alrededores de Terrassa (cuenca del Vallés, España) y problemas de su adaptación. *Boletín Geológico y Minero, 93–94*, 287–296.

Golpe-Posse, J. M., & Crusafont-Pairó, M. (1981). Presencia de un hirácido en el Vallesiense de Can Llobateres (Sabadell, cuenca del Vallés, depresión catalana, España). *Boletín de la Real Sociedad Española de Historia Natural, 79*, 265–276.

Gray, J. E. (1821). On the natural arrangement of vertebrose animals. *London Medical Repository Record, 15*, 296–310.

Harris J. H., & Liu, L.-P. (2007). Superfamily Suoidea. In D. R. Prothero & E. F. Foss (Eds.), *The evolution of artiodactyls* (pp. 130–150). Baltimore: Johns Hopkins University Press.

Harrison, T., Van der Made, J., & Ribot, F. (2002). A new middle Miocene pliopithecid from Sant Quirze, northern Spain. *Journal of Human Evolution, 42*, 371–377.

Heissig, K. (1989). *Conohyus huenermanni* n. sp., eine kleine Schweineart aus der Oberen Süßwassermolasse Bayerns. *Mitteilungen der Bayerischen Staatssammlung für Paläontologie und Historische Geologie, 29*, 235–240.

Hernández-Pacheco, E. (1914). Los vertebrados terrestres del Mioceno de la Península Ibérica. *Memorias de la Real Sociedad Española de Historia Natural, 9*, 443–488.

Hofmann, A. (1893). Die Fauna von Göriach. A*bhandlungen der kaiserlich-königlichen geologischen Reichsanstalt, 15*(6), 1–87.

Hou, S., & Deng, T. (2014). A new species of *Chleuastochoerus* (Artiodactyla: Suidae) from the Linxia Basin, Gansu Province, China. *Zootaxa, 3872*, 401–439.

Hünermann, K. A. (1968). Die Suidae (Mammalia, Artiodactyla) aus den Dinotheriensanden (Unterpliozän = Pont) Rheinhessens (Sudwestdeutschland). *Schweizerische Paläontologische Abhandlungen, 86*, 1–96.

Hünermann, K. A. (1999). Superfamily Suoidea. In G. Rössner & K. Heissig (Eds.), *The Miocene land mammals of Europe* (pp. 209–216). München: Verlag Dr. Friedrich Pfeil.

Iannucci, A., & Begun, D. R. (2022). Suidae (Mammalia, Artiodactyla) from the Late Miocene hominoid locality of Alsótelekes (Hungary). *Geobios, 71*, 39–49.

Iannucci, A., Cherin, M., Sorbelli, L., & Sardella, R. (2021). Suidae transition at the Miocene-Pliocene boundary: A reassessment of the taxonomy and chronology of *Propotamochoerus provincialis*. *Journal of Mammalian Evolution, 28*, 323–335.

Institut Cartogràfic i Geològic de Catalunya. (2024). *VISSIR v3.26 (VISor del Servidor d'Imatges Ràster)*. Generalitat de Catalunya. http://www.icc.cat/vissir3/. Accessed 26 March 2024.

Jeppsson, L., & Merrill, G. K. (1982). How best to designate obsolete taxonomic names and concepts: Examples among conodonts. *Journal of Paleontology, 56*, 1489–1493.

Kaup, J.-J. (1833). *Description d'ossements fossiles de Mammifères inconnus jusqu'à présent, qui se trouvent au Muséum Grand-Ducal de Darmstadt. Second Cahier.* Darmstadt: J.G. Heyer.

Kaup, J. J. (1859). *Beitraege zur naeheren Kenntniss der urweltlichen Saeugethiere. Viertes Heft*. Darmstadt: Eduard Zernin.

Kirscher, U., Prieto, J., Bachtadse, V., Abdul Aziz, H., Doppler, G., Hagmaier, M., & Böhme, G. (2016). A biochronologic tie-point for the base of the Tortonian stage in European terrestrial settings: Magnetostratigraphy of the topmost Upper Freshwater Molasse sediments of the North Alpine Foreland Basin in Baviera (Germany). *Newsletters on Stratigraphy, 49*, 445–467.

Kubiak, H. (1981). Suidae and Tayassuidae (Artiodactyla, Mammalia) from the Miocene of Przeworno in Lower Silesia. *Acta Geologica Polonica, 31*, 59–70.

Lartet, E. (1851). *Notice sur la Colline de Sansan, suivie d'une récapitulation des diverses espèces d'Animaux Vertébrés fossiles, trouvés soit a Sansan, soit dans d'autres gisements du terrain Tertiaire Miocène dans le Bassin Sous-Pyréneen.* Auch: J.-A. Portes.

Leakey, L. S. B. (1958). Some East African Pleistocene Suidae. *Fossil Mammals of Africa, 14*, 1–132.

Linnaeus, C. (1758). *Systema naturae per regna tria naturae, secundum classes, ordines, genera, species, cum characteribus, differentiis. Synonymis, locis. Tomus I. Editio decima, reformata.* Stockholm: Laurentius Salvius.

Liu, J.-H., & Pickford, M. (2007). Comparison of European and Chinese Late Miocene Suoidea: Implications for biostratigraphy and palaeoecology. *Vertebrata PalAsiatica, 45*, 59–73.

Llenas i Avellaneda, M. (1996). *Datació per mètodes paleontològics amb micromamífers dels materials neògens que afloren a l'àmbit dels fulls N. 392-4-3, 392-4-4 i 420-3-1 a escala 1/10.000*. [Unpublished report]. Institut Cartogràfic de Catalunya.

Luján, À. H., Delfino, M., Robles, J. M., & Alba, D. M. (2016). The Miocene tortoise *Testudo catalaunica* Bataller, 1926 and a revised phylogeny of extinct species of genus *Testudo* (Testudines: Testudinidae). *Zoological Journal of the Linnean Society, 178*, 312–342.

Lydekker, R. (1876 [1874–1880]). Molar teeth and other remains of Mammalia. In *Palaeontologia Indica. Ser. X. Indian Tertiary and post-Tertiary Vertebrata. Vol. I. Memoirs of the Geological Survey of India* (pp. 19–87). Calcutta.

Lydekker, R. (1877). Notices of new and rare mammals from the Siwaliks. *Records of the Geological Survey of India, 10*, 76–83.

Lydekker, R. (1878). Notices of Siwalik mammals. *Records of the Geological Survey of India, 11*, 64–104.

Marigó, J., Susanna, I., Minwer-Barakat, R., Madurell-Malapeira, J., Moyà-Solà, S., Casanovas-Vilar, I., Robles, J. M., & Alba, D. M. (2014). The primate fossil record in the Iberian Peninsula. *Journal of Iberian Geology, 40*, 179–211.

McKenzie, S., Arranz, S. G., Almécija, S., DeMiguel, D., & Alba, D. M. (2024). Tetraconodontines and suines (Artiodactyla: Suidae) from the earliest Vallesian site of Castell de Barberà (Vallès-Penedès Basin, NE Iberian Peninsula). *Journal of Mammalian Evolution, 31*, 7.

McKenzie, S., Casanovas-Vilar, I., & Alba, D. M. (2023b). Tetraconodont dental remains (Suidae, Tetraconodontinae) from the Middle Miocene site of Ca l'Almirall (Vallès-Penedès Basin, NE Iberian Peninsula). *Historical Biology, 35*, 597–606.

McKenzie, S., Sorbelli, L., Cherin, M., Almécija, S., Pina, M., Abella, J., Luján, À. H., DeMiguel, D., & Alba, D. M. (2023a). Earliest Vallesian suid remains from Creu de Conill 20 (Vallès-Penedès Basin, NE Iberian Peninsula). *Journal of Mammalian Evolution, 30*, 155–212.

Mein, P. (1975). Resultats du groupe de travail des Vertébrés: Biozonation du Néogène méditerranéen à partir des Mammifères. In J. Senes (Ed.), *Report on Activity of the R.C.M.N.S. Working Groups (1971–1975)* (pp. 78–81). Bratislava: International Union of Geological Sciences, Committee on Mediterranean Neogene Stratigraphy.

Mein, P. (1986). Chronological succession of hominoids in the European Neogene. In J. G. Else & P. C. Lee (Eds.), *Primate evolution* (pp. 59–70). Cambridge: Cambridge University Press.

Mein, P. (1990). Updating of MN zones. In E. H. Lindsay, V. Fahlbush, & P. Mein (Eds.), *European Neogene mammal chronology* (pp. 73–90). New York: Plenum Press.

Mein, P., & Ginsburg, L. (2002). Sur l'âge relatif des différents dépôts karstiques miocènes de La Grive-Saint-Alban (Isère). *Cahiers Scientifiques, 2*002(2), 7–47.

Morales, J., & Soria, D. (1985). Carnívoros y artiodáctilos de la provincia de Madrid. In M. T. Alberdi (Ed.), *Geología y paleontología del Terciario continental de la provincia de Madrid* (pp. 81–97). Madrid: Consejo Superior de Investigaciones Científicas.

Moyà-Solà, S., Pons-Moyà, J., & Köhler, M. (1990). Primates catarrinos (Mammalia) del Neógeno de la península Ibérica. *Paleontologia i Evolució, 23*, 41–45.

Orliac, M. J., Antoine, P.-O., & Ducrocq, S. (2010). Phylogenetic relationships of the family Suidae (Mammalia, Cetartiodactyla), new insights on the relationships within Suoidea. *Zoologica Scripta, 39*, 315–330.

Owen, R. (1848). Description of teeth and portions of jaws of two extinct Anthracotherioid quadrupeds (*Hyopotamus vectianus* and *Hyop. bovinus*) discovered by the Marchioness of Hastings in the Eocene deposits on the N.W. coast of the Isle of Wight: With an attempt to develop Cuvier's idea of the classification of pachyderms by the number of their toes. *The Quarterly Journal of the Geological Society of London, 4*, 103–141.

Pickford, M. (1981). *Parachleuastochoerus* (Mammalia, Suidae). *Estudios Geológicos, 37*, 313–320.

Pickford, M. (1993). Old World suoid systematics, phylogeny, biogeography and biostratigraphy. *Paleontologia i Evolució, 26–27*, 237–269.

Pickford, M. (2012). Les Suoidea (Artiodactyla) de Sansan : systématique, paléoécologie, biogéographie et biochronologie. In S. Peigné, & S. Sen (Eds.), Mammifères de Sansan. *Mémoires du Muséum National d'Histoire Naturelle, 203*, 249–277.

Pickford, M. (2013a). Reassessment of Dinotheriensande Suoidea: Biochronological and biogeographic implications (Miocene Eppelsheim Formation). *Mainzer Naturwissenschaftliches Archiv, 50*, 155–193.

Pickford, M. (2013b). *Conohyus simorrensis* (Lartet, 1851) (Suidae, Mammalia) from the Middle Miocene of Carpetana (Madrid, Spain). *Spanish Journal of Palaeontology, 28*, 91–102.

Pickford, M. (2014). *Sus valentini* Filhol (1882) from St Gaudens (MN 8–9) France: Blighted from the outset but a key to understanding late Middle Miocene Tetraconodontinae (Suidae, Mammalia) of Europe. *Mainzer Naturwissenschaftliches Archiv, 51*, 167–220.

Pickford, M. (2015). Late Miocene Suidae from Eurasia: *Hippopotamodon* and *Microstonyx* problem revisited. *Münchner Geowissenschaftliche Abhandlungen A, 42*, 1–126.

Pickford, M. (2016). Biochronology of European Miocene Tetraconodontinae (Suidae, Artiodactyla, Mammalia) flowing from recent revision of the subfamily. *Annalen des Naturhistorischen Museums in Wien A, 118*, 175–244.

Pickford, M. (2017). Revision of "peccary-like" Suoidea (Artiodactyla: Mammalia) from the Neogene of the Old World. *Münchener Geowissenschaftliche Abhandlungen A, 46*, 1–144.

Pickford, M., & Laurent, Y. (2014). Valorisation of palaeontological collections: Nomination of a lectotype for *Conohyus simorrensis* (Lartet, 1851), Villefranche d'Astarac, France, and description of a new genus of tetraconodont. *Estudios Geológicos, 70*, e002.

Pickford, M., & Liu, L. (2001). Revision of the Miocene Suidae of Xiaolongtan (Kaiyuan), China. *Bollettino della Società Paleontologica Italiana, 40*, 275–283.

Pickford, M., Moyà Solà, S., & Mein, P. (1997). A revised phylogeny of Hyracoidea (Mammalia) based on new specimens of Pliohyracidae from Africa and Europe. *Neues Jahrbuch für Geologie und Paläontologie – Abhandlungen, 205*, 265–288.

Pickford, M., Nakaya, H., Kunimatsu, Y., Saegusa, H., Fukuchi, A., & Ratanasthien, B. (2004). Age and taxonomic status of the Chiang Muan (Thailand) hominoid. *Comptes Rendus Palevol, 3*, 65–75.

Pilgrim, G.E. (1925). Presidential address to the Geological Section of the 12th Indian Science Congress. In Indian Science Congress Association (Ed.), *Proceedings of the 12th Indian Scientific Congress* (pp. 200–218). Calcutta.

Pilgrim, G.E. (1926). The fossil Suidae of India. *Memoirs of the Geological Survey of India. Palaeontologia Indica, 8*(4), 1–105.
Quintana Cardona, J. (1995). *Memoria sobre las excavaciones paleontológicas en Sant Quirze del Vallès (Vallès Occidental, provincia de Barcelona).* [Unpublished report]. Institut de Paleontologia "M. Crusafont".
Robles, J.M., Alba, D.M., Casanovas-Vilar, I., Galindo, J., Cabrera, L., Carmona, R., & Moyà-Solà, S. (2011). On the age of the paleontological site of Can Missert (Terrassa, Vallès-Penedès Basin, NE Iberian Peninsula). In A. Pérez-García, F. Gascó, J.M. Gasulla, & F. Escaso (Eds.), *Viajando a mundos pretéritos* (pp. 339–346). Morella: Ayuntamiento de Morella.
Robles, J. M., Alba, D. M., Fortuny, J., De ESteban-Trivigno, S., Rotgers, C., Balaguer, J., Carmona, R., Galindo, J., Almécija, S., Bertó, J. V., & Moyà-Solà, S. (2013). New craniodental remains of the barbourofelid *Albanosmilus jourdani* (Filhol, 1883) from the Miocene of the Vallès-Penedès (NE Iberian Peninsula) and the phylogeny of the Barbourofelini. *Journal of Systematic Palaeontology, 11*, 993–1022.
Roman, F. (1907). *Le Néogène continental dans la Basse Vallée du Tage (rive droite). 1re partie—Paléontologie*. Commission du Service Lisbonne: Géologique du Portugal.
Salmerón i Bosch, C. (1988). *El tren del Vallès: Història dels ferrocarrils de Barcelona a Sabadell i Terrassa*. Barcelona: Terminus.
Santafé Llopis, J.V. (1978). *Rinocerótidos fósiles de España*. [Unpublished doctoral dissertation]. Universidad de Barcelona.
Schaub, S. (1944). Cricetodontiden der Spanischen Halbinsel. *Eclogae Geologicae Helvetiae, 37*, 453–457.
Schaub, S. (1947). Los cricetodóntidos del Vallés-Panadés. *Estudios Geológicos, 6*, 55–67.
Seehuber, U. (2008). *Litho- und biostratigraphische Untersuchungen in der Oberen Süßwassermolasse in der Umgebung von Kirchheim in Schwaben*. [Unpublished doctoral dissertation]. Ludwig–Maximilians–Universität München.
Simpson, G. G. (1945). The principles of classification and a classification of mammals. *Bulletin of the American Museum of Natural History, 85*, 1–350.
Stehlin, H. G. (1900). Ueber die Geschichte des Suiden-Gebisses. Zweiter Teil. *Abhandlungen der Schweizerischen Paläontologischen Gesellschaft, 27*, 337–527.
Swofford, D.L. (2003). *PAUP*. Phylogenetic Analysis Using Parsimony (*and Other Methods). Version 4*. Sunderland: Sinauer Associates.
Thaung-Htike. (2009). The first discovery of *Parachleuastochoerus* (Mammalia, Artiodactyla, Suidae) from the Late Miocene of Myanmar. *Shwebo Degree College Research Journal, 1*, 109–119.
The NOW Community. (2024). New and Old Worlds Database of Fossil Mammals (NOW). Licensed under CC BY 4.0. Retrieved July 3, 2024 from https://nowdatabase.org/now/database/
Thenius, E. (1956). Die Suiden und Tayassuiden des steirischen Tertiärs. Beiträge zur Kenntnis der Säugetierreste des steirischen Tertiärs VIII. *Sitzungsberichten der Österreichische Akademie der Wissenschaften, mathematisch-naturwissenschaftlichen Klasse, 165*, 337–382.
Van der Made, J. (1989). A *Conohyus*-lineage (Suidae, Artiodactyla) from the Miocene of Europe. *Revista Española de Paleontología, 4*, 19–28.
Van der Made, J. (1990). *Iberian Suoidea. Paleontologia i Evolució, 23*, 83–97.
Van der Made, J. (1996a). Listriodontinae (Suidae, Mammalia), their evolution, systematics and distribution in time and space. *Contributions to Tertiary and Quaternary Geology, 33*, 3–254.
Van der Made, J. (1996b). *Albanohyus*, a small Miocene pig. *Acta Zoologica Cracoviensia, 39*, 293–303.
Van der Made, J. (1997). Los Suoidea de la Península Ibérica. In J. P. Calvo & J. Morales (Eds.), *Avances en el conocimiento del Terciario ibérico* (pp. 109–112). Cuenca.
Van der Made, J. (1998). *Aureliachoerus* from Oberdorf and other Aragonian pigs from Styria. *Annalen des Naturhistorischen Museums in Wien, 99A*, 225–277.
Van der Made, J. (1999). Biometrical trends in the Tetraconodontinae, a subfamily of pigs. *Transactions of the Royal Society of Edinburgh, Earth Sciences, 89*, 199–225.
Van der Made, J. (2020). The Suoidea from the Middle Miocene of Gračanica (Bugojno Basin, Bosnia and Herzegovina)—evolution, taxonomy, and biostratigraphy. *Palaeobiodiversity and Palaeoenvironments, 100*, 321–349.
Van der Made, J., Aiglstorfer, M., & Böhme, M. (2014). Taxonomic study of the pigs (Suidae, Mammalia) from the late Middle Miocene of Gratkorn (Austria, Syria). *Palaeobiodiversity and Palaeoenvironments, 94*, 595–617.
Van der Made, J., Krakhmalnaya, T., & Kubiak, H. (1999). The pig *Propotamochoerus palaeochoerus* from the Upper Miocene of Grytsiv, Ukraine. *Estudios Geológicos, 55*, 283–292.
Van der Made, J., & Morales, J. (2003). The pig *Conohyus simorrensis* from the Upper Aragonian of Alhambra, Madrid, and a review of the distribution of European *Conohyus*. *Estudios Geológicos, 59*, 303–312.
Van der Made, J., & Moyà-Solà, S. (1989). European Suinae (Artiodactyla) from the Late Miocene onwards. *Bollettino della Società Paleontologica Italiana, 28*, 329–339.
Van der Made, J., & Salesa, M.J. (2004). Early remains of the pig *Conohyus simorrensis* from the Middle Aragonian of Somosaguas near Madrid—Its dispersal into Europe and evolution. *Neues Jahrbuch für Geologie und Paläontologie – Abhandlungen, 233*, 153–168.
Villalta, J. F. de, & Crusafont, M. (1946). Les gisements de Mammifères du Néogène espagnol. I. Bassin du Valles-Penaeés (Catalogne) Vindobonien. Sant Quirze de Galliners. *Comptes Rendus Sommaires de la Societé Géologique de France, 1946*(3/4), 49–51.
Villalta-Comella, J. F. de, & Crusafont-Pairó, M. (1933). Primera nota sobre vertebrats fòssils miocènics del Vallès. La presència del *Dinotherium giganteum* Kaup var. *laevius* Jourdan a Sant Quirze de Galliners. *Butlletí de la Institució Catalana d'Història Natural, 33*, 258–261.
Villalta, J. F., & Crusafont, P. (1934). Segona nota sobre els mamífers miocènics del Vallès. *Butlletí de da Institució Catalana d'Història Natural, 34*, 128–130.
Villalta-Comella, J. F. de, & Crusafont-Pairó, M. (1941a). Noticia preliminar sobre la fauna de carnívoros del Mioceno continental del Vallés-Penedés. *Boletín de la Real Sociedad Española de Historia Natural, 39*, 201–208.
Villalta-Comella, J. F. de, & Crusafont-Pairó, M. (1941b). Los vertebrados fósiles del Mioceno continental del Vallés-Penedés (provincia de Barcelona). *Publicaciones del Museo de Sabadell, 1*, 1–16.
Villalta-Comella, J. F. de, & Crusafont-Pairó, M. (1943a). Los vertebrados del Mioceno continental de la cuenca del Vallés-Panadés (provincia de Barcelona). I. Insectívoros. II. Carnívoros. *Boletín del Instituto Geológico y Minero de España, 56*, 145–336.
Villalta-Comella, J. F. de, & Crusafont-Pairó, M. (1943b). *Contribución al conocimiento de Albanosmilus jourdani Filhol*. Madrid: Consejo Superior de Investigaciones Científicas.
Villalta-Comella, J. F. de, & Crusafont-Pairó, M. (1944a). Nuevos carnívoros del Vindoboniense de la Cuenca del Vallés-Panadés. *Notas y Comunicaciones del Instituto Geológico y Minero de España, 13*, 53–88.
Villalta-Comella, J. F. de, & Crusafont-Pairó, M. (1944b). El "Stephanocemas elegantulus" Roger, nuevo cérvido del Vindoboniense del Vallés-Panedés. *Boletín de la Real Sociedad Española de Historia Natural, 42*, 397–410.
Villalta-Comella, J. F. de, & Crusafont-Pairó, M. (1944c). Nuevos insectívoros del Mioceno continental del Vallés-Panadés. *Notas y Comunicaciones del Instituto Geológico y Minero de España, 12*, 39–65.
Villalta-Comella, J. F. de, & Crusafont-Pairó, M. (1945). Los vertebrados del Mioceno continental de la cuenca del Vallés-Panadés (Provincia de Barcelona). III.—Ungulados: A Perisodáctilos i. Chalicotheriinae. *Estudios Geológicos, 1*, 113–167.
Von Meyer, H. (1834). *Die fossilen Zähne und Knochen und ihre Ablagerung in der Gegen von Georgensmünd in Bayern*. Frankfurt am Mein: J.D. Sauerländer.
Von Meyer, H. (1846). Mittheilungen an Professor Bronn gerichtet. *Neues Jahrbuch für Mineralogie, Geologie. Geognosie und Petrefakten-Kunde, 1846*, 462–476.

Publisher's Note